Oncology and Translational Medicine

Volume 7 • Number 1 • February 2021

Oncology and Translational Medicine Volume 7 • Number 1 • February 2021 pp 1–49

邮发代号：38-121
ISSN 2095-9621

GENERAL INFORMATION
≫otm.tjh.com.cn

ISSN 2095-9621
CN 42-1865/R

Oncology and Translational Medicine

肿瘤学与转化医学（英文）

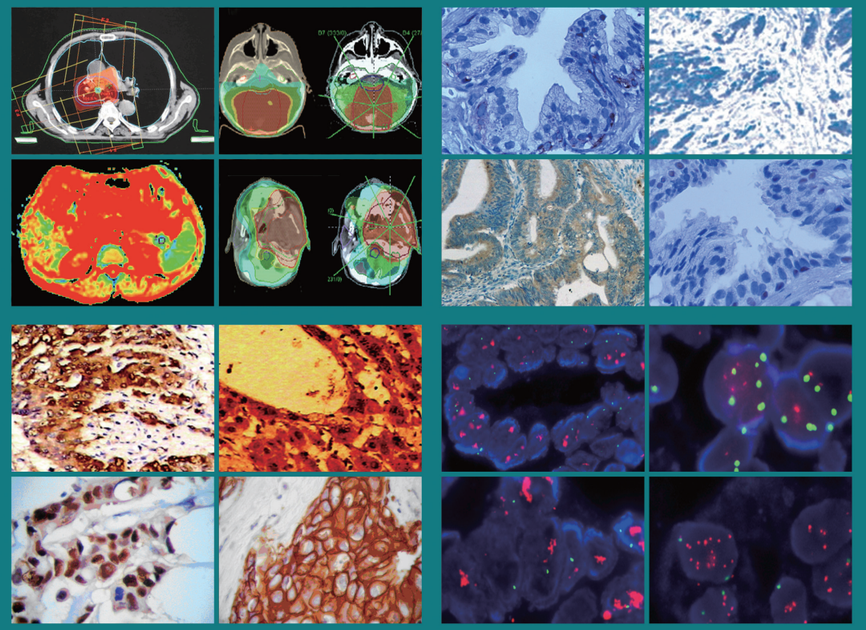

Volume 7
Number 1
February 2021

Oncology and Translational Medicine

Oncology and Translational Medicine
February 2021 Volume 7 Number 1

Contents

Oncology and Translational Medicine

Volume 7 • Number 1 • February 2021

Aims & Scope

Oncology and Translational Medicine is an international professional academic periodical. The Journal is designed to report progress in research and the latest findings in domestic and international oncology and translational medicine, to facilitate international academic exchanges, and to promote research in oncology and translational medicine as well as levels of service in clinical practice. The entire journal is published in English for a domestic and international readership.

Copyright

Supervised by

Ministry of Education of the People's Republic of China.

Administered by

Tongji Medical College, Huazhong University of Science and Technology.

Submission information

Manuscripts should be submitted to:
http://otm.tjh.com.cn
dmedizin@sina.com

Subscription information

ISSN edition: 2095-9621
CN: 42-1865/R

■ Subscription rates
Subscription may begin at any time. Remittances made by check, draft or express money order should be made payable to this journal. The price for 2021 is as follows: US $ 30 per issue; RMB ￥28.00 per issue.

Database

Oncology and Translational Medicine is abstracted and indexed in EMBASE, Index Copernicus, Chinese Science and Technology Paper Citation Database (CSTPCD), Chinese Core Journals Database, Chinese Journal Full-text Database (CJFD), Wanfang Data; Weipu Data; Chinese Academic Journal Comprehensive Evaluation Database.

Business correspondence

All matters relating to orders, subscriptions, back issues, offprints, advertisement booking and general enquiries should be addressed to the editorial office.

Mailing address
Editorial office of
Oncology and Translational Medicine
Tongji Hospital
Tongji Medical College
Huazhong University of Science and Technology
Jie Fang Da Dao 1095
430030 Wuhan, China
Tel.: +86-27-69378388
Email: dmedizin@sina.com

Printer
Changjiang Spatial Information Technology Engineering Co., Ltd. (Wuhan) Hangce Information Cartorgraphy Printing Filial, Wuhan, China
Printed in People's Republic of China

Editors-in-Chief

Managing director

Executive editors

Oncology and Translational Medicine
DOI 10.1007/s10330-020-0455-5

February 2021, Vol. 7, No. 1, P1–P6

ORIGINAL ARTICLE

Efficacy and safety of berberine in the prophylactic treatment of acute radiation proctitis in postoperative patients with cervical cancer: a randomized controlled study*

Kai Qin, Yi Cheng, Xianglin Yuan, Jing Zhang, Le Huang (✉)

Department of Oncology, Tongji Hospital, Tongji Medical College, Huazhong University of Science and Technology, Wuhan 30030, China

Abstract

Objective The aiom of this study was to study the efficacy and safety of berberine as a prophylactic treatment of acute radiation proctitis in postoperative patients with cervical cancer.

Methods A total of 120 postoperative patients with cervical cancer were enrolled between July 2016 and October 2019, and randomly divided into a treatment group (berberine 300 mg three times a day, $n = 60$) and a control group (receiving vitamin C tablets, 100 mg three times a day; $n = 60$) using the random number table method. All patients received pelvic intensity-modulated radiation therapy (IMRT) and concurrent sensitizing chemotherapy weekly. The difference in the percentage of irradiation volume to the rectum and small intestine as well as the incidence, onset time, severity, and duration of acute radiation proctitis and cystitis during radiotherapy were compared between the two groups. The completion rate, completion time, number of chemotherapy sessions, and quality of life during radiotherapy were also compared.

Results There were no statistical differences in age, FIGO stage, pathological type, complications, high-risk factors, and rectum and small intestine irradiation dose distribution (V_{20}, V_{30}, V_{40}, and V_{50}) between the two groups ($P > 0.05$). No acute radiation proctitis of grade 3 or above occurred in the two groups. There was no significant difference in the incidence of acute radiation cystitis, grade 2 acute radiation proctitis, completion rate of IMRT, and frequency of sensitization chemotherapy between the two groups. After prophylactic treatment with berberine, the incidence of grade 1 acute radiation proctitis, occurrence of grade 1 radiation proctitis, and completion time of radiotherapy in the treatment group were significantly lower than those in the control group ($P < 0.05$). The SF-36 score of the treatment group after radiotherapy was 67.53 ± 4.21, which was significantly better than that of the control group (64.90 ± 6.32; $P < 0.05$). The incidence of grade 3-4 neutropenia in the treatment group was 10% and lower than that in the control group (31.7%, $P = 0.003$). No adverse reactions related to berberine were observed.

Conclusion Prophylactic prescription with oral berberine can reduce the incidence, onset time, and duration of grade 1 acute radiation proctitis, and improve the quality of life of postoperative patients with cervical cancer receiving concurrent chemoradiotherapy.

Received: 16 September 2020
Revised: 20 October 2020
Accepted: 12 November 2020

Key words: berberine; adjvuant therapy; cervical cancer; intensity-modulated radiation therapy (IMRT); acute radiation proctitis

Cervical cancer is a major public health problem worldwide that seriously threatens women's health. The incidence of cervical cancer in young women is still rising [1]. Cervical cancer was the eighth leading cause of cancer death in China in 2015, accounting for 2.83% of the total new malignant tumors and 3.96% of deaths [2]. Adjuvant concurrent chemoradiotherapy has been proven to improve the progression-free survival and overall survival of patients with early-stage cervical cancer (stage IB to stage IIA) with poor prognosis (positive margin, positive lymph node, or para-uterine involvement) after radical hysterectomy [3–4]. Radiation proctitis, with

✉ Correspondence to: Le Huang. Email: huang7181@163.com
* Supported by a grant from The Health Commission of Hubei Province Scientific Research Project (No. WJ2019M118).

symptoms of nausea, vomiting, diarrhea, pain, bleeding, weight loss, and intestinal fistula, is the most frequent complication of radiotherapy for cervical cancer [5]. Acute radiation proctitis usually occurs within 3 months after radiotherapy, and its incidence is as high as 50%–75% [5–6]. Common risk factors for acute radiation proctitis include previous abdominal surgery history, low body mass index, cardiovascular disease, diabetes, advanced age, female sex, and smoking history [6]. However, there are only a few preventive strategies for acute radiation proctitis, including the drug, amifostine, and physical intervention [7].

Berberine is an isoquinoline alkaloid isolated from plants that has been used as an antidiarrheal, antiarrhythmic, and anti-inflammatory agent [8]. Studies have shown that berberine can regulate the expression and secretion of tumor necrosis factor-α and interleukin-10, and plays an important role in inhibiting radiation-induced intestinal injury and improving survival, thus serving as an effective treatment strategy for radiation-induced intestinal injury [9]. The purpose of this study was to explore the clinical efficacy and safety of berberine as a preventive treatment of acute radiation proctitis caused by intensity-modulated radiation therapy (IMRT) in postoperative patients with cervical cancer.

Materials and methods

Patient characteristics

Postoperative cervical cancer patients with high-risk factors who received pelvic IMRT between July 2016 and October 2019 at Tongji Hospital, Tongji Medical College, Huazhong University of Science and Technology were enrolled in this study. All patients signed an informed consent form. The inclusion criteria were as follows: patients categorized as stage IB to IIA cervical cancer according to the guideline of the International Federation of Gynecology and Obstetrics (FIGO), those diagnosed with cervical adenocarcinoma via postoperative pathology, without radiotherapy, patients aged 20–70 years, and those who recovered well from radical operation of cervical cancer within 3 months. The exclusion criteria were as follows: patients with KPS score < 80, defecation ≥ 3 times a day, patients with gastroduodenal ulcer, chronic gastroenteritis, cholecystitis, diabetes, history of inflammatory bowel disease, severe damage to vital organ function, allergy to the experimental drug, hemolytic anemia, secondary primary cancer, and expected poor compliance.

Patients were randomly divided into treatment and control groups using the random number table method. They received pelvic radiotherapy and weekly synchronous sensitization chemotherapy. The baseline characteristics of patients were listed in Table 1.

Treatment plan

A total of 100 and 120 postoperative cervical cancer patients with high-risk factors were randomly divided into the treatment and control groups, respectively, and received pelvic radiotherapy and weekly synchronous sensitization chemotherapy based on the random number table method.

Treatment group (n = 60): all patients received 300 mg of prophylactic berberine (dosage: 0.1 g × 100 tablets; Shenyang No.1 Pharmaceutical Co., Ltd., China) orally three times a day before radiotherapy. Control group (n = 60): all patients received prophylactic treatment with 100 mg vitamin C tablets (dosage: 0.1 g × 100 tablets; Guangdong South China Pharmaceutical Group Co., Ltd., China) as a placebo three times a day.

Postoperative patients with cervical cancer were received IMRT and concurrent sensitization chemotherapy, and IMRT comprised a total PTV D48 of 48.6 Gy in a fraction of 1.8 Gy five fractions a week. The target delineation of IMRT in postoperative cervical cancer was based on the Consensus Guidelines for Clinical Target Delimitation published by Small, W in 2008 [4, 10], and the target delineation of normal tissues referred to the Consensus Atlas of Radiation Therapy Oncology Group published by GAY H [4, 11]. Synchronous sensitization chemotherapy was performed once weekly using an intravenous drip of cisplatin 30 mg/m^2 (dosage: 20 mg/piece; Nanjing Pharmaceutical Factory Co., Ltd., China). Upon contraindications or intolerance to chemotherapy, sensitization chemotherapy was terminated within the week.

Patients with grade 3 or higher acute proctitis or other adverse reactions related to radiotherapy (according to the RTOG/EORTC) were suspended from radiotherapy [11]. If the adverse reactions returned to grade 2 or below, radiotherapy was continued. The time of occurrence, duration, and grade of gastrointestinal reactions were recorded. The quality of life score (the MOS 36-item short-form health survey) was completed before and after radiotherapy.

Endpoints and evaluations

Primary endpoints

(a) Incidence, onset time, severity, and duration of acute radiation proctitis and cystitis

The common symptoms of acute radiation proctitis included nausea, vomiting, diarrhea, pain, hemorrhage, weight loss, and intestinal fistula. Acute radiation proctitis usually occurs within 3 months of radiotherapy. Radiation cystitis was characterized by painless hematuria, mild frequent micturition, or dysuria. In accordance with the RTOG/EORTC, the symptoms and severity of radiation proctitis and cystitis were recorded every day within 3 months after radiotherapy, and the duration of

adverse reactions was the sum of adverse reaction time at all levels. The incidence of radiation proctitis and cystitis of different grades was defined as the number of patients with radiation proctitis and cystitis divided by the total number of patients. The occurrence time of radiation proctitis and cystitis of different grades was the number of days when the corresponding symptoms first appeared within 3 months after receiving radiotherapy. By comparing the primary endpoints between the two groups, the clinical efficacy of the treatment against acute radiation proctitis and cystitis was evaluated. The blood parameters and liver and kidney function of patients were monitored weekly.

(b) Quality of life: Quality of life was assessed using the SF-36 scores before and at 1-2 weeks after radiotherapy. The scores were compared between the two groups. A lower SF-36 score indicates worse quality of life.

Secondary endpoints:

(a) Completion time, completion rate of radiotherapy, and frequency of sensitization chemotherapy. Completion time of radiotherapy: the days from receiving radiotherapy to completing radiotherapy, excluding the time of treatment suspension due to machine failure and holidays. The completion rate of radiotherapy was the proportion of patients who completed external radiotherapy. Preventive treatment with berberine was evaluated by comparing the days of radiotherapy completion, completion rate, and times of sensitization chemotherapy between the two groups.

(b) Normal tissue assessment

To evaluate the effect of irradiation volume on radiation proctitis, the percentage of irradiation volume to the small intestine and rectum was compared between the two groups. The radiation doses were 20, 30, 40, and 50 Gy.

Statistical analysis

Data were analyzed using SPSS20.0 software (SPSS Inc, USA). Measurement data are presented as mean ± standard deviation and compared between the two groups using *t*-test. Calculated data are expressed as percentages, and compared between the two groups using the chi-square test. Differences with $P < 0.05$ were considered significant [12].

Results

Characteristics of the treatment and control groups

The age, FIGO stage of cervical cancer, pathological type, complications, and postoperative high-risk factors of the two groups were compared ($P > 0.05$). The results showed no obvious difference between the two groups, as shown in Table 1.

Percentage of irradiation dose volume to organs at risk (rectum and small intestine)

The percentages of irradiation volumes V20, V30, V40, and V50 to the rectum in the treatment group were higher than those in the control group, but with no significant difference ($P > 0.05$). The percentages of irradiation volumes V30, V40, and V50 to the small intestine in the treatment group were lower than those in the control group, but without significant difference ($P > 0.05$). The percentages of irradiation volume V20 to the small intestine in the treatment group was higher than that in the control group, but the difference was not

Table 1 Baseline clinical characteristics of postoperative patients with cervical cancer

Parameter	Treatment (*n* = 60)	Control (*n* = 60)	*t*	*P*
Mean age (years)	50.17 ± 3.54	49.57 ± 3.43	1.069	0.289
Stage			0.135	0.713
IB	34 (56.7%)	32 (53.3%)		
IIA	26 (43.3%)	28 (46.7%)		
Complication				
History of abdominal surgery	2 (3.3%)	3 (5%)	0.209	0.648
Low body mass index	0	0		
Cardiovascular diseases	6 (10%)	8 (13.3%)	0.323	0.57
Diabetes	0	0		
Smoking	6 (10%)	7 (11.7%)	0.086	0.769
Histological type				
Adenocarcinoma	60 (100%)	60 (100%)		
High risk factors				
Tumor size ≥ 3cm	10 (16.7%)	8 (13.3%)	0.261	0.609
LVSI*	38 (63.3%)	40 (66.7%)	0.147	0.702
Infiltrate 1/3 of the stroma outside the cervix	10 (16.7%)	12 (20%)	0.223	0.637
Preoperative neoadjuvant chemotherapy	20 (33.3%)	28 (46.7%)	2.222	0.136

* Lymph-vascular space invasion

Table 2 Distribution of irradiation volume to the small intestine and rectum (%)

Organs at risk	Group	*n*	V_{20}	V_{30}	V_{40}	V_{50}
Small intestine	Treatment	60	79.30 ± 4.31	44.40 ± 3.25	18.20 ± 1.41	8.37 ± 1.96
	Control	60	77.83 ± 2.92	44.57 ± 2.20	18.55 ± 1.41	8.40 ± 1.85
	t		1.948	–0.323	–1.725	–0.111
	P		0.056	0.748	0.09	0.912
Rectum	Treatment	60	76.28 ± 1.64	57.47 ± 1.27	38.35 ± 1.39	4.73 ± 1.33
	Control	60	76.08 ± 1.83	57.03 ± 1.85	38.03 ± 1.48	4.63 ± 1.34
	t		0.666	1.776	1.329	0.365
	P		0.508	0.081	0.189	0.716

significant ($P > 0.05$), as shown in Table 2.

Evaluation of endpoints

There was a significant difference in the incidence of grade 1 acute radiation proctitis between the treatment and control groups (61.7% *vs* 36.7%, $P = 0.006$); however, there was no significant difference in the incidence of grade 2 acute radiation proctitis between the two groups (11.7% *vs* 6.7%, $P = 0.342$). No acute radiation proctitis of grade 3 or above occurred in the two groups. There was no significant difference in the incidence of acute radiation cystitis between the two groups. The incidence of grade 3-4 neutropenia in the treatment group was lower than that in the control group (10% *vs* 31.7%, $P = 0.003$). Both the treatment and control groups completed radiotherapy. The radiotherapy time of the treatment group was slightly shorter than that of the control group, showing a significant difference (38.10 ± 1.17 *vs* 39.37 ± 1.59 days, $P = 0.001$). The SF-36 score after treatment was significantly higher than that of the control group (67.53 ± 4.21 *vs* 64.90 ± 6.32, $P = 0.001$). However, there was no significant difference in the frequency of completing sensitization chemotherapy between the two groups (4.20 ± 0.75 *vs* 4.10 ± 0.84, $P = 0.522$), as shown in Table 3.

The occurrence time of grade 1 radiation proctitis in the treatment group was slightly later than that in the control group (5.55 ± 1.26 *vs* 4.27 ± 1.28 days). In the treatment group, the duration of grade 1 radiation proctitis was significantly shorter (3.64 ± 0.90 *vs* 4.57 ± 0.90 days). Grade 2 radiation proctitis occurred slightly earlier in the treatment group than in the control group (10.50 ± 1.20 *vs* 9.75 ± 0.96 days). The duration of grade 2 radiation proctitis in the treatment group was relatively shorter than that in the control group (3.0 ± 0.82 *vs* 2.25 ± 0.89 days), but the difference was not significant, as shown in Table 4.

No adverse reactions related to berberine were observed in the study (as evaluated according to CTCAE4.0)

Discussion

Radiotherapy is one of the most effective treatments for pelvic tumors, and acute radiation proctitis is a major factor that seriously affects the completion rate

Table 3 Endpoints and acute adverse reactions according to concurrent chemoradiotherapy

Characteristics	Treatment group (*n* = 60)	Control group (*n* = 60)	*t*	*P*
Acute radiation proctitis				
Grade 1	22	37	7.502	0.006
Grade 2	4	7	0.901	0.342
Grade 3	0	0		
Grade 4	0	0		
Acute radiation cystitis				
Grade 1	2	4	0.702	0.402
≥ Grade 2	0	0		
Hematologic complications (Grade 3–4)				
Neutropenia	6	19	8.539	0.003
Anemia	4	9	2.157	0.142
Thrombocytopenia	4	7	0.901	0.343
SF-36 score (before radiotherapy)	67.10 ± 4.02	66.17 ± 4.47	1.609	0.113
SF-36 score (after radiotherapy)	67.53 ± 4.21	64.90 ± 6.32	3.615	0.001
Radiotherapy completion rate	100%	100%		
Radiotherapy completion time/day	38.10 ± 1.17	39.37 ± 1.59	–4.75	0.001
Number of sensitization chemotherapy	4.20 ± 0.75	4.10 ± 0.84	0.644	0.522

Table 4 Treatment course for acute radiation proctitis ($\bar{x} \pm s$)

Items	Grade 1		Grade 2	
	Onset time (days)	Duration (days)	Onset time (days)	Duration (days)
Treatment group	5.55 ± 1.26	3.64 ± 0.90	10.50 ± 1.20	3.0 ± 0.82
Control group	4.27 ± 1.28	4.57 ± 0.90	9.75 ± 0.96	2.25 ± 0.89
P	0.001	0.001	0.304	0.188

of radiotherapy and quality of life in patients receiving pelvic radiotherapy [7]. Gastrointestinal side effects are the most important dose-limiting factor in radiotherapy for malignant tumors [13]. To date, there have been only a few preventive strategies for acute radiation proctitis, which include preventive treatment with amifostine and physical intervention [7, 12]. In 2014, the MASCC/ISOO clinical practice guidelines recommended intravenous amifostine to prevent acute radiation proctitis [13]. Amifostine has been proven to exert protective effects in acute radiation-induced intestinal mucosal injury caused by various radiation types and doses. However, its protective effect on tissues is controversial [14]. Thus, for the radiotherapy for pelvic tumors, there is a necessity to develop new protective agents to reduce the occurrence of radiation proctitis [12, 15]. Song *et al*. found that abnormal expression of proteins in the Fas and glycolysis pathways is a possible molecular mechanism of acute radiation proctitis [16]. Li *et al*. found that berberine can protect against intestinal mucosa injury caused by radiotherapy by regulating the expression and secretion of TNF-α and IL-10 [17]. Li *et al*. found through follow-up clinical research that berberine significantly reduced the incidence and severity of acute radiation proctitis, and delayed the occurrence time of acute radiation proctitis [18]. In this study, we observed no significant difference in the irradiation volume to the rectum and small intestine between the two groups. Compared with those in the control group, the incidence of grade 1 acute radiation proctitis in patients in the treatment group was significantly reduced, the occurrence time was delayed, and the duration was shortened. There was no significant difference in the incidence, occurrence time, and duration of grade 2 acute radiation proctitis in patients between the two groups. No acute radiation proctitis of grade 3 or above occurred in the two groups. Liu *et al*. reported that the emission rate of acute radiation proctitis of grade 3 and above in patients with cervical cancer after the operation was 1.02% [3]. In this study, the incidence of grade 1 acute radiation proctitis was significantly higher than that reported by Li *et al*. (the incidence in the treatment and control groups reported by Li was 9.5% and 33.3%, respectively [18]), which may be related to the higher radiotherapy dose in the treatment target area (the clinical radiotherapy dose was 48.6 Gy in our study and 36–46 Gy in Li *et al*). In addition, the irradiated volume to the rectum was relatively larger in patients with cervical cancers who underwent surgery than in those who did not. Both groups of patients completed IMRT, and the patients in the treatment group completed radiotherapy in a shorter time than those in the control group, which may be related to the occurrence of grade 3-4 neutropenia during chemoradiotherapy. There was no significant difference in the frequency of sensitization chemotherapy and the incidence of radiation cystitis between the two groups. This indicated that IMRT can be used as a safe treatment for postoperative cervical cancers with good tolerance. Moreover, the SF-36 scores in patients in the treatment group were significantly higher than those in the control group after radiotherapy. No berberine-related side effects were observed in this study. Thus, this study suggested that preventive treatment with berberine can significantly reduce the incidence of grade 1 acute radiation proctitis in postoperative patients with cervical cancer caused by IMRT, delay the occurrence time, shorten the duration of symptoms, and improve the quality of life of patients. However, for the prevention and treatment of serious radiation proctitis (≥ grade 2), it may be necessary to improve the radiotherapy plan, reduce the range of irradiation volume to organs at risk, optimize the radiotherapy methods, and use other additional drugs.

Conclusion

In conclusion, the prophylactic treatment with berberine can effectively reduce grade 1 acute radiation proctitis in postoperative patients with cervical cancer receiving concurrent chemoradiotherapy, and improve the quality of life of these patients. This treatment is therefore worthy of further verification and promotion through randomized multicenter clinical studies.

Conflicts of interest

The authors declare no potential conflicts of interest.

References

1. Siegel RL, Miller KD, Jemal A. Cancer statistics, 2019. CA Cancer J Clin, 2019, 69: 7–34.
2. Zheng RS, Sun KX, Zhang SW, *et al*. Report of cancer epidemiology in China, 2015. Chin J Oncol (Chinese), 2019, 41:19–28.
3. Liu YM, Ni LQ, Wang SS, *et al*. Outcome and prognostic factors in cervical cancer patients treated with surgery and concurrent chemoradiotherapy: a retrospective study. World J Surg Oncol, 2018, 16: 18.
4. Zhou H, Wang YD, Luo M, *et al*. FIGO 2018 Gynecological tumor report--interpretation of cervical cancer guidelines. Chin J Pract Gynecol Obstet (Chinese), 2019, 35: 95–103.
5. Wang Y, Kong W, Lu N, *et al*. Incidence of radiation enteritis in cervical cancer patients treated with definitive radiotherapy versus adjuvant

radiotherapy. J Cancer Res Ther, 2018, 14: S120–S124.
6. Harb AH, Abou FC, Sharara AI. Radiation enteritis. Curr Gastroenterol Rep, 2014, 16: 383.
7. Surgeon Branch of Chinese Medical Doctor Association, Colorectal Surgery Group of Surgery Branch in the Chinese Medical Association. Chinese consensus on diagnosis and treatment of radiation proctitis (2018). Chin J Gastr Surg (Chinese), 2018, 21: 1321–1336.
8. Kuo CL, Chi CW, Liu TY. The anti-inflammatory potential of berberine *in vitro* and *in vivo.* Cancer Lett, 2004, 203: 127–137.
9. Li GH, Zhang YP, Tang JL, *et al*. Effects of berberine against radiation-induced intestinal injury in mice. Int J Radiat Oncol Biol Phys, 2010, 77: 1536–1544.
10. Small WJ, Mell LK, Anderson P, *et al*. Consensus guidelines for delineation of clinical target volume for intensity-modulated pelvic radiotherapy in postoperative treatment of endometrial and cervical cancer. Int J Radiat Oncol Biol Phys, 2008, 71: 428–434.
11. Gay HA, Barthold HJ, O'Meara E, *et al*. Pelvic normal tissue contouring guidelines for radiation therapy: A Radiation Therapy Oncology Group consensus panel atlas. Int J Radiat Oncol Biol Phys, 2012, 83: e353–e362.
12. Zhang J, Gong C, Qin K, *et al*. Effect of kangfuxin fluid combined with compound berberine retention enema in the treatment of 25 cases of patients with radiotherapy-induced acute proctitis. Herald of Med, 2019, 38: 1030–1032.
13. Lalla RV, Bowen J, Barasch A, *et al*. MASCC/ISOO clinical practice guidelines for the management of mucositis secondary to cancer therapy. Cancer, 2014, 120: 1453–1461.
14. Tas S, Ozkul F, Arik MK, *et al*. The effect of amifostine on bacterial translocation after radiation induced acute enteritis. Acta Cir Bras, 2016, 31: 156–160.
15. Harb AH, Abou FC, Sharara AI. Radiation enteritis. Curr Gastroenterol Rep, 2014, 16: 383.
16. Song S, Chen D, Ma T, *et al*. Molecular mechanism of acute radiation enteritis revealed using proteomics and biological signaling network analysis in rats. Dig Dis Sci, 2014, 59: 2704–2713.
17. Li GH, Zhang YP, Tang JL, *et al*. Effects of berberine against radiation-induced intestinal injury in mice. Int J Radiat Oncol Biol Phys, 2010, 77: 1536–1544.
18. Li GH, Wang DL, Hu YD, *et al*. Berberine inhibits acute radiation intestinal syndrome in human with abdomen radiotherapy. Med Oncol, 2010, 27: 919–925.

DOI 10.1007/s10330-020-0455-5
Cite this article as: Qin K, Cheng Y, Yuan XL, *et al*. Efficacy and safety of berberine in the prophylactic treatment of acute radiation proctitis in postoperative patients with cervical cancer: a randomized controlled study. Oncol Transl Med, 2021, 7: 1–6.

Oncology and Translational Medicine
DOI 10.1007/s10330-020-0441-1
February 2021, Vol. 7, No. 1, P7–P14

ORIGINAL ARTICLE

The prognostic significance of ALI, PLR, and Ki-67 expression in stage III–IV inoperable non-small cell lung cancer*

Ying Li[1] (✉), Qiaofang Li[2], Yanluqi He[1], Hongzhen Zhang[2] (✉)

[1] Graduate School of Hebei North University, Shijiazhuang 075000, China
[2] Fifth Department of Oncology, Hebei General Hospital, Shijiazhuang 050000, China

Abstract

Objective The aim of the study was to investigate and compare the prognostic value of advanced inflammatory index, platelet/lymphocyte ratio (PLR), and Ki-67 expression in stage III–IV inoperable non-small cell lung cancer (NSCLC) before treatment.

Methods The clinical data of 98 inoperable patients with stage III–IV NSCLC in our hospital (Fifth Department of Oncology, Hebei General Hospital, Shijiazhuang, China) before treatment were retrospectively analyzed, and advanced lung cancer inflammation index (ALI) was calculated using body mass index (BMI) × serum albumin (ALB) ÷ neutrophil/lymphocyte ratio (NLR). he optimal cutoff values of ALI and PLR for predicting prognosis is determined. Chi-square test was used to analyze the relationship between patients and clinical characteristics. Kaplan-Meier method was used to calculate the total survival of patients, and log-rank test was used for comparison. Independent prognostic factors were assessed by univariate and multivariate analyses. Spearman correlation was used to analyze the relationship among ALI, PLR, and Ki-67.

Results In our study of the 98 cases, the survival time of the patients with ALI < 18 was significantly lower than that of patients with ALI > 18 ($P < 0.001$), with a median survival time of 10 months and 25 months, respectively. The survival time of patients with a PLR < 185 was significantly higher than that of patients with a PLR > 185 (median survival time was 27 months vs. 10 months, $P < 0.001$).The higher the Ki-67 expression, the shorter the survival time ($P < 0.005$).The combined ALI and PLR detection results indicated that the survival time of patients with high ALI and low PLR was significantly longer than that of patients with low ALI and high PLR ($P < 0.001$). Univariate analysis showed that smoking history, degree of differentiation, KPS score, Ki-67 expression, ALI value, and PLR affected the prognosis of patients. Multivariate analysis showed that KPS score, ALI value, and Ki-67 expression were independent prognostic factors.

Conclusion ALI, PLR, and Ki-67 expression are important predictors of stage III-IV inoperable NSCLC. In terms of the prognostic value, ALI seems to have the best ability to predict patient survival. In addition, the combined detection of ALI and PLR levels before treatment seems to be more helpful in improving our prediction of patient prognosis. Moreover, it is expected to play a role in future clinical applications.

Received: 23 June 2020
Revised: 15 October 2020
Accepted: 6 November 2020

Key words: non-small cell lung cancer (NSCLC); advanced lung cancer inflammation index (ALI); expression of Ki-67; prognosis

Lung cancer is still the leading cause of cancer-related deaths in the world today, with more than 600 000 mortalities every year [1]. Lung cancer is divided according to different biological and morphological characteristics into small cell lung cancer and non-small cell lung cancer (NSCLC), with NSCLC accounting for more than 80% of all cancers. To our knowledge, more than half of all patients with NSCLC are diagnosed at an advanced stage and have a low 5-year survival rate. Therefore, early detection, timely diagnosis, and formulation of targeted

✉ Correspondence to: Ying Li. Email: 349546474@qq.com;
Hongzhen Zhang. Email: hongzhenzhang456@sohu.com
* Supported by a grant from the Key Research Project of Medical Science in Hebei Province (No. 20180006).

treatment programs are of great importance for early control of the disease, arrest of its development, and improvement of patients' quality of life.

Inflammation is an important occurrence in the tumor microenvironment and is involved in the formation and development of tumors. Studies have found that the prognosis of cancer patients depends not only on the characteristics of the tumor itself but also on the inflammatory response of the patients [2]. An increasing number of reports have confirmed that tumor-related inflammation, especially host-related systemic inflammatory response, is closely related to disease development and progression and survival of cancer patients [3]. Some studies have assessed the degree of systemic inflammation by analyzing acute protein markers such as albumin (ALB) [4]. In the process of inflammation regulation, neutrophils, lymphocytes, and platelets are important mediators of tumor inflammation; they have been demonstrated to have potential prognostic predictors of inflammation [5–7]. In addition, a new inflammatory predictor called the advanced lung cancer inflammation index (ALI) that uses body mass index (BMI), ALB, and neutrophil/lymphocyte ratio (NLR) to arrive at a value. ALI has been proven to be a valuable prognostic factor for patients with lung cancer [8]. Platelet aggregation not only plays an important role in hemostasis and thrombosis but also in the immune response, and thus it has arole in the progression of tumors [9]. Ki-67 is an indicator of the ability of all cells to proliferate. It is also useful in determining the degree of malignancy as well as in assessing the prognosis of patients and in guiding the adjuvant therapy of tumors. According to previous studies, high Ki-67 is closely related to low overall survival (OS) rate in NSCLC patients [10–11]. Therefore, Ki-67 expression is a valuable biomarker for predicting the prognosis of lung cancer patients. The traditional method to detect Ki-67 expression is immunohistochemistry, which requires invasive methods such as biopsy or surgery to obtain specimens. Since we selected patients with unresectable stage III–IV NSCLC, our pathological results were all obtained from biopsy specimens. Because of this, biopsy may miss more aggressive lesions in the tumor, leading to an underestimation of the disease. However, this pathological result still has important reference value.

To the best of our knowledge, no studies have assessed all three indicators of ALI, platelet/lymphocyte ratio (PLR), and Ki-67 expression in NSCLC. Therefore, we retrospectively analyzed the prognostic value of ALI, PLR, and Ki-67 expressions in patients with stage III–IV NSCLC, and we also compared the relationship between ALI, PLR, and the clinical characteristics of tumor patients and Ki-67 expression.

Patients and methods

A retrospective descriptive study was conducted, from 2014 to 2018 at Hebei General Hospital (Shijiazhang, China), on 98 patients with stage III–IV inoperable NSCLC diagnosed by biopsy. The basic information of patients (age, sex, height, weight, smoking history, etc.), clinicopathological features, immunohistochemical results, time of death, and final follow-up were all collected and summarized. NLR, lymphocyte to monocyte ratio (LMR), PLR, and ALI (ALI = BMI × ALB/NLR) were also recorded. According to published articles [12], the critical values of ALI and PLR were set at 18 and 185.

The inclusion criteria of the patients were as follows: (1) patients with a pathological diagnosis of inoperable, stage III–IV NSCLC; (2) no signs of infection or history of infectious diseases or diseases affecting inflammatory indicators, such as leukemia. The exclusion criteria were as follows: (1) presence of other malignant tumors; (2) patients with severe diseases in organs such as heart, brain, liver, and kidney, or presence of mental diseases; (3) patients with other pathological types of NSCLC such as squamous cell carcinoma and adenocarcinoma were excluded; (4) signs of infection at the initial diagnosis, history of diseases of the blood system affecting the inflammatory indicators, or recent intake of drugs affecting the inflammatory indicators; and (5) missing clinical data.

The use of clinical data (from the medical records as well as the paraffin-embedded sections) was approved by the hospital ethical committee, and consent was received from the patients' families for use of this data. The main reagent, rabbit anti-human Ki-67 monoclonal antibody, was purchased from Bioworld, USA. In using the mouse anti-human SP detection reagent, sections were routinely dewaxed to water, followed by antigen repair, incubation at room temperature, placement in 3% H_2O_2 for 15 min, and then mixing with the primary antibody in a dropwise manner and incubation at 4 °C overnight, based on the instructions on the kit. Phosphate buffer saline (PBS) was using for washing, and then horseradish peroxidase-labeled secondary antibody was added; the samples were incubated at room temperature for 30 min. This was followed by another round of PBS washing, and then DAB was added for color development. The samples were washed again and hematocrit redyeing was done. Subsequently, samples were dehydrated, made transparent, and sealed with a neutral resin adhesive. The final samples were observed under the microscope.

For the positive control, Ki-67 was used to select human breast cancer-positive tablets, while for the negative control, PBS was used in place of the primary antibody. After staining, all sections were assessed by pathologists and researchers in a double-blind manner.

Ki-67 positivity was demonstrated as brown-yellow granules in the nucleus, and a value < 5% was (–), 5%–25% was (+), 25%–50% was (++), > 50% was (+++). The (–) and (+) are defined as low expression, and (++) and (+++) as high expression.

Quality of life assessment: the Karnofsky performance status (KPS, in percentile) functional status score was used, which has a total score of 100 points. The higher the score, the better the physical condition. We divided the patients into two groups based on KPS as: KPS ≥ 90 and < 90.

Statistical analysis

The enumeration data were expressed as mean ± standard deviation. The relationship among ALI, PLR, and Ki-67 expression was evaluated by chi-square test. Kaplan-Meier analysis was used to estimate OS expression based on ALI, PLR, and Ki-67 expression in patients with stage III–IV NSCLC. Single-factor and Cox multivariate analysis were performed on the clinical data, and Spearman correlation analysis was performed on the three indicators.

Follow-up

The main endpoint assessed in this study was OS, that is, the time from diagnosis to death or the last follow-up. The patients were followed up by telephone and by their visits to the outpatient services. The patients were followed up every 3 months within 2 years after diagnosis, and every 6 months thereafter. The follow-up period started on August 2018.

Results

Patient characteristics

The clinical characteristics of the 98 patients are shown in Table 1. Among them, 63 were male and 35 were female, and they were aged 33–86 years [mean: (63.15 ± 10.19) years]. There were 52 cases with poorly differentiated tumors and 46 cases with highly differentiated tumors. There were 58 cases aged < 65 years, and 40 cases aged 65 years and older. Regarding risk factors, 60 cases had either adenocarcinoma or squamous cell carcinomas, 50 cases had a history of smoking, and 48 cases had no history of smoking. Regarding laboratory values, 47 cases had KPS ≥ 90, while 51 cases had KPS < 90; 25 cases had ALI < 18, while ALI > 18 in 73 patients; and finally PLR < 185 in 75 patients, while PLR > 185 in 23 patients. There was low expression of Ki-67 in 30 cases and high expression of Ki-67 in 68 cases. The median follow-up time was 16.6 months (1–64 months). At the end of the follow-up period, 48 patients died and 50 survived.

Table 1 Patient characteristics

	n (%)
Gender	
Male	63 (64.3)
Female	35 (35.7)
Age (years)	
< 65	58 (59.2)
≥ 65	40 (40.8)
Smoking history	
No	48 (49.0)
Yes	50 (51.0)
Differentiation	
Poorly differentiated	52 (53.1)
Medium and high differentiation	46 (46.9)
Pathological pattern	
Adenocarcinoma	60 (61.2)
Squamous cell carcinomas	38 (38.8)
KPS	
≥ 90	47 (48.0)
< 90	51 (52.0)
ALI	
High	73 (74.5)
Low	25 (25.5)
PLR	
High	23 (23.5)
Low	75 (76.5)
Ki-67 expression	
High	68 (69.4)
Low	30 (30.6)

Relationships among the ALI, PLR, expression cof Ki-67, and clinicopathological factors

Table 2 shows the relationship between ALI and clinicopathological factors. ALI had no significant relationship with any of the clinicopathological factors, except for differentiation ($P = 0.008$), gender ($P = 0.049$), and KPS score ($P = 0.005$). PLR had no significant relationship with any of the clinicopathological factors, except for differentiation ($P = 0.006$) and KPS score ($P = 0.016$). As seen in Table 3, Ki-67 expression was increased in men ($P = 0.001$), patients with a history of smoking ($P = 0.020$), patients with poorly differentiated tumors ($P = 0.007$), and patients with pathological squamous cell carcinomas ($P = 0.037$; Tables 2 and 3).

Survival analyses according to the ALI

The OS rate in the low ALI groups was significantly lower than that in the high-ALI group ($P < 0.0001$; Fig. 1). The OS rates for the high PLR group and the high Ki-67 expression group were significantly lower than that for the high ALI group ($P < 0.0001$, $P < 0.005$; Fig. 2 and 3).

Survival analyses according to the PLR

The OS rate of patients with a low PLR was significantly better than that of those with a high PLR (Fig. 2).

Table 2 Association among ALI, PLR, and clinical characteristics [*n* (%)]

	ALI		*P*	PLR		*P*
	High	Low		High	Low	
Gender			0.049			0.374
Male	51 (81.0)	12 (19.0)		13 (20.6)	50 (79.4)	
Female	22 (62.9)	13 (37.1)		10 (28.6)	25 (71.4)	
Age (years)			0.397			0.205
< 65	45 (77.6)	13 (22.4)		11 (19.0)	47 (81.0)	
≥ 65	28 (70.0)	12 (30.0)		12 (30.0)	28 (70.0)	
Smoking history			0.082			0.408
No	32 (66.7)	16 (33.3)		13 (27.1)	35 (72.9)	
Yes	41 (82.0)	9 (18.0)		10 (20.0)	40 (80.0)	
Differentiation			0.008			0.006
Poorly	33 (63.5)	19 (36.5)		18 (34.6)	34 (65.4)	
Medium and high	40 (87.0)	6 (13.0)		5 (10.9)	41 (89.1)	
Pathological			0.884			0.309
Adenocarcinoma	45 (25.0)	15 (75.0)		12 (20.0)	48 (80.0)	
Squamous cell carcinomas	28 (73.7)	10 (26.3)		11 (28.9)	27 (71.1)	
KPS			0.005			0.016
≥ 90	41 (87.2)	6 (12.8)		6 (12.8)	41 (87.2)	
< 90	32 (62.7)	19 (37.3)		17 (33.3)	34 (66.7)	
Ki-67 expression			0.743			0.205
High	50 (73.5)	18 (26.5)		20 (29.4)	48 (70.6)	
Low	23 (76.7)	7 (23.3)		3 (10.0)	27 (90.0)	

Survival analyses according to the expression of Ki-67

The OS rate of the high Ki-67 expression group was significantly lower than that of the low Ki-67 expression group ($P < 0.005$; Fig. 3).

Survival analyses according to combined assessment

We found a significant negative correlation between ALI and PLR; so we divided the patients into three groups: Group 1 had high ALI and low PLR, Group 2 had low ALI and high PLR, and Group 3 had either high ALI and high PLR or low ALI and low PLR. Among the 84 patients, there were 65, 17, and 16 patients classified into Groups 1, 2, and 3, respectively. The results showed that the total survival time of patients in the three groups was significantly different ($P < 0.001$). The median survival time (30 months vs. 10 months vs. 20 months) is shown in Fig. 4.

Prognostic factors influencing the OS

The correlations between OS and various clinicopathological factors are shown in Table 3. Univariate analysis showed that OS was significantly associated with age ($P < 0.001$), smoking history ($P = 0.009$), differentiation ($P < 0.001$), KPS score ($P < 0.001$), ALI ($P < 0.001$), PLR ($P < 0.001$), and Ki-67 expression ($P = 0.001$). A multivariate analysis of these significant variables indicated that the KPS score ($P = 0.040$), Ki-67 expression ($P = 0.008$), and ALI ($P = 0.048$) were independently associated with OS (Table 4).

Table 3 Relationship between Ki-67 and clinical characteristics [*n* (%)]

	Ki-67		*P*
	Low	High	
Gender			0.001
Male	12 (19.0)	51 (81.0)	
Female	18 (51.4)	17 (48.6)	
Age (years)			0.913
< 65	18 (31.0)	40 (69.0)	
≥ 65	12 (30.0)	28 (70.0)	
Smoking history			0.020
No	20 (41.7)	28 (58.3)	
Yes	10 (20.0)	40 (80.0)	
Differentiation			0.007
Poorly	9 (17.3)	43 (82.7)	
Medium and high	21 (45.7)	25 (54.3)	
Pathological			0.037
Adenocarcinoma	7 (18.4)	31 (81.6)	
Squamous cell carcinomas	23 (38.3)	37 (61.7)	
KPS			0.252
≥ 90	17 (36.2)	30 (63.8)	
< 90	13 (25.5)	38 (74.5)	

Correlation between expression of Ki-67, ALI, and PLR in NSCLC

Spearman correlation analysis results showed that ALI

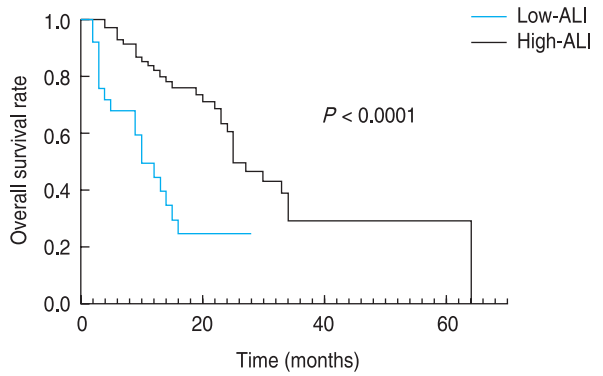

Fig. 1 Kaplan-Meier survival curves for the overall survival (OS) according to the advanced lung cancer inflammation index (ALI). A low ALI has a detrimental effect on the OS ($P < 0.0001$)

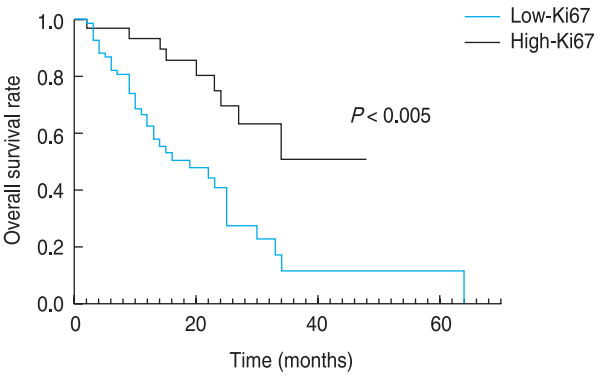

Fig. 3 Kaplan-Meier survival curves for the overall survival (OS) according to the expression of Ki-67. Low expression of Ki-67 has a detrimental effect on OS ($P < 0.005$).

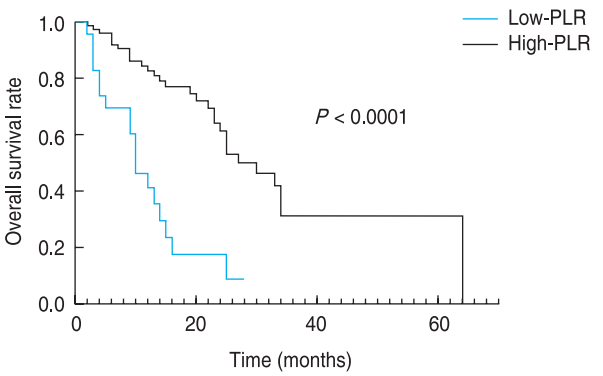

Fig. 2 Kaplan-Meier survival curves for the overall survival (OS) according to the platelet-lymphocyte ratio (PLR). The OS rate of patients with a low PLR was significantly better than that of those with a high PLR ($P < 0.0001$)

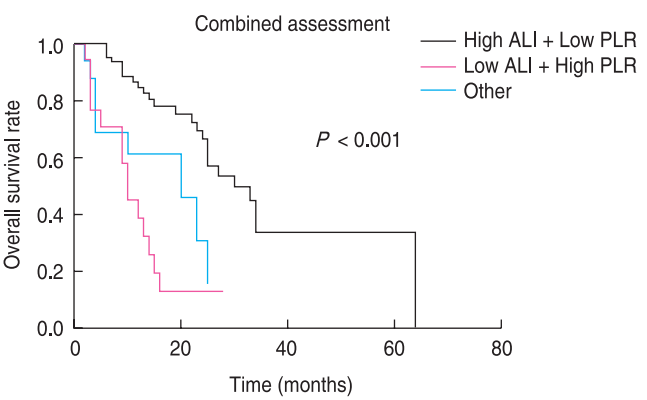

Fig. 4 Kaplan-Meier survival curves for the overall survival (OS) according to the combined assessment. A low ALI and high PLR have a significant lydetrimental effect on the OS ($P < 0.001$).

value was negatively correlated with PLR ($r_s = -0.615$, $P < 0.05$), and PLR was positively correlated with Ki-67 expression ($r_s = 0.211$, $P < 0.05$). There was no significant correlation between ALI and Ki-67 expression (Table 5).

Discussion

In recent years, the association between systemic inflammation and cancer has been extensively studied. Epidemiological observations have shown that inflammatory markers are evident in the tumor

Table 4 The correlations between the overall survival (OS) and various clinicopathological factors by univariate and multivariate analysis

	Univariate analysis		*P*	Multivariate analysis		*P*
	Hazard ratio	95% CI		Hazard ratio	95% CI	
Gender	1.388	0.761–2.530	0.285	–	–	–
Age	1.441	0.810–2.566	0.214	–	–	–
Smoking history	2.190	1.199–4.000	0.011	1.601	0.860–2.979	0.138
Differentiation	0.325	0.169–0.627	0.001	0.574	0.279–1.181	0.131
Pathological pattern	1.416	0.798–2.542	0.243	–	–	–
KPS	3.109	1.662–5.815	0.000	2.074	1.033–4.161	0.040
Ki-67 expression	3.387	1.622–7.072	0.001	3.023	1.342–6.813	0.008
ALI	0.291	0.155–0.546	0.000	0.380	0.145–0.991	0.048
PLR	4.142	2.240–7.660	0.000	1.253	0.487–3.224	0.640

Table 5 Correlation between expression of Ki-67, ALI, and PLR in NSCLC

		Ki-67	ALI	PLR
Ki-67	r_s	–	–0.033	0.211
	P	–	0.746	0.037
ALI	r_s	–0.033	–	–0.615
	P	0.746	–	0.000
PLR	r_s	0.211	–0.615	–
	P	0.037	0.000	–

microenvironment, and tumors often form at sites of chronic inflammation [13]. Recent studies have also shown a clear relationship between markers of systemic inflammatory response and poor prognosis in patients with tumors [14–16]. More specifically, our study also confirmed an independent prognostic factor – ALI – in NSCLC, but its mechanism is still unclear.

ALI is a systemic inflammatory indicator based on BMI, ALB, and NLR. In this study, the median survival time of patients in the low ALI group (10 months, 2–28 months) was significantly lower than that in the high ALI group (25 months, 1–64 months). We can hypothesize that low ALI as low BMI, low ALB, and high NLR.

BMI is a common nutritional indicator. BMI levels can vary depending on health and disease status or in obese and non-obese people and can even aid indistinguishing health status and malnutrition. Therefore, BMI is important for assessing cancer progression. Gu *et al* [17] confirmed that the survival rate of patients with high BMI before treatment or no reduction in BMI during treatment could be prolonged. ALB accounts for about half of the serum protein and is involved in scavenging free radicals, maintaining colloid osmotic pressure, and protecting nerve cells, and it is also closely related to nutritional status and systemic inflammatory response. In recent years, it has been reported that hypoalbuminemia is mainly found in tumor patients and is considered as a prognostic marker of human cancers, such as endometrial cancer, gastrointestinal tumors, and even lung cancer [18–20].

The NLR is an early indicator of systemic inflammation and has been reported to have a significant impact on the prognosis of tumors [21–22]. High NLR represents an increase in neutrophil count and/or a decrease in lymphocyte count as well as a relative decrease in lymphocytes. Lymphocytes play a crucial role in tumor defense by inducing cytotoxic cell death and inhibiting tumor cell proliferation and migration [23].

ALI is an easy assessment to evaluate systemic inflammation in patients [24]. It has been reported to be a better predictor of cancer survival than any single indicator; ALI can be seen as a simple, inexpensive, and useful biomarker in clinical practice. In a study by Mandaliya *et al* [25], ALI was regarded as a meaningful biomarker in elderly patients with stage IV NSCLC. The current study sought to find evidence of ALI as a meaningful clinical indicator. In this study, ALI was also closely related to the degree of differentiation in patients with NSCLC. That is, with poor differentiation, ALI is higher, which is similar to the results of Feng *et al* [26]. In theory, ALI could indicate both nutritional status and inflammatory response, providing guidance on how patients should be treated. In our study, ALI showed great potential as a prognostic indicator. Given the low cost of these markers and the availability of results of the same in pre-treatment evaluation, they can be easily used for routine clinical identification of high-risk patients. ALI is a reliable, objective, and inexpensive evaluation indicator for patients with NSCLC and can be considered for routine clinical use.

PLR has also received extensive attention as an inflammatory indicator, and activation of the coagulation system is often associated with tumor metastasis, invasion, and poor prognosis. Thrombus formation is a problem that tumor patients often face. There is evidence that [27] high platelet count is associated with a low survival rate in patients with lung cancer. It has been reported [28] that in addition to their role in hemostasis, platelets are increasingly recognized as regulators of inflammation. This influences the inflammatory response of cancer by affecting the activation state of endothelial cells and recruiting white blood cells to the sites of primary and metastatic tumors and to distant organs not affected by tumor growth as yet. In addition, platelets are involved in the formation of neutrophil extracellular traps, which can promote metastasis and thrombosis, and lead to organ failure. Tumor growth depends on blood vessels, and platelets contain platelet-derived cytokines that play a role in tumor angiogenesis, such as vascular endothelial growth factor (VEGF) and platelet-derived growth factor (PDGF). Similarly, lymphocytopenia has been shown to predict poor prognosis in patients with advanced cancer [29]. This may be due to its role in mediating tumor cell destruction and inhibiting tumor growth. T cells in the tumor microenvironment may secrete cytokines such as IL-4 and IL-5 to regulate the proliferation, apoptosis, angiogenesis, and metastasis of cancer cells [30]. A cohort study with a large sample size by Ding *et al* [31] showed that PLR can be used as a representative indicator of systemic inflammation. They also showed that a PLR threshold of 150–200 is more significant than a PLR threshold of > 200. The critical value used in the current study was 185; thus, we can consider our results as being more reliable. Similarly, in our statistical analysis, we concluded that low PLR was associated with improved survival (median survival was 27 months vs. 10 months) and is an independent prognostic factor for NSCLC. This

study shows that patients with high levels of PLR have poorly differentiated tumors, which is similar to the findings of Messager *et al* [32]. In addition, recent studies have reported that low molecular weight heparin, aspirin, and other drugs have anti-tumor effects [33–35]. Therefore, in addition to considering PLR as a prognostic predictor for patients with inoperable stage III–IV NSCLC, we can also expect anticoagulation as a new antitumor therapy in the future.

Ki-67 is a widely used proliferation-related indicator related to the development, metastasis, and prognosis of a variety of tumors [36]. Except for the G0 phase of the cell cycle, Ki-67 can be detected in every mitotic phase, especially in the M phase, which can directly and sensitively reflect the proliferation activity of tumor cells and more comprehensively reflect the number of proliferating cells [37]. It has been reported that the higher the Ki-67 proliferation index, the lower the degree of tumor differentiation; this is useful since the tumor proliferation capacity often represents the malignancy of the tumor [38]. This study confirmed that in NSCLC tissues, the factors included gender, smoking status and pathological type, and there were significant differences in Ki-67 expression, and the differences were statistically significant ($P < 0.05$). Survival analysis showed that the survival time of patients with high Ki-67 expression was significantly lower than that of patients with low Ki-67 expression ($P < 0.01$). Univariate and Cox multivariate results showed that Ki-67 expression level was an independent prognostic factor in patients with stage III–IV inoperable NSCLC, and the difference was statistically significant ($P < 0.05$). The results were similar to those of Ji *et al* [39].

Pearson's correlation analysis was conducted to identify whether there was a connection between ALI, PLR, and Ki-67. Results showed that ALI was negatively correlated with PLR ($r_s = –0.615$, $P < 0.001$), while ALI and Ki-67 had no correlation ($P > 0.05$). However, Ki-67 had a weak positive correlation with PLR ($r_s = 0.211$, $P < 0.05$). Very little research has been done on the relationship between the three afore mentioned factors. Platelets involved in the formation of neutrophiltraps can be used to regulate inflammatory factors, while Ki-67 is a cell proliferation factor, and inflammation is involved in the process of cell proliferation. Given this link, perhaps ALI is associated with PLR and Ki-67. However, the mechanism behind this association is still unknown and requires further research and exploration. However, in terms of detection methods, compared with Ki-67, inflammatory markers in the peripheral blood are more easily assessed than immunohistochemical indicators.

In the study by Zhuang *et al* [40], the important role of clinicians in determining which patients will receive follow-up treatment and which will receive palliative care is emphasized. In fact, the clinician is the one who assesses the quality of life and decides on the antitumor medication regimen. Therefore, they need an appropriate prognostic indicator that will help them predict patient response and the value of antitumor therapy [41].

Our study had several limitations. First, the number of patients included was small, although the study population was histologically uniform. Second, the optimal cutoff values of ALI and PLR have not yet been determined. We determined the optimal cutoff value by reading a large number of studies; however, there are bound to be deviations in prior studies that could have affected this. Furthermore, our conclusions are limited by the retrospective nature of the study. This indicators discussed herein may be influenced by other factors, such as infection or cancer-related complications, and prospective studies with a large sample size are needed to confirm our study.

To the best of our knowledge, this is the first study to compare inflammatory markers and immunohistochemic al indicators. We conclude that ALL, PLR, and Ki-67 are some of the most important prognostic factors in stage III–IV inoperable NSCLC patients. In particular, we observed that ALI is not only an independent prognostic indicator, but, compared with PLR, seems to provide a more precise, comprehensive evaluation index in terms of its ability to predict survival in patients with NSCLC. In addition, ALI is easier to obtain than the Ki-67 values and can be easily applied in clinical practice. Statistically, ALI and PLR have a significant negative correlation. By combining ALI and PLR before treatment, we found that patients with low ALI and high PLR had a worse prognosis. In the future, we may combine these two indicators to improve the accuracy of prognosis prediction. Further prospective studies will help to confirm our findings.

Conflicts of interest

The authors indicated no potential conflicts of interest.

References

1. Siegel RL, Miller KD, Jemal A. Cancer statistics, 2020. CA Cancer J Clin, 2020, 70: 7–30.
2. Korniluk A, Koper O, Kemona H, *et al*. From inflammation to cancer. Ir J Med Sci, 2017, 186: 57–62.
3. Rogovskii VS. The linkage between inflammation and immune tolerance: interfering with inflammation in cancer. Curr Cancer Drug Targets, 2017, 17: 325–332.
4. Hong TT, Shen D, Chen XP, *et al*. Preoperative plasma fibrinogen, but not D-dimer might represent a prognostic factor in non-metastatic colorectal cancer: A prospective cohort study. Cancer Biomarker, 2017, 19: 103–111.
5. Schwartz PB, Poultsides G, Roggin K, *et al*. PLR and NLR are poor predictors of survival outcomes in sarcomas: a new perspective from the USSC. J Surg Res, 2020, 251: 228–238.

6. Quan XY. The combined prognostic value of pretreatment neutrophil-to-lymphocyte ratio, lymphocyte-to-monocyte ratio, and platelet-to-lymphocyte ratio in stage IE/IIE extranodal natural killer/T-cell lymphoma. Oncol Transl Med, 2019, 5: 137–146.
7. Yu QQ, Qiu H, Zhang MS, *et al*. Prognostic value of neutrophil-to-lymphocyte ratio in metastatic colorectal cancer. Oncol Transl Med, 2016, 2: 75–79.
8. Jafri SH, Shi RH, Mills G. Advance lung cancer inflammation index (ALI) at diagnosis is a prognostic marker in patients with metastatic non-small cell lung cancer (NSCLC): a retrospective review. BMC Cancer, 2013, 13: 158.
9. Herzog BH, Fu JX, Wilson SJ, *et al*. Podoplanin maintains high endothelial venule integrity by interacting with platelet CLEC-2. Nature, 2013, 502: 105–109.
10. Ahn HK, Jung M, Ha SY, *et al*. Clinical significance of Ki-67 and p53 expression in curatively resected non-small cell lung cancer. Tumour Biol, 2014, 35: 5735–5740.
11. Wen S, Zhou W, Li CM, *et al*. Ki-67 as a prognostic marker in early-stage non-small cell lung cancer in Asian patients: a meta-analysis of published studies involving 32 studies. BMC Cancer, 2015, 15: 520.
12. Komurcuoglu B, Evkan A, Karakurt G. Are pretreatment neutrophil-lymphocyte ratio (NLR), platelet-lymphocyte ratio (PLR) and advanced lung cancer inflamation index (ALI) levels useful in predicting the outcomes of patients with advanced non-small cell lung cancer? J Thorac Oncol, 2018, 13: 113–114.
13. Balkwill F, Mantovani A. Inflammation and cancer: back to Virchow? Lancet, 2001, 357: 539–545.
14. Ozyurek BA, Ozdemirel TS, Ozden SB, *et al*. Does advanced lung inflammation index (ALI) have prognostic significance in metastatic non-small cell lung cancer? Clin Respir J, 2018, 12: 2013–2019.
15. He XB, Zhou T, Yang YP, *et al*. Advanced lung cancer inflammation index, a new prognostic score, predicts outcome in patients with small-cell lung cancer. Clin Lung Cancer, 2015, 16: e165–e171.
16. Jank BJ, Kadletz L, Schnöll J, *et al*. Prognostic value of advanced lung cancer inflammation index in head and neck squamous cell carcinoma. Eur Arch Otorhinolaryngol, 2019, 276: 1487–1492.
17. Gu WS, Fang WZ, Liu CY, *et al*. Prognostic significance of combined pretreatment body mass index (BMI) and BMI loss in patients with esophageal cancer. Cancer Manag Res, 2019, 11: 3029–3041.
18. Lei J, Wang Y, Guo XQ, *et al*. Low preoperative serum ALB level is independently associated with poor overall survival in endometrial cancer patients. Future Oncol, 2020, 16: 307–316.
19. Shibutani M, Maeda K, Nagahara H, *et al*. Prognostic significance of the preoperative ratio of C-reactive protein to albumin in patients with colorectal cancer. Anticancer Res, 2016, 36: 995–1001.
20. Ni XF, Wu J, Ji M, *et al*. Effect of C-reactive protein/albumin ratio on prognosis in advanced non–small-cell lung cancer. Asia Pac J Clin Oncol, 2018, 14: 402–409.
21. Ozyurek BA, Ozdemirel TS, Ozden SB, *et al*. Prognostic value of the neutrophil to lymphocyte ratio (NLR) in lung cancer cases. Asia Pac J Cancer Prev, 2017, 18: 1417–1421.
22. Brkic FF, Kadletz L, Jank B, *et al*. Impact of pretherapeutic neutrophil-to-lymphocyte ratio, serum albumin, body-mass index, and advanced lung cancer inflammation index on clinical outcome in sinonasal squamous cell carcinoma. J Craniomaxillofac Surg, 2020, 48: 33–37.
23. Tan TT, Coussens LM. Humoral immunity, inflammation and cancer. Curr Opin Immunol, 2007, 19: 209–216.
24. Starnes SL, Pathrose P, Wang J, *et al*. Clinical and molecular predictors of recurrence in stage I non-small cell lung cancer. Ann Thorac Surg, 2012, 93: 1606–1612.
25. Mandaliya H, Jones M, Oldmeadow C, *et al*. Prognostic biomarkers in stage IV non-small cell lung cancer (NSCLC): neutrophil to lymphocyte ratio (NLR), lymphocyte to monocyte ratio (LMR), platelet to lymphocyte ratio (PLR) and advanced lung cancer inflammation index (ALI). Transl Lung Cancer Res, 2019, 8: 886–894.
26. Feng JF, Huang Y, Chen QX. A new inflammation index is useful for patients with esophageal squamous cell carcinoma. Onco Targets Ther, 2014, 7: 1811–1815.
27. Wen JH, Yang YN, Ye F, *et al*. The preoperative plasma fibrinogen level is an independent prognostic factor for overall survival of breast cancer patients who underwent surgical treatment. Breast, 2015, 24: 745–750.
28. Olsson AK, Cedervall J. The pro-inflammatory role of platelets in cancer. Platelets, 2018, 29: 569–573.
29. Lissoni P, Brivio F, Fumagalli L, *et al*. Efficacy of cancer chemotherapy in relation to the pretreatment number of lymphocytes in patients with metastatic solid tumors. Int J Biol Markers, 2004, 19: 135–140.
30. Hiraoka K, Miyamoto M, Cho Y, *et al*. Concurrent infiltration by CD8+ T cells and CD4+ T cells is a favourable prognostic factor in non-small-cell lung carcinoma. Br J Cancer, 2006, 94: 275–280.
31. Ding N, Pang ZF, Shen HC, *et al*. The prognostic value of PLR in lung cancer, a meta-analysis based on results from a large consecutive cohort. Sci Rep, 2016, 6: 34823.
32. Messager M, Neofytou K, Chaudry MA, *et al*. Prognostic impact of preoperative platelets to lymphocytes ratio (PLR) on survival for oesophageal and junctional carcinoma treated with neoadjuvant chemotherapy: A retrospective monocentric study on 153 patients. Eur J Surg Oncol, 2015, 41: 1316–1323.
33. Sheng LM, Luo M, Sun XJ, *et al*. Serum fibrinogen is an independent prognostic factor in operable nonsmall cell lung cancer. Int J Cancer, 2013, 133: 2720–2725.
34. Santilli F, Boccatonda A, Davì G. Aspirin, platelets, and cancer: The point of view of the internist. Eur J Intern Med, 2016, 34: 11–20.
35. Elaskalani O, Berndt MC, Falasca M, *et al*. Targeting platelets for the treatment of cancer. Cancers (Basel), 2017, 9: 94.
36. Sun GY, Wang SY, Wang Y. Expressions of Topo IIα and Ki-67 in breast cancer and its clinicopathologic features and prognosis. Pak J Med Sci, 2019, 35: 715–720.
37. Antonarakis ES, Keizman D, Zhang Z, *et al*. An immunohistochemical signature comprising PTEN, MYC, and Ki-67 predicts progression in prostate cancer patients receiving adjuvant docetaxel after prostatectomy. Cancer, 2012, 118: 6063–6071.
38. Zheng Y, Wang L, Zhang JP, *et al*. Expression of p53, c-erbB-2 and Ki-67 in intestinal metaplasia and gastric carcinoma. World J Gastroenterol, 2010, 16: 339–344.
39. Ji Y, Zheng MF, Ye SG, *et al*. PTEN and Ki-67 expression is associated with clinicopathologic features of non-small cell lung cancer. J Biomed Res, 2014, 28: 462–467.
40. Zhuang H, Ma Y, Wang L, *et al*. Effect of early palliative care on quality of life in patients with non-small-cell lung cancer. Curr Oncol, 2018, 25: e54–e58.
41. Zhou T, Zhao YY, Zhao S, *et al*. Comparison of the prognostic value of systemic inflammation response markers in small cell lung cancer patients. J Cancer, 2019, 10: 1685–1692.

DOI 10.1007/s10330-020-0441-1
Cite this article as: Li Y, Li QF, He YLQ, *et al*. The prognostic significance of ALI, PLR, and Ki-67 expression in stage III–IV inoperable non-small cell lung cancer. Oncol Transl Med, 2021, 7: 7–14.

Oncology and Translational Medicine
DOI 10.1007/s10330-020-0449-9

February 2021, Vol. 7, No. 1, P15–P19

ORIGINAL ARTICLE

Expression of PD-1/PD-L1 in lung adenocarcinoma and its clinical significance*

Jian Li (✉), Yimin Chen

Department of Respiration, Emeishan People's Hospital, Emeishan 614200, China

Abstract

Objective This study aimed to investigate PD-1/PD-L1 expression in lung adenocarcinoma and its relationship with EGFR/KRAS mutation.

Methods The expression levels of PD-1 and PD-L1 in lung adenocarcinoma were detected. Clinicopathological parameters were collected and followed up. The effects of PD-1 and PD-L1 expression on clinicopathological parameters and prognosis of patients with lung adenocarcinoma were statistically analyzed.

Results PD-L1 and PD-1 were mainly located in the membrane and cytoplasm of tumor cells. The positive expression rates of PD-1 and PD-L1 were 53% and 40%, respectively. Positive PD-1 expression had a significant effect on the incidence of KRAS mutation ($P < 0.05$), while PD-L1 expression significantly affected the incidence of EGFR mutation ($P < 0.05$). Overexpression of PD-1 and PD-L1 had a significant negative effect on disease-free survival (DFS) in patients with lung adenocarcinoma ($P<0.05$) but had no significant effect on overall survival ($P > 0.05$). EGFR gene mutation, high PD-1 expression, high PD-L1 expression, N stage, and AJCC stage were independent risk factors of DFS ($P < 0.05$).

Conclusion High PD-1/PD-L1 expression is closely related to the occurrence of lung adenocarcinoma and can be used as an independent factor to assess the prognosis of patients with lung adenocarcinoma. There were negative correlations between PD-L1 expression and EGFR mutation and between PD-1 expression and KRAS mutation.

Received: 9 August 2020
Revised: 15 September 2020
Accepted: 17 October 2020

Key words: lung adenocarcinoma; PD-1; PD-L1; gene mutation

Lung cancer is the most common malignant tumor and the leading cause of cancer-related death worldwide. In China, lung cancer also ranks first in incidence and mortality rates [1]. Non-small-cell lung cancer (NSCLC) accounts for 80%–85% of all lung cancer cases. Although the chemotherapy regimen has achieved great progress in recent decades, platinum-based chemotherapy has an effective rate of 20%–35% and provides only 8–12 months median survival [2–3]. NSCLC is a disease characterized by molecular subgroups with driver mutations. The two most important driver genes are EGFR and KRAS. About 35% of East Asian patients have tumor-associated EGFR mutations [4], and approximately 50%–65% of EGFR mutations respond to EGFR tyrosine kinase inhibitors. Cancer immunotherapy achieved an important breakthrough with the discovery of "immune checkpoints," including programmed cell death protein 1 (PD-1) and programmed death-ligand 1 (PD-L1) [5]. It is unclear whether specific genomic subsets of NSCLC use the PD-1/PD-L1 pathway to achieve immune escape. The correlation between EGFR/KRAS mutation and PD-1/PD-L1 has been reported, but the results vary. Therefore, this study aimed to explore the clinical significance of PD-1/PD-L1 expression in lung cancer and its correlation with mutated EGFR and KRAS to provide additional potential targets for individualized immunotherapy of lung cancer patients.

✉ Correspondence to: Jian Li. Email: zhongzhonglw199@aliyun.com
* Supported by a grant from the Sichuan Health Appropriate Technology Promotion Project (No. 2017yz-00158).

Materials and methods

Subjects and clinical data collection

Patients with lung adenocarcinoma admitted to the cardiothoracic surgery department of our hospital from February 2014 to December 2017 were selected as the research subjects. Inclusion criteria: (1) All patients were diagnosed with lung adenocarcinoma after operation. (2) Patients were at first diagnosis and treatment. (3) Surgical resection was performed. (4) The clinical data and follow-up data were complete. Exclusion criteria: (1) Death occurred in hospital or within 30 days after discharge. (2) The follow-up compliance was poor. Finally, 100 patients were included in the study, comprising 51 males and 49 females with average ages of 57.1 ± 14.3 and 55.2 ± 12.2 years, respectively. Clinical data including age, gender, T stage, N stage, and AJCC stage were collected in the electronic medical record system.

Immunohistochemical staining

A representative tumor region was carefully selected from a section stained with hematoxylin and eosin. After dewaxing in xylene and gradient ethanol, the antigen was heat repaired, the endogenous peroxidase was blocked by 0.3% hydrogen peroxide, and nonspecific binding was blocked by serum incubation. The sections were incubated with anti-PD-L1 antibody and anti-PD-1 antibody for 24 h. The biotin-labeled secondary antibody and horseradish peroxidase-labeled avidin were incubated with the samples and stained using the DAB method. Two doctors independently evaluated the patients' sections. The staining intensity was randomly divided into 4 grades: 0 (no staining), 1 (weak staining), 2 (moderate staining), and 3 (strong staining). The percentage of positive cells was 0 (0%), 1 (1%–30%), 2 (31%–50%), and 3 (> 50%). The formula of positive staining is: total integral = positive percentage fraction × intensity fraction. A score of 0–2 was negative and > 2 was positive.

Follow up

All patients were followed up by outpatient visits or telephone for every 3 months in the first year and every 6 months from the second year until the patients died or the study ended. Overall survival (OS) was defined as the time from the date of surgery to death or the last follow-up, and disease-free survival (DFS) was defined as the time from the beginning of randomization to recurrence or (for any reason) death. Postoperative recurrence was diagnosed by imaging. All subjects provided informed consent for this study.

Statistical analysis

All data were analyzed by SPSS 20.0. The counting data were expressed by case number and the chi-square test. The Kaplan-Meier method and log rank test were used to analyze the survival rate. Factors showing statistically significant differences in univariate survival analysis were included in Cox regression for multivariate analysis. $P < 0.05$ was considered as statistically significant.

Results

EGFR and KRAS mutations in lung adenocarcinoma

In total, 100 patients (51 males and 49 females) with primary lung adenocarcinoma were selected. EGFR mutation was found in 60 cases (60%), and KRAS mutation in 10 cases (10%). Among cases with EGFR mutations, 19 had mutations in exon 21, 5 in exons 21/20, 3 in exons 21/19, 2 in exons 21/20/19, 2 in exons 21/18, 27 in exon 19, and 2 in exons 20/18. Among KRAS mutations, there were 4 mutations in codon 1, 1 in codon 4, 3 in codon 5, 1 in codon 6, and 1 in codon 7.

PD-1/PD-L1 immunohistochemical staining

Immunohistochemical analysis showed that the expression of PD-L1 and PD-L2 was mainly located in the cell membrane and cytoplasm of tumor cells. The positive expression rates of PD-1 and PD-L1 were 53% and 40%, respectively (Fig. 1).

Relationships between the expression of PD-1/PD-L1 and clinicopathological features

The chi-square test showed that positive PD-1 expression had a significant impact on the incidence of KRAS mutation ($P < 0.05$), and PD-L1 expression significantly influenced the incidence of EGFR mutation ($P < 0.05$). However, the expression of PD-1/PD-L1 had

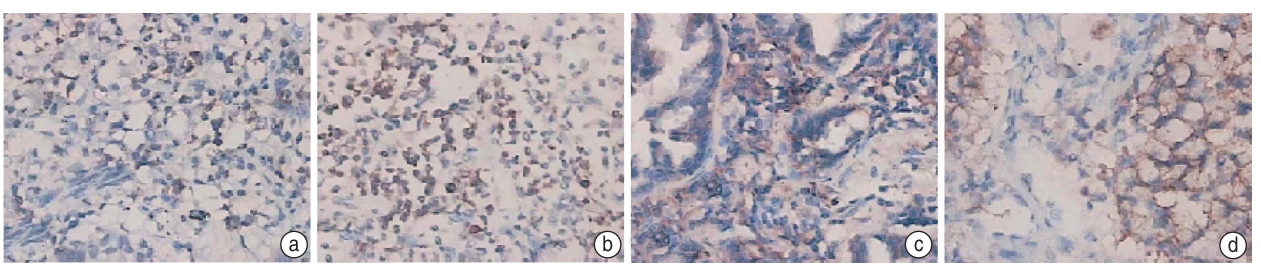

Fig. 1 Immunohistochemical staining of PD-1 / PD-L1

Table 1 Relationship between expression of PD-1 / PD-L1 and clinicopathological features

Indicators	PD-1 (–) (*n* = 47)	PD-1 (+) (*n* = 53)	χ^2	*P*	PD-1 (–) (*n* = 60)	PD-1 (+) (*n* = 40)	χ^2	*P*
Age (years)			0.117	0.732			0.168	0.682
< 60	22	23			28	17		
≥ 60	25	30			32	23		
Gender			0.662	0.416			3.528	0.060
Male	26	25			26	25		
Female	21	28			34	15		
History of smoking			0.661	0.416			0.035	0.852
No	33	41			44	30		
Yes	14	12			16	10		
EGFR mutations			1.311	0.252			6.250	0.012
No	16	24			18	22		
Yes	31	29			42	18		
KRAS mutations			4.857	0.028			0.463	0.496
No	39	51			55	35		
Yes	8	2			5	5		
PD-1 expression							0.107	0.744
Low	–	–			29	18		
High	–	–			31	22		
PD-L1 expression			0.107	0.744				
Low	29	31			–	–		
High	18	22			–	–		
T stage			0.479	0.489			1.891	0.169
T1–2	45	49			58	36		
T3–4	2	4			2	4		
N stage			0.133	0.715			1.311	0.252
N0	23	24			31	16		
> N0	24	29			29	24		
AJCC stage			1.655	0.437			0.662	0.718
I	20	22			26	16		
II	15	12			16	11		
III	12	19			28	13		

Table 2 Relationship between expression of PD-1 / PD-L1 and clinicopathological features

Indicators	β	SE	Wald	*P*	HR	95%CI
No EGFR mutations	0.867	0.325	7.138	0.008	2.553	1.262–4.503
PD-1 high expression	1.276	0.588	4.746	0.029	3.575	1.022–11.910
PD-L1 high expression	0.262	0.264	1.117	0.040	1.311	0.768–1.894
T stage	–0.594	0.352	2.935	0.084	0.548	0.274–1.092
N stage	–1.573	0.187	77.633	0.003	0.330	0.103–0.598
AJCC stage	–0.451	0.283	2.592	0.032	0.631	0.362–1.125

no significant effect on T, N, and AJCC stages ($P > 0.05$; Table 1).

Effect of PD-1/PD-L1 expression on the OS rate of patients

Kaplan-Meier survival analysis showed that overexpression of PD-1 and PD-L1 had a significant negative effect on DFS in patients with lung adenocarcinoma ($\chi^2 = 14.52$, $P < 0.05$; $\chi^2 = 7.54$, $P < 0.05$), but had no significant effect on OS ($\chi^2 = 2.74$, $P = 0.152$; $\chi^2 = 1.63$, $P = 0.405$; Fig. 2).

Cox multivariate analysis

Cox multivariate analysis showed that EGFR gene mutation, high PD-1 expression, high PD-L1 expression, N stage, and AJCC stage were independent risk factors of DFS ($P < 0.05$) (Table 2).

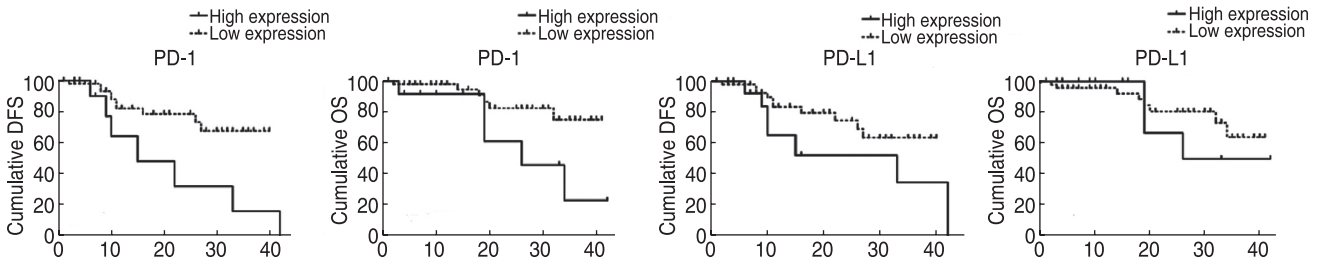

Fig. 2 Effect of PD-1 / PD-L1 expression on overall survival rate of patients

Discussion

PD-1 and its ligand, PD-L1, are immune checkpoints for cancer cells to escape destruction by T cells. PD-1 encoded by the PDCD1 gene interacts with PD-L1 to inhibit T cell activation and render immune surveillance ineffective. Accumulating evidence from experimental studies and clinical trials has shown that PD-1/PD-L1 receptor blockers exhibit good potential for application in the treatment of respiratory cancer. In a multicenter clinical trial of patients with PD-L1-positive advanced gastric cancer, the anti-PD-1 antibody pembrolizumab revealed an acceptable toxicity level and strong anti-tumor effect [6]. In another study, IFN-γ increased PD-1 expression in tumor cells through JAK signal transduction and activation of transcription pathways [7]. PD-1 and PD-L1 block immunotherapy as an effective means of treatment of various types of cancer, including lung cancer in patients with various clinical characteristics. However, currently, the specific regulatory mechanism of this new immune pathway remains unclear. Therefore, we systematically studied the expression of PD-1 and PD-L1 in lung cancer tissues to explore its relationship with the clinical parameters and survival time of lung cancer.

The frequency of EGFR mutation is highest in the East Asian population, ranging from 36.4% to 66.3% in lung adenocarcinoma [8,9]. The mutation frequency of KRAS varies from 2.3% to 9.4% in East Asia [10]. EGFR is overexpressed in about 40%–80% of NSCLC cases, and its expression level is related to the mutation of the EGFR tyrosine kinase domain. KRAS mutation is found in about 30% of lung adenocarcinoma cases but is rare in squamous cell carcinoma [11]. In this study, we found that PD-1 and PDL1 expression varied with the characteristics of patients. The expression level of PD-1 in patients without EGFR and KRAS mutations was higher than that in patients with these mutations. Current clinical studies have shown that blocking the PD-1/PD-L1 immune checkpoint can prolong the progression-free survival of NSCLC cancer patients; moreover, it is also the only new treatment option that has improved the prognosis of lung cancer patients in the past ten years. The PD-1 pathway plays an important role in inhibiting cytotoxic immune response [12]. However, not all lung cancer patients respond to the targeted therapy of these immunosuppressive checkpoints. In this sense, the clinicopathological characteristics of NSCLC patients, the changes in these inhibitory pathways, and the expected therapeutic response to these drugs are still worth further exploration. This study also found that overexpression of PD-1 and PD-L1 had a significant negative effect on DFS in patients with lung adenocarcinoma. Further Cox multivariate analysis showed that EGFR gene mutation, high PD-1 expression, high PD-L1 expression, N stage, and AJCC stage were independent risk factors for DFS. However, no correlation was found between smoking status and high PD-1/PD-L1 expression, which may be due to the relatively small sample size and sample bias.

In conclusion, this study found that the high expression of PD-1/PD-L1 is closely related to the occurrence of lung adenocarcinoma and can be used as an independent factor to assess the prognosis of patients with lung adenocarcinoma. There were negative correlations between PD-L1 expression and EGFR mutation and between PD-1 expression and KRAS mutation. These findings may provide new insights for improving the immunotherapy of PD-1/PD-L1/PD-L2 in patients with lung cancer.

References

1. Feng WN, Gu WQ, Zhao N, *et al*. Comparison of the SuperARMS and droplet digital PCR for detecting EGFR mutation in ctDNA from NSCLC patients. Transl Oncol, 2018, 11: 542–545.
2. Planchard D, Boyer M, Lee JS, *et al*. 1280 Osimertinib vs standard of care (SoC) EGFR-TKI as first-line therapy in patients (pts) with untreated EGFRm advanced NSCLC: FLAURA post-progression outcomes. J Thoracic Oncol, 2018, 13: S72–S73.
3. Wei CC, Nie FQ, Jiang LL, *et al*. The pseudogene DUXAP10 promotes an aggressive phenotype through binding with LSD1 and repressing LATS2 and RRAD in non small cell lung cancer. Oncotarget, 2017, 17, 8: 5233–5246.
4. Ito M, Codony-Servat C, Codony-Servat J, *et al*. 25P A non-pathway-specific approach in EGFR and KRAS mutant or squamous cell histology non-small cell lung cancer (NSCLC). Tumor Biol Pathol, 2018, 13: S13–S14.
5. Zarredar H, Ansarin K, Baradaran B, *et al*. Potential molecular targets

in the treatment of lung cancer using siRNA technology. Cancer Invest, 2018, 36: 37–58.
6. Muro K, Chung HC, Shankaran V, *et al*. Pembrolizumab for patients with PD-L1-positive advanced gastric cancer (KEYNOTE-012): a multicentre, open-label, phase 1b trial. Lancet Oncol, 2016, 17: 717–726.
7. Mimura K, Teh JL, Okayama H, *et al*. PD-L1 expression is mainly regulated by interferon gamma associated with JAK-STAT pathway in gastric cancer. Cancer Sci, 2018, 109: 43–53.
8. Castellanos E, Feld E, Horn L. Driven by mutations: The predictive value of mutation subtype in EGFR-mutated non-small cell lung Cancer. J Thorac Oncol, 2017, 12: 612–623.
9. Leduc C, Merlio JP, Besse B, *et al*. Clinical and molecular characteristics of non-small-cell lung cancer (NSCLC) harboring EGFR mutation: results of the nationwide French Cooperative Thoracic Intergroup (IFCT) program. Ann Oncol, 2017, 28: 2715–2724.
10. Park S, Kim JY, Lee SH, *et al*. KRAS G12C mutation as a poor prognostic marker of pemetrexed treatment in non-small cell lung cancer. Korean J Intern Med, 2017, 32: 514–522.
11. Liu L, Wei S. Research progress of KRAS mutation in non-small cell lung cancer. Chin J Lung Cancer, 2018, 21: 419–424.
12. Lin ZY, Gu JC, Cui XX, *et al*. Deciphering microenvironment of NSCLC based on CD8+ TIL density and PD-1/PD-L1 expression. J Cancer, 2019, 10: 211–222.

DOI 10.1007/s10330-020-0449-9
Cite this article as: Li J, Chen YM. Expression of PD-1/PD-L1 in lung adenocarcinoma and its clinical significance. Oncol Transl Med, 2021, 7: 15–19.

Oncology and Translational Medicine
DOI 10.1007/s10330-020-0427-7

February 2021, Vol. 7, No. 1, P20–P24

ORIGINAL ARTICLE

The optional extent of lymph node dissection for pancreatic head cancer

Guangcai Niu, Xiangdong Ma (✉)

Department of Oncological Surgery, Xuzhou Central Hospital, Xuzhou 221009, China

Abstract

Objective The extent of lymph node dissection for pancreatic head cancer (PHC) is uncertain and controversial; therefore, this study evaluated whether PHC patients can benefit from different extents of lymph node dissection.

Methods A total of 106 PHC patients underwent standard regional lymphadenectomy (SRLN; *n* = 56, 52.8%) and extended regional lymphadenectomy (ERLN; *n* = 50, 47.2%) between September 2015 and September 2019. None of the study participants had distant metastases. The median survival time and complications were compared between the two groups.

Results The median survival time in the SRLN and ERLN groups was 27.01 months and 21.17 months, respectively ($P = 0.30$). The postoperative major morbidity and mortality rates were 37.50% and 1.79% in the SRLN group, and 46.00% and 2.00% in the ERLN group, respectively. Moreover, the tumor differentiation, tumor diameter, lymph node involvement, perineural invasion, vascular invasion, and margin status all correlated with survival ($P < 0.05$).

Conclusion For PHC patients, ERLN cannot provide a significant survival benefit over SRLN. Moreover, ERLN increased morbidity and mortality, although without statistical significance. This indicates that ERLN should not be considered in PHC patients.

Received: 10 May 2020
Revised: 23 August 2020
Accepted: 3 September 2020

Key words: pancreatic head cancer (PHC); standard regional lymphadenectomy (SRLN); extended regional lymphadenectomy (ERLN); survival; complication

Pancreatic cancer is one of the most fatal tumors for which the poor survival rate is often attributable to inefficient therapy. According to some reports, patients with pancreatic head cancer (PHC) who underwent pancreaticoduodenectomy had a median overall survival of only 13 months, and a 5-year survival rate of only 7%–8% [1–3]. Lymph node metastasis is very high among PHC patients and is one of the adverse prognostic factors that indicate progressively decreased survival [4]. To date, radical surgery is the only option to increase survival in PHC patients; therefore, there is a need for studies evaluating whether PHC patients can benefit from different extents of lymph node dissection.

Extended regional lymphadenectomy (ERLN) was originally intended to remove the entire pancreas as well as the adjacent tissues (nervous, adipose, and lymphatic tissues, among others). In Japan, radical pancreaticoduodenectomy has been used most extensively and has been thought to guarantee a better survival [5–6]. Nevertheless, as per some reports, it did not prolong the survival time, but increased postoperative complications [7–8]. Our paper aimed to evaluate the benefits of different extents of lymphadenectomy in PHC patients.

Patients and methods

A total of 166 PHC patients were admitted to the Xuzhou Central Hospital (Xuzhou, China) from September 2015 and September 2019. Of them, 60 patients were excluded because of preoperative chemoradiation therapy, the presence of tumors other than adenocarcinoma, and the absence of informed consent. In total, 106 patients were eligible for the study, and all patients received ethical and written consent.

Standard regional lymphadenectomy (SRLN) included the removal of the following lymphatic fat tissue: No.

✉ Correspondence to: Xiangdong Ma. Email: m10046@sina.com

5/6/8a/12b1/12b2/12c/13a/13b/14a/14b/17a/17b. By contrast, ERLN included the additional removal of all lymphatic, connective, and neural tissue No. 8p/9/16 [9].

The 106 patients were divided between the SRLN and ERLN groups according to the lymphadenectomy extent. The SRLN group included 56 patients (27 males and 29 females). The ERLN group included 50 patients (29 males and 21 females). No patient with macroscopically positive resection margins was included in the study. Matched-pair analysis was performed to assess the impact of the different extents of lymphadenectomy in PHC patients. Patients in both groups were matched for the gender, performance status, tumor differentiation, tumor diameter, lymph node involvement, surgery type, perineural invasion, vascular invasion, and margin status.

Statistical analyses were performed using SPSS 13.0 software (SPSS Inc., Chicago, Illinois). Data were presented as mean ± standard deviation or median (range). Chi-square test or Fisher's exact test was used for categorical variables. The Kaplan-Meier method was used to calculate overall survival rates. A P value < 0.05 was considered statistically significant.

Results

The mean age of the all patients was 49 years (range: 30–70 years), and there were 56 males and 50 females. In the SRLN group, 48% of the patients were male, compared to 58% in the ERLN group (P = 0.314). As for the surgery type, the patients underwent traditional pancreaticoduodenectomy (PD) (SRLN: 36; ERLN: 26; P = 0.20). Tumor differentiation was also comparable between the two groups (P = 0.677). In the SRLN and ERLN groups, 32 and 24 patients had tumors with a diameter of > 2 cm, respectively. The SRLN group had microscopic carcinoma at a surgical margin in 27% of patients; by contrast, this was in 14% of patients in the ERLN group. Perineural invasion was identified in the majority of patients, but no difference was observed between the two groups. For both groups, 34% of patients had histologically positive lymph node metastases in the resection specimen (Table 1).

Univariate analysis showed that the tumor differentiation, diameter, lymph node involvement, perineural invasion, vascular invasion, and margin status was closely related to survival (Table 2). However, there was no difference in the median survival time between the two groups (27.01 *vs.* 21.17 months, P = 0.30). Fig. 1 shows the survival curves for all PHC patients.

As seen in Table 3, the morbidity and mortality rates of patients in the ERLN group were higher than those in the SRLN group. Postoperative major morbidity and mortality rates were 37.50% and 1.79% in the SRLN group, and 46.00% and 2.00% in the ERLN group, respectively.

Table 1 Comparison of PHC patients between SRLN and ERLN groups (*n*)

	SRLN group	ERLN group	*P*
Gender			0.314
Male	27	29	
Female	29	21	
Performance status			0.713
Score 90–100	26	25	
Score 70–80	30	25	
Differentiation			0.677
Well	10	6	
Moderately	28	28	
Poorly	18	16	
Tumor diameter (cm)			0.347
≤ 2	24	26	
> 2	32	24	
Lymph node metastasis (N)			0.994
Yes	19	17	
No	37	33	
Surgery type			0.200
PD	36	26	
PPPD	20	24	
Perineural invasion			0.872
Yes	40	35	
No	16	15	
Vascular invasion			0.727
Yes	14	14	
No	42	36	
Margin status			0.411
R0	51	43	
R1	5	7	

Note: PD, pancreaticoduodenectomy; PPPD, pylorus-preserving pancreaticoduodenectomy

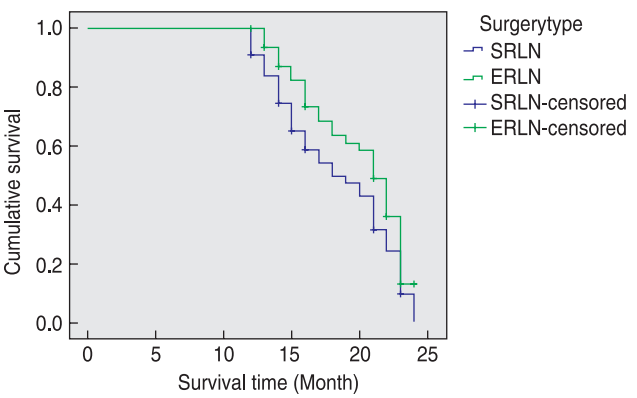

Fig. 1 The survival curves for all PHC patients

The most common postoperative complication was delayed gastric emptying and pancreatic fistula, which were observed in 8 patients. Other complications, such as wound infection, intraabdominal abscess, intraperitoneal hemorrhage, cholangitis, bile leak,

Table 2 Univariate analysis and Cox multivariate analysis to identify independent prognostic factors

	Median Survival	Univariate *P*	Multivariate *P*
Gender		0.102	
Male	27.65		
Female	19.05		
Performance status		0.935	
Score 90–100	24.31		
Score 70–80	23.82		
Differentiation		0.000	0.000
Well	34.91		
Moderately	28.50		
Poorly	12.08		
Tumor diameter (cm)		0.006	0.128
≤ 2	30.39		
> 2	18.16		
Lymph node metastasis (N)		0.033	0.033
Yes	15.03		
No	27.48		
Surgery type		0.100	
PD	23.35		
PPPD	12.00		
Extent of lymph node dissection		0.300	
SRLN	27.01		
ERLN	21.17		
Perineural invasion		0.008	0.040
Yes	19.97		
No	30.77		
Vascular invasion		0.000	0.005
Yes	10.85		
No	30.26		
Margin status		0.008	0.048
R0	25.73		
R1	8.13		

Note: PD, pancreaticoduodenectomy; PPPD, pylorus-preserving pancreaticoduodenectomy

Table 3 The morbidity and mortality of PHC patients between SRLN and ERLN groups (*n*)

	SRLN group	ERLN group	*P*
Morbidity	21 (37.50%)	23 (46.00%)	0.375
Delayed gastric emptying	3	5	
Pancreatic fistula	4	4	
Wound abscess	3	3	
Intraabdominal abscess	3	2	
Intraperitoneal hemorrhage	1	2	
Cholangitis	2	2	
Bile leak	2	2	
Lymphocele dysfunction	1	1	
Diarrhea	2	2	
Mortality	1 (1.79%)	1 (2.00%)	0.935
Cardiac & Respiratory failure	1	0	
Bleeding	0	1	

lymphocele dysfunction, and diarrhea occurred with similar frequency between the two groups. In the SRLN group, 1 death was directly related to respiratory failure resulting in multi-organ failure. There was also 1 death in the ERLN group, due to acute abdominal bleeding. Postoperative complications were graded according to the Clavien-Dindo classification [10].

Discussion

Despite improvements in techniques associated with extended regional lymph nodes, we have not established the appropriate extent of lymphadenectomy. More radical surgical strategies have been developed to improve the survival of PHC patients, with extensive lymph node dissection being the most important aspect. Nevertheless, extended radical surgery remains controversial because of the high rates of complications.

Some East Asian surgeons have advocated for aggressive radical lymph node dissection, with PHC patients gaining long-term survival time through ERLN. For example, Ishikawa *et al* [11] reported a significantly different ($P < 0.05$) 3-year survival rate between patients receiving SRLN (13%) and ERLN (38%). Moreover, Manabe *et al* [12] showed that for pancreatic cancer without lymph node metastasis, the 2-year survival rate was 22% and 48% in the standard and radical groups, respectively ($P < 0.05$). By contrast, two randomized controlled trials (RCTs) have not found better outcomes in PHC patients who underwent extended lymph node dissection versus standard lymphadenectomy [13–14]. However, these RCT studies were of low quality, having numerous confusing factors that made it less convincing to compare the results between the two groups and determine the preferred lymphadenectomy method. In our study, we also found no significant difference in the survival rates between the two groups; the median survival time was 27.01 months and 21.17 months for the SRLN and ERLN groups, respectively ($P = 0.30$; Fig. 1). Therefore, ERLN serves no benefit for PHC patients.

In addition to the tumor diameter, our study showed that tumor grade was a significant prognostic factor when tumor differentiations were compared. The tumors of patients under the T3 and T4 stages extend out of the capsule of the pancreas; therefore, the risk of direct perineural invasion is probably very high. Moreover, perineural invasion was identified in the majority of the patients, and was also an important survival predictor.

In other reports, lymph node metastasis represents a strong negative prognostic factor. Hellan *et al* [15] found that the number of lymph node dissections directly affects prognosis. The median survival for patients with < 11 lymph nodes and > 11 lymph nodes was 20 months and 15 months, respectively. Riediger *et al* [16] also reported

the relationship between lymph nodes ratio (LNR) and 5-year survival rate after surgery: when LNR > 0.2, the 5-year survival rate was 6%, whereas when LNR ≤ 0.2, the 5-year survival rate was 19%. In our study, patients with positive lymph nodes had a median survival time of 15.03 months, whereas that of the patients with negative lymph nodes was 27.48 months ($P = 0.033$).

In most series, the portal or mesenteric vein infiltration is correlated with poor prognosis and a very low 5-year survival rate. Our current study showed that the portal involvement was significantly associated with the worst prognosis. The median overall survival was 10.85 months and 30.26 months for patients with and without the portal vein involvement, respectively ($P < 0.001$). Nevertheless, because these operations could guarantee a better survival, and morbidity and mortality rates did not increase, we can proceed intraoperatively with segmental resection if there is a possibility to achieve an R0 resection.

With improvements in surgical techniques, some surgeons have sought to perform more radical surgeries. However, it was shown in our study that R0 resection rates were similar in patients between the two groups (91.07% and 86.00% in the SRLN and ERLN groups, respectively). Even if the surgery was performed to cure, pancreatic cancer recurrence rates were as high as that of classical R0 resection. Thus, controlling the local tumor recurrence through extended lymphadenectomy cannot overcome the lymph node metastasis after surgery.

Some studies have reported that the most important factor for improved overall survival of PHC patients following pancreatoduodenectomy is proper systemic chemoradiotherapy rather than extensive surgery. According to some research, chemoradiotherapy and targeted therapy may improve survival outcomes after curative resection [14, 17–18]. A large multicenter RCT suggested that aggressive systemic treatment could lead to long-term survival [19–20]. With emerging chemotherapeutic agents and targeted medicines, we must pay more attention to the benefits of adjuvant treatment and not focus only on pure resection. In our study, the patients did not receive any postoperative adjuvant therapy, which could explain their low survival time. Nevertheless, by eliminating adjuvant therapy in our study, we were able to judge if there were any benefits derived exclusively from the extended lymphadenectomy.

There are 2 surgical techniques performed in the treatment of pancreatic head surgery. Several RCTs have compared these 2 techniques in terms of postoperative complications and survival; there was no evidence of superiority for one procedure over the other in terms of overall survival, and the differences in mortality and morbidity were not statistically significant [21–22]. Similar to the findings of our study, the type of surgery did not have an influence on survival or postoperative morbidity.

The mortality and morbidity rates in the two groups are summarized in Table 3. The results in our study were similar to those previously reported. The overall postoperative morbidity and mortality in the ERLN group was higher, but the difference was not statistically significant. Postoperative major morbidity and mortality rates were 37.50% and 1.79% in the SRLN group, and 46.00% and 2.00% in the ERLN group, respectively, which were similar to the previous reports of 40% to 50%, respectively [23–24]. Pancreatic fistula and delayed gastric emptying were the most frequent complications, which tended to be higher in patients who underwent ERLN, but no statistically significant differences were observed. Some studies reported that the rates of postoperative diarrhea tended to be higher in patients who underwent ERLN, mainly due to extended excision of the retroperitoneal and pancreatic head plexus. In our paper, 2 out of 56 patients and 2 out of 50 patients in the SRLN and ERLN groups, respectively, had diarrhea, which differed from the conclusion of other studies. Finally, 2 studies have also reported that postoperative quality of life was poorer among patients in the extended lymphadenectomy group [13, 25].

Since ERLN increases morbidity and does not appear to improve survival, it should be noted that extended lymphadenectomy does not provide a better survival rate. Therefore, PHC patients should be treated with caution. Surgery combined with comprehensive treatments should be considered for PHC patients.

Conflict of interest

The authors indicated no potential conflicts of interest.

References

1. Chen WQ, Zheng RS, Baade PD, *et al*. Cancer statistics in China, 2015. CA Cancer J Clin, 2016, 66: 115–132.
2. Zeng HM, Chen WQ, Zheng RS, *et al*. Changing cancer survival in China during 2003-15: a pooled analysis of 17 population-based cancer registries. Lancet Glob Health, 2018, 6: e555–e567.
3. Siegel RL, Miller KD, Jemal A. Cancer statistics, 2018. CA Cancer J Clin, 2018, 68: 7–30.
4. Kamisawa T, Wood LD, Itoi T, *et al*. Pancreatic cancer. Lancet, 2016, 388: 73–85.
5. Satake K, Nishiwaki H, Yokomatsu H, *et al*. Surgical curability and prognosis for standard versus extended resection for T1 carcinoma of the pancreas. Surg Gynecol Obstet, 1992, 175: 259–265.
6. Kayahara M, Nagakawa T, Ueno K, *et al*. Surgical strategy for carcinoma of the pancreas head area based on clinicopathologic analysis of nodal involvement and plexus invasion. Surgery, 1995, 117: 616–623.
7. Orci LA, Meyer J, Combescure C, *et al*. A meta-analysis of extended versus standard lymphadenectomy in patients undergoing pancreatoduodenectomy for pancreatic adenocarcinoma. HPB (Oxford), 2015, 17: 565–572.
8. Dasari BVM, Pasquali S, Vohra RS, *et al*. Extended versus standard

lymphadenectomy for pancreatic head cancer: meta-analysis of randomized controlled trials. J Gastrointest Surg, 2015, 19: 1725–1732.
9. Tol JAMG, Gouma DJ, Bassi C, *et al*. Definition of a standard lymphadenectomy in surgery for pancreatic ductal adenocarcinoma: a consensus statement by the International Study Group on Pancreatic Surgery (ISGPS). Surgery, 2014, 156: 591–600.
10. Dindo D, Demartines N, Clavien PA. Classification of surgical complications: a new proposal with evaluation in a cohort of 6336 patients and results of a survey. Ann Surg, 2004, 240: 205–213.
11. Ishikawa O, Ohhigashi H, Sasaki Y, *et al*. Practical usefulness of lymphatic and connective tissue clearance for the carcinoma of the pancreas head. Ann Surg, 1988, 208: 215–220.
12. Manabe T, Ohshio G, Baba N, *et al*. Radical pancreatectomy for ductal cell carcinoma of the head of the pancreas. Cancer, 1989, 64: 1132–1137.
13. Nimura Y, Nagino M, Takao S, *et al*. Standard versus extended lymphadenectomy in radical pancreatoduodenectomy for ductal adenocarcinoma of the head of the pancreas: long-term results of a Japanese multicenter randomized controlled trial. J Hepatobiliary Pancreat Sci, 2012, 19: 230–241.
14. Jang JY, Kang MJ, Heo JS, *et al*. A prospective randomized controlled study comparing outcomes of standard resection and extended resection, including dissection of the nerve plexus and various lymph nodes, in patients with pancreatic head cancer. Ann Surg, 2014, 259: 656–664.
15. Hellan M, Sun CL, Artinyan A, *et al*. The impact of lymph node number on survival in patients with lymph node-negative pancreatic cancer. Pancreas, 2008, 37: 19–24.
16. Riediger H, Keck T, Wellner U, *et al*. The lymph node ratio is the strongest prognostic factor after resection of pancreatic cancer. J Gastruintest Surg, 2009, 13: 1337–1344.
17. Neoptolemos JP, Stocken DD, Bassi C, *et al*. Adjuvant chemotherapy with fluorouracil plus folinic acid vs gemcitabine following pancreatic cancer resection: a randomized controlled trial. JAMA, 2010, 304: 1073–1081.
18. Regine WF, Winter KA, Abrams R, *et al*. Fluorouracil-based chemoradiation with either gemcitabine or fluorouracil chemotherapy after resection of pancreatic adenocarcinoma: 5-year analysis of the U.S. Intergroup/RTOG 9704 phase III trial. Ann Surg Oncol, 2011, 18: 1319–1326.
19. Neoptolemos JP, Dunn JA, Stocken DD, *et al*. Adjuvant chemoradiotherapy and chemotherapy in resectable pancreatic cancer: a randomised controlled trial. Lancet, 2001, 358: 1576–1585.
20. Neoptolemos JP, Stocken DD, Friess H, *et al*. A randomized trial of chemoradiotherapy and chemotherapy after resection of pancreatic cancer. N Engl J Med, 2004, 350: 1200–1210.
21. Seiler CA, Wagner M, Bachmann T, *et al*. Randomized clinical trial of pylorus-preserving duodenopancreatectomy versus classical Whipple resection-long term results. Br J Surg, 2005, 92: 547–556.
22. Tran KTC, Smeenk HG, van Eijck CHJ, *et al*. Pylorus preserving pancreaticoduodenectomy versus standard Whipple procedure: a prospective, randomized, multicenter analysis of 170 patients with pancreatic and periampullary tumors. Ann Surg, 2004, 240: 738–745.
23. Addeo P, Delpero JR, Paye F, *et al*. Pancreatic fistula after a pancreaticoduodenectomy for ductal adenocarcinoma and its association with morbidity: a multicentre study of the French Surgical Association. HPB (Oxford), 2014, 16: 46–55.
24. Glazer ES, Amini A, Jie T, *et al*. Recognition of complications after pancreaticoduodenectomy for cancer determines inpatient mortality. JOP, 2013, 14: 626–631.
25. Farnell MB, Pearson RK, Sarr MG, *et al*. A prospective randomized trial comparing standard pancreatoduodenectomy with pancreatoduodenectomy with extended lymphadenectomy in resectable pancreatic head adenocarcinoma. Surgery, 2005, 138: 618–628.

DOI 10.1007/s10330-020-0427-7
Cite this article as: Niu GC, Ma XD. The optional extent of lymph node dissection for pancreatic head cancer. Oncol Transl Med, 2021, 7: 20–24.

Oncology and Translational Medicine
DOI 10.1007/s10330-020-0438-8
February 2021, Vol. 7, No. 1, P25–P30

ORIGINAL ARTICLE

Expression of mir-34c-5p and mir-150-5p in nasopharyngeal carcinoma and up-regulated expression after invasion and apoptosis of nasopharyngeal carcinoma cells*

Xiaojun Zhou[1] (✉), Baorui Lin[1], Yun Wang[2]

[1] Department of Otolaryngology, Zhongshan Hospital affiliated to Guangzhou University of Chinese Medicine, Zhongshan 528401, China
[2] Department of Pathology, Zhongshan Hospital affiliated to Guangzhou University of Chinese Medicine, Zhongshan 528401, China

Abstract

Objective MiRNAs are closely related to tumors, and we hypothesized there is specific miR expression in nasopharyngeal carcinoma (NPC). We intended to investigate the expression of mir-34c-5p and mir-150-5p in NPC and to investigate the effects of mir-34c-5p and mir-150-5p on apoptosis and invasion following up-regulated expression in HNE1 NPC cells.

Methods MiR-34c-5p and miR-150-5p expression levels in 30 individual cases of NPC and nasopharyngitis were detected with gene chip and qRT-PCR techniques. miR-34c-5p and miR-150-5p were transfected into the NPC cell line HNE1 via liposomes. Their expression levels were detected with qRT-PCR, apoptosis was evaluated by flow cytometry, and invasion ability was assessed via Transwell migration assay.

Results MiR-150-5p expression levels in NPC and nasopharyngitis were 0.165 ± 0.092 and 1.062 ± 0.280 respectively, and miR-34c-5p expression levels in NPC and nasopharyngitis were 0.417 ± 0.220 and 1.385 ± 0.739, respectively, which indicated miR-34c-5p and miR-150-5p were weakly expressed in NPC. Apoptosis rates in HNE1 cells transfected by miR-34c-5p and miR-150-5p were increased, by 12.7% and 7.6%, respectively, which were significantly higher compared to blank control (3.9%). The Transwell assay demonstrated that invasive HNE1 cell counts were 32.00 ± 2.00 and 28.33 ± 2.08, respectively, compared to 60.66 ± 8.50 in the blank control ($P < 0.001$).

Conclusion MiR-34c-5p and miR-150-5p are lowly expressed in NPC, and their down-regulation may be associated with NPC.

Received: 18 June 2020
Revised: 10 July 2020
Accepted: 25 July 2020

Key words: miR-150-5p; miR-34c-5p; nasopharyngeal carcinoma; apoptosis; invasion

Nasopharyngeal carcinoma (NPC) is a common malignancy mostly seen in southern China. Many years of research have found that although the factors of heredity, region, and EB virus exposure are implicated in its etiology, the most distinguishing feature is that its occurrence has a particular regionalism; it is also called "canton tumor," the only malignant carcinoma named after a region. This phenomenon indicates that genetic and environmental regulations together are closely associated with its occurrence. Regarding regulation, the relationship between micro RNA and tumor has received increased attention. Related studies report that miR-34c-5p and miR-150-5p are lowly expressed in many types of tumors and are closely associated with tumor progression and invasive activities, representing potential targets for tumor therapy [1–2]. The expression of miR-34c-5p and miR-150-5p in NPC and related cytobiological activities after reverse-regulation in the cultured NPC cell line

✉ Correspondence to: Xiaojun Zhou. Email: zd1232@126.com
* Supported by grants from the National Natural Science foundation of China (No. 81373698), Joint Special Scientific Research Project of the Department of Science and Technology of Guangdong Province-Guangdong Provincial Academy of Chinese Medical Sciences (No. 2017A020213020); Zhongshan Key Scientific and Technological Project (No. 2015B1003, 2019B1096).

HNE1 are yet to be studied, which provided the basis for the present study.

Materials and methods

Clinical materials

Thirty cases of NPC from outpatients of the Zhongshan Hospital, affiliated with Guangzhou University of Chinese Medicine, from between May 2014 and October 2016 were sampled, comprising 18 men and 12 women, ages from 22 to 64 years, with an average age of 46.67 ± 11.17 years. The clinical stages of NPC included 10 cases of stage II, 13 cases of stage III, and 7 cases of stage IV. There were 20 cases of differentiated nonkeratinizing carcinoma and 10 cases of undifferentiated carcinoma in pathological categorization. Thirty cases of nasopharyngitis were used as a control group, including 17 men and 13 women, ages from 20 to 55 years, with an average age of 34.17 ± 11.25 years.

Experimental materials

The NPC cell line HNE1 was purchased from American Type Culture Collection (ATCC).

Main reagents and apparatus

Experimental reagents

The miRCURY LNA™ microRNA Array (Exiqon, Denmark) was used. Three thousand and one hundred capture probes were employed, covering human, mouse, and rat microRNA in miRBase, as well as viral microRNA related to these species. Other reagents included the miRCURYTM Array Power Labeling kit (Cat #208032-A, Exiqon), 2X PCR master mix (Arraystar), RPMI1640 basic culture medium (Hyclone Co., cat: SH30022.03B), fetal bovine serum (FBS, GIBCO Co., cat: 16400-044), bispecific antibody (Prospec Co., cat: SV30010), Lipofectamine 2000(Invitrogen Co., cat: 11668-027), and real-time PCR kit (Thermo Co., cat: 11762-100), TRIZOL (Invitrogen Co., cat: 15596-026), and primer synthesis was done by Shanghai Sangon Biotech Co.

Experimental apparatus

An axon GenePix 4000B microarray scanner, real-time fluorescent quantification PCR cycler (Eppendorf Co., lot No.:X226488N), primer design software Primer 5.0, CO_2 incubator (Shanghai Boxun Biotech Co., cat:BC-J160S), sterile bench (Shang Boxun Biotech Co., type:SW-CJ-2FD), transwell chamber (Costar Co., cat: 3422), and fluorescence microscope (Olympus IX71) were employed in this study.

Experimental methods

Determination of miR-34c-5p and miR-150-5p expression in NPCs via gene chip technique.

RNA was extracted from 100 mg of -80°C frozen fragmented nasopharynx tissues by Trizol, including 6 cases each of NPC and nasopharyngitis.

RNA was labeled with the miRCURY™ Array Power Labeling kit after quality control by gel electrophoresis detection. Labeled RNA samples were hybridized to the microarray with the miRCURY LNA™ microRNA Array and washed with buffer kit.

The microarrays were scanned using the Axon GenePix 4000B microarray scanner (Axon Instruments, Foster City, CA), and results were saved after being transformed into data; then, the original data were analyzed with corresponding software.

Determination of miR-34c-5p and miR-150-5p expression in NPC by RT-PCR.

RNA was extracted from tissues of 30 patients with NPC and 30 patients with nasopharyngitis, and quality was controlled via gel electrophoresis detection. For cDNA sample synthesis, a compound RT mixed reaction solution, which included 5 μL of 2x Master Mix, 0.5 μL of 10 uM PCR specific primer F, 0.5 μL of 10 uM PCR specific primer R, and water to a total volume of 8 μL. cDNA samples of 2 μL were amplified by mixing with the reaction solution, then running 40 PCR cycles (95°C for 10 s, 60°C for 60 s). PCR primer sequences were listed below, Table 1.

miRNA transfection into NPC cell line HNE1

Cells were digested and seeded one day before transfection. Into each of two centrifuge tubes (No.1 and No.2), 100 μL of RPMI-1640 was added. With the pipette tip well below the liquid level, 3 μL of lipofectamine 2000 was added into tube 1 and 1 μg of DNA (100 pmol siRNA) into tube 2. Both were homogenized by flicking, and placed at 25°C for 5 min. The liposome dilution in tube 1 was transferred into tube 2 with the pipette tip well below the liquid level; then, the mixture was homogenized by flicking and placed at room temperature for 20 min. RPMI-1640 (0.8 mL/well) was added to HNE1 cells for transfection. Blank and negative controls were made for siRNA transfection. Next, 0.2 mL of DNA-liposome (siRNA-liposome) mixture was dripped into culture plates. They were then homogenized and incubated in an incubator at 37°C with 5% CO_2. Five hours later, the culture solution was changed to 10% FBS-RPMI-1640, and the culture continued for 48 h. After 48 h of transfection, RNA was routinely extracted using Trizol reagent. RNA reverse transcription (37°C for 60 min, 65°C for 20 min) and RT-PCR was performed (hU6 was used as the internal standard, the primer design software was Primer5, and primer sequences of all target genes were listed below, Table 1).

Table 1 Primer sequences for all target genes

miRNA mimics	Sequence
hsa-miR-150-5p mimics-Sense	5'-UCUCCCAACCCUUGUACCAGUG-3'
hsa-miR-150-5p mimics-anti sense	5'-CUGGUACAAGGGUUGGGAGAUU-3'
hsa-miR-34c-5p mimics- Sense	5'-AGGCAGUGUAGUUAGCUGAUUGC-3'
hsa-miR-34c-5p mimics-anti sense	5'-AAUCAGCUAACUACACUGCCUUU-3'
Mimics-sense	5'-UCACAACCUCCUAGAAAGAGUAGA-3'
Mimics-anti sense	5'-UACUCUUUCUAGGAGGUUGUGAUU-3'
RT primer	
hsa-miR-150-5p	TGCTCCAACCCTTGTACCAGTG
hsa-miR-34c-5p	TGCTAGTGTAGTTAGCTGATTGC
hU6	CGCAAGGATGACACGCAAATTC

Determination of apoptosis by flow cytometry

HNE1 cells were classified into the following groups: hsa-miR-150-5p mimics transfection group, hsa-miR-34c-5p mimics transfection group, negative control transfection group, and normal control group. At 48 h after transfection, the supernatant was discarded. The cell pellet was washed twice with PBS solution and digested with trypsin. Then, 500 μL of AnnexinV binding buffer was added to prepare the cell suspension, 5 μL of AnnexinV-FITC was added, and the mixture homogenized. Next, 5 μL of propidium iodide was added and the mixture homogenized and placed at room temperature in darkness for 10 min. Apoptosis was examined by flow cytometry (Ex = 488 nm; Em = 530 nm).

Determination of cell invasion ability by Transwell assay

HNE1 cells were classified into the following groups: hsa-miR-150-5p mimics transfection group, hsa-miR-34c-5p mimics transfection group, negative control transfection group, and normal control group. They were digested and passaged with routine methods. Cell suspension was prepared, cell counting was performed, and cell concentration was adjusted to 2×10^5/mL. Next, 100 μL of diluted Matrigel was perpendicularly added to the bottom center of the upper chamber and incubated at 37°C for 4–5 h to form a gel. Afterwards, 100 μL of cell suspension was pipetted into the chamber and 600-800 μL of 10% serum culture medium was added into the lower chamber (the bottom of 24-well plate), and the culture continued for 48 h. Then the chamber was taken out, washed twice with PBS solution, and transferred into 100% methanol to fix at room temperature for 20 min. Then it was transferred into 800 μL of Giemsa solution to stain at room temperature for 15–30 min, and washed with PBS. With a wet cotton swab, cells were carefully removed from Matrigel and the surface of the bottom membrane in the upper chamber. After the chamber was completely dry, counting and photography were performed under a fluorescent inverted microscope.

Statistical analysis

Statistical analyses and plotting were performed with GraphPad prism 5.0. Data were processed with MS EXCEL. Relative quantification was used to analyze RT-PCR results, and relative expression levels were calculated with $RQ = 2^{-\Delta\Delta CT}$. Expression of mir-34c-5p and mir-150-5p are expressed as mean ± standard deviation, and Student's *t*-test was performed for two-group comparisons. The data on apoptosis ratio were analyzed by non-parametric statistical methods, while the numbers on cell invasion were analyzed with a variance analysis test. $P < 0.05$ indicated statistical significance.

Results

Expression of miR-150-5p and miR-34c-5p in NPC

The original data were preprocessed and homogenized, and the results of microRNA Array chip detection indicated certain characteristic microRNA expression profiles in NPC. miR-34c-5p expression levels in nasopharyngitis and NPC were 1.099 ± 1.015 and 0.361 ± 0.659, respectively, and miR-150-5p expression levels in nasopharyngitis and NPC were 5.884 ± 4.374 and 2.236 ± 1.708, respectively, which indicated miR-34c-5p and miR-150-5p were weakly expressed in NPC.

RT-PCR detection of microRNA expression levels are displayed in Table 2. Statistical testing indicated miR-150-5p and miR-34c-5p were weakly expressed in NPC, and the expression levels were significantly lower compared to nasopharyngitis, with $t = 16.673$, $P < 0.01$ and $t = 6.874$, $P < 0.01$, respectively. Both gene chip detection and RT-PCR amplification results indicated miR-150-5p and miR-34c-5p were weakly expressed in NPC.

Transfection and amplification of NPC cell line HNE1

Expression levels were elevated in HNE1 cells

Table 2 Expression of miR-150-5p and miR-34c-5p in NPC by RT-PCR

Groups	*n*	miR-150-5p	miR-150-5p
NPC	30	0.165 ± 0.092	0.417 ± 0.220
nasopharyngitis	30	1.062 ± 0.280	1.385 ± 0.739

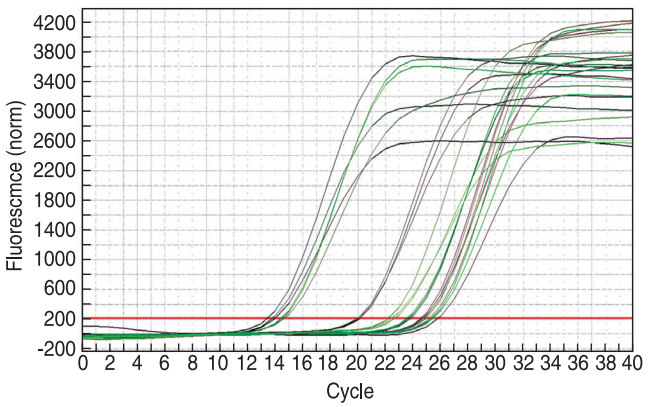

Fig. 1 Amplification curves of the NPC cell line HNE1 when transfected with hsa-miR-150-5p and hsa-miR-34c-5p

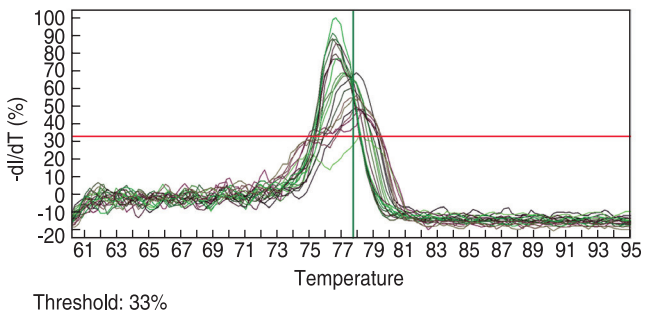

Fig. 2 Solubility curves of the NPC cell line HNE1 when transfected with hsa-miR-150-5p and hsa-miR-34c-5p

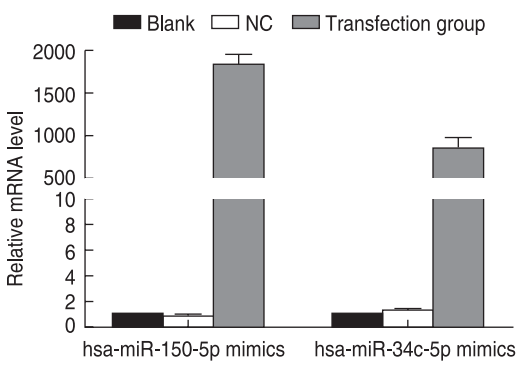

Fig. 3 Expression levels of the NPC cell line HNE1 when transfected with hsa-miR-150-5p and hsa-miR-34c-5p

transfected with hsa-miR-150-5p mimics and hsa-miR-34c-5p mimics (Fig. 1–3).

Apoptosis analysis by flow cytometry

After transfection, the average apoptosis rates in HNE1 cells of the-miR-34c-5p mimics (12.7%) and hsa-miR-150-5p mimics (7.6%) groups were significantly higher compared to the blank control (3.9%) and negative control (5.7%) groups (Fig. 4).

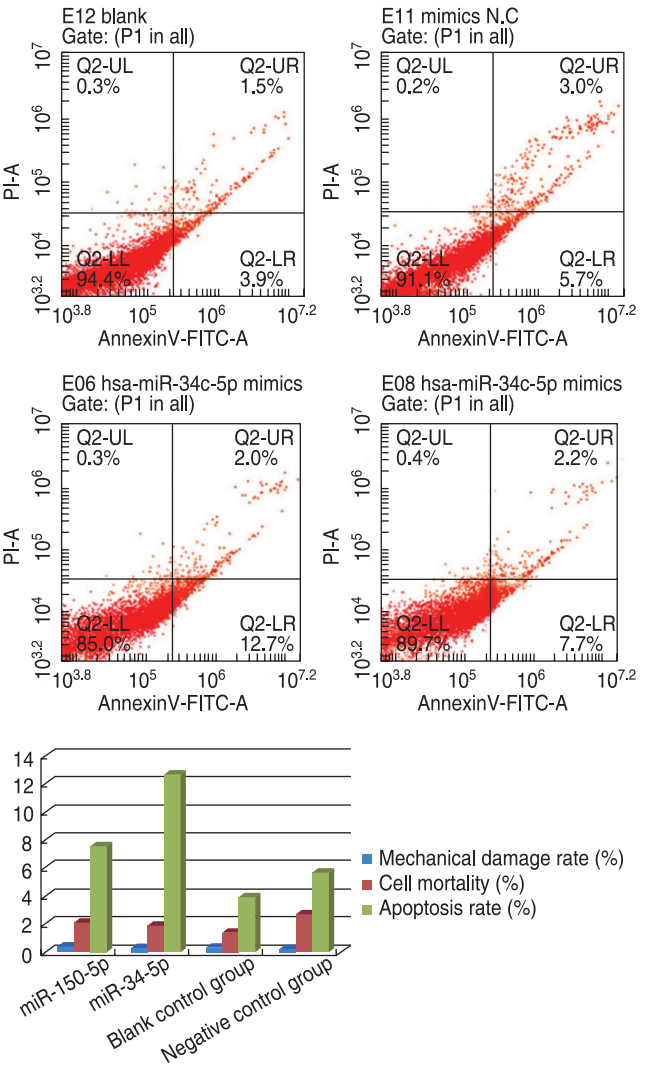

Fig. 4 Photographs of HNE1 cell apoptosis after up-regulation of hsa-miR-34c-5p and hsa-miR-150-5p

Transwell cell invasion test

A Transwell cell invasion test showed that migration (invasion) counts of HNE1 cells in the miR-150-5p mimics and miR-34c-5p mimics groups were 32.00 ± 2.00 and 28.33 ± 2.08, respectively, while they were 60.66 ± 8.50 and 56.6 ± 12.09 in the blank control and negative control groups, respectively ($F = 14.572$, $P < 0.001$). There was a significant difference when the miR-150-5p mimics and miR-34c-5p mimics groups were compared with the blank control and negative control groups ($P < 0.01$). There was no significant difference between either the miR-150-5p mimics and miR-34c-5p mimics groups or between the blank control and negative control groups (Fig. 5).

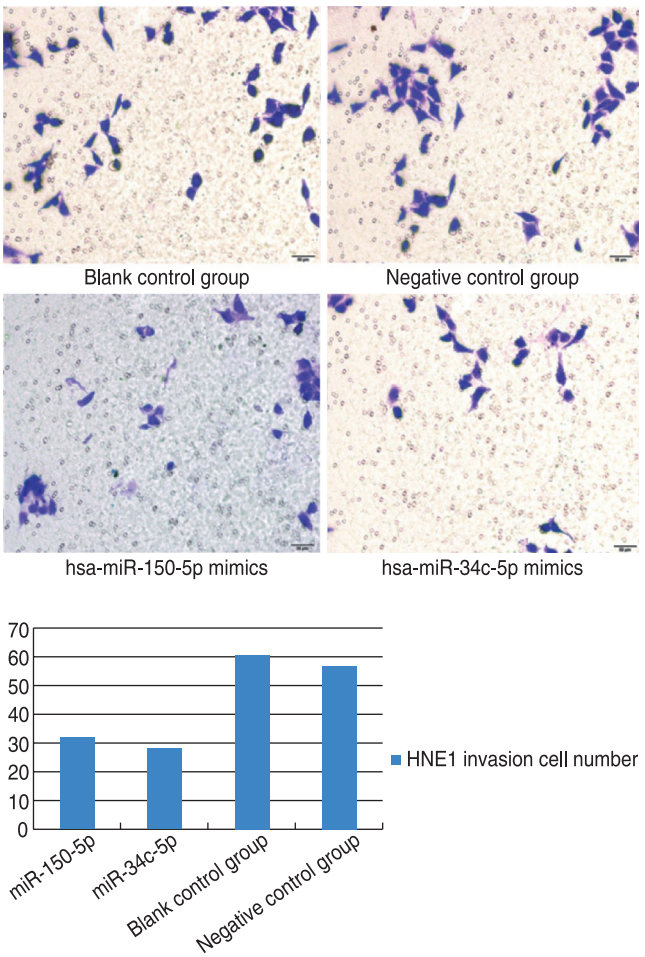

Fig. 5 Photographs of HNE1 cell invasion after up-regulation of hsa-miR-34c-5p and hsa-miR-150-5p

Discussion

MicroRNAs (miRNAs) are a group of endogenous and highly conserved non-encoding RNAs that regulate the expression of related target genes by complementary combination with the 3′ non-translated region of the genes. Because miRNA regulation is closely associated with cancer, it has become a hotspot in cancer research. Among the many miRNAs associated with cancer, down-regulation of miR-150-5p and miR-34c-5p has been associated with various types of tumors. For example, over-expression of miR-34c-5p may block the cell cycle at the G1 phase and inhibit the proliferation and metastasis of cervical carcinoma [3], inhibit MAPT gene expression in gastric cancer tissues and promote apoptosis of cancer cells [4], and regulate the KITLG gene to inhibit the proliferation and metastasis of colon cancer cells [5], while miR-150-5p can inhibit the proliferation and invasion of liver cancer cells [6] and Mir-150-5p inhibits the proliferation and migration of glioma cells by targeting matrix metalloproteinases [7]; these studies all show that Mir-34C-5p and Mir-150-5p are closely related to tumors. Thus, further study is warranted to uncover whether miR-34c-5p and miR-150-5p are related to NPC.

Our study on gene chip detection indicated certain characteristic microRNA expression profiles in NPC, among which miR-34c-5p and miR-150-5p were significantly downregulated in NPC. Thus, we selected miR-34c-5p and miR-150-5p for further study in NPC. First, we started with enlarging the number of clinical samples to 30 cases of NPC and nasopharyngitis each, and RT-PCR amplification result for those samples indicated miR-150-5p and miR-34c-5p were down-regulated in NPC, and the difference was statistically significant. Then, interference experiments on miR-150-5p and miR-34c-5p were performed using the NPC cell line HNE1, and the results indicated that after up-regulation of miR-150-5p and miR-34c-5p in the HNE1 cell line by transfection, apoptosis rates of HNE1 cells as examined by flow cytometry were significantly increased. A Transwell invasion test indicted that the invasion ability of NPC HNE1 cells was significantly decreased, demonstrating that decreased expression of miR-34c-5p and miR-150-5p was associated with malignant changes in NPC cells. Other studies [8] have indicated similar cytobiological activities of miR-34c-5p in NPC HONE1 cells, which provides corroborative evidence to our conclusions.

The present study reveals the relationship between down-regulation of miR-150-5p and miR-34c-5p and NPC, but additional research is needed to clarify the related mechanism and its relevance in the molecular diagnosis of NPC.

Conflicts of interest

The authors indicated no potential conflicts of interest.

References

1. Leoncini PP, Bertaina A, Papaioannou D, *et al*. MicroRNA fingerprints in juvenile myelomonocytic leukemia (JMML) identified miR-150-5p as a tumor suppressor and potential target for treatment. Oncotarget, 2016, 7: 55395–55408.
2. Wu Z, Wu Y, Tian Y, *et al*. Differential effects of miR-34c-3p and miR-34c-5p on the proliferation, apoptosis and invasion of glioma cells. Oncol Lett, 2013, 6: 1447–1452.
3. López JA, Alvarez-Salas LM. Differential effects of miR-34c-3p and miR-34c-5p on SiHa cells proliferation apoptosis, migration and invasion. Biochem Biophys Res Commun, 2011, 409: 513–519.
4. Wu H, Huang M, Lu M, *et al*. Regulation of microtubule-associated protein tau (MAPT) by miR-34c-5p determines the chemosensitivity of gastric cancer to paclitaxel. Cancer Chemother Pharmacol, 2013, 71: 1159–1171.
5. Yang S, Li WS, Dong F, *et al*. KITLG is a novel target of miR-34c that is associated with the inhibition of growth and invasion in colorectal cancer cells. J Cell Mol Med, 2014, 18: 2092–2102.

6. Liang ZK, Cheng FT, Hu ZX, *et al*. Inhibitory effect of miR-150-5p on migration and invasion of hepatocellular carcinoma cells and its mechanism. Chin J Gen Surg (Chinese), 2016, 25: 1175–1179.
7. Moustafa S,Takahisa T,Hemragul S, *et al*. MiR-150-5p and miR-133a suppress glioma cell proliferation and migration through targeting membrane-type-1 matrix metalloproteinase. Gene, 2016, 587: 155–162.
8. Ma FF, Hao YQ, Wang GQ, *et al*. The effect of up-regulating miR-34c-5p on the proliferation and invasion of nasopharyngeal carcinoma cell line HONE-1. Tianjin Med J, 2015, 43: 1097–1099.

DOI 10.1007/s10330-020-0438-8
Cite this article as: Zhou XJ, Lin BR, Wang Y. Expression of mir-34c-5p and mir-150-5p in nasopharyngeal carcinoma and up-regulated expression after invasion and apoptosis of nasopharyngeal carcinoma cells. Oncol Transl Med, 2021, 7: 25–30.

Oncology and Translational Medicine
DOI 10.1007/s10330-020-0414-4

February 2021, Vol. 7, No. 1, P31–P34

ORIGINAL ARTICLE

Application of dynamic contrast-enhanced magnetic resonance imaging (DCE-MRI) combined with magnetic resonance spectroscopy (MRS) in prostate cancer diagnosis

Yakun He, Min Wang (✉), Heping Deng, Jin Ren

Department of Radiology, Sichuan Cancer Hospital, Chengdu 610041, China

Abstract

Objective The aim of the study was to investigate the application of dynamic contrast-enhanced magnetic resonance imaging (DCE-MRI) combined with magnetic resonance spectroscopy (MRS) in prostate cancer diagnosis.

Methods In the outpatient department of our hospital (Sichuan Cancer Hospital, Chengdu, China), 60 patients diagnosed with prostate disease were selected randomly and included in a prostate cancer group, 60 patients with benign prostatic hyperplasia were included in a proliferation group, and 60 healthy subjects were included in a control group, from January 2013 to January 2017. Using Siemens Avanto 1.5 T high-field superconducting MRI for DCE-MRI and MRS scans, after the MRS scan was completed, we used the workstation spectroscopy tab spectral analysis, and eventually obtained the crest lines of the prostate metabolites choline (Cho), creatine (Cr), citrate (Cit), and the values of Cho/Cit, and (Cho + Cr)/Cit.

Results Participants who had undergone 21-s, 1-min, and 2-min dynamic contrast-enhanced MR revealed significant variations among the three groups. The spectral analysis of the three groups revealed a significant variation as well. DCE-MRI and MRS combined had a sensitivity of 89.67%, specificity of 95.78%, and accuracy of 94.34%.

Conclusion DCE-MRI combined with MRS is of great value in the diagnosis of prostate cancer.

Received: 27 March 2020
Revised: 28 August 2020
Accepted: 20 December 2020

Key words: prostate cancer; magnetic resonance imaging (MRI); dynamic contrast-enhanced (DCE); spectroscopy

Today, with the change in diet and lifestyle due to westernization, the extension of life expectancy, the aging of the population, and the popularity of prostate-specific antigen (PSA) examinations in China, the incidence of prostate cancer in China has increased significantly [1]. It has become one of the most common malignant tumors that endangers the health of middle-aged and elderly males [2]. In order to ensure the proper treatment and physical health of prostate cancer patients, a reasonable treatment plan is required. The patient's treatment plan and prognosis mainly depend on the early diagnosis of patients and the stage of the disease before the operation [3]. Early examination is beneficial for early detection, diagnosis, and treatment of prostate cancer [4].

In recent years, reports from the United States have shown that PSA audits in a large population have reduced the incidence of and overall mortality due to advanced prostate cancer in the United States by 50% and 30%, respectively, compared with the rates in the early 1990s [5]. In addition, recent reports reveal about 90% of newly diagnosed prostate cancer cases in Europe and the United States as localized prostate cancer at the first diagnosis, and 85% of localized prostate cancer can be cured by radical prostatectomy, thereby reducing the overall mortality rate of prostate cancer and improving the survival rate and quality of life of patients [6].

Magnetic resonance imaging (MRI) has a high applied value in the diagnosis of prostate cancer. Dynamic contrast-enhanced MRI (DCE-MRI) has a higher sensitivity in evaluating hemodynamics, morphology,

✉ Correspondence to: Min Wang. Email: 273795600@qq.com

and functionality, and can improve the diagnostic rate and staging accuracy of MRI in prostate cancer. At present, magnetic resonance spectroscopy (MRS) has also been widely used in the diagnosis of breast, brain, and prostate disease [7–8]. The purpose of this study was to investigate the application of DCE-MRI combined with MRS in prostate cancer diagnosis.

Materials and methods

Baseline characteristics of participants

In the outpatient department of our hospital (Sichuan Cancer Hospital, Chengdu, China), 60 patients diagnosed with prostate disease (confirmed by biopsy, surgical pathology, or follow-up) were selected randomly and included in a prostate cancer group, 60 patients with benign prostatic hyperplasia were included in a proliferation group, and 60 healthy subjects were included in a control group, from January 2013 to January 2017. The age ranges of the three groups were 48–78 years, 45–75 years, and 43–83 years; the mean age was 65.47 years, 60.56 years, and 68.43 years, respectively. There was no significant difference in the age factor among the three groups, which ensured the comparability of the subsequent data.

Equipment and inspection methods

The magnetic resonance examination was performed using a Siemens Avanto 1.5 T high-field intensity superconducting MR imager, and a body phased array coil. Before examination, the patient was cleaned intestinal tract, and after confirming that there was no stool in the rectum, the patient was examined by MRS.

DCE-MRI

The parameters and conditions of the DCE-MRI: TR 5.56 ms, TE 2.72 ms, the length of the echo chain (ETL) 1, Average 1, matrix 64 × 265, the layer thickness was 3 mm, the layer spacing was 0.6 mm, field of view (FOV) 350 mm × 250 mm, dynamic enhancement scan of the horizontal axis was 60 layers, scanning time 22 s. Prior to scanning, Gd-DTPA was injected through the anterior cubital vein at an injection flow rate of approximately 2 mL/s by a high-pressure syringe. Then, we performed the first scan after 21 s, and it was scanned once every minute. We obtained three scans in total.

MRS

An MRS scan is a three-dimensional imaging sequence of the axial plane. First the patients were scanned in the coronal, transverse, and sagittal sections. Then, the scanning was performed on the location phase in three directions, and the range of the scan included the entire prostate of the patients. After localization, eight saturated bands were added around the scanning area, and the saturation bands were as close as possible to the prostate, in order to suppress the influence of the surrounding tissue on the area of concern to the greatest extent. Prior to MRS scanning, band shimming was performed. The MRS scan was carried out under the following parameters: TR 700 ms and TE 120 ms scan sequence. The average number was 6 times, the reverse angle was 90°, the layer thickness was 50 mm, and the scanning time was 12 min. After scanning, spectrum analysis was performed on the spectroscopy TAB of the workstation to obtain the crest spectra of the prostatic metabolites choline (Cho), creatine (Cr), and citrate (Cit), and the ratio and mean values of Cho/Cit and (Cho + Cr)/Cit.

Image analysis

All images were analyzed by two MRI experts without knowledge of the patients' physical condition. In different impact conditions, the scope of the location of the tumor, hyperplasia and capsule invasion, seminal vesicle, and involvement of the neurovascular bundle were determined, and the results were compared with pathological results.

DCE-MRI

The signals of the same patient at the same position on the same level were measured at different times. The positions of the three measurements were as follows: the cancerous signals of patients with prostate cancer were measured separately, as well as the signals of the hyperplasia sites of patients with benign prostatic hyperplasia. The signals of the central glandular region and peripheral zone of members in the control group were measured and averaged. At the same time, the signal values of the obturator internus muscle at the same level for all participants were measured, and the relative signal intensity values were obtained after comparing the two signal values. During the measurement process, each partition of each research object had more than three selected districts, the values were recorded, and the average value was calculated.

MRS

MRS data were processed by a post-processing workstation. Three or more layers with the most clear lesions were selected to observe and measure the wave peaks of metabolites in the periprostatic region and central glandular region of the control group, in the lesion zone of the prostatic hyperplasia and prostate cancer groups, respectively. The data of Cho, Cr, and Cit were recorded, and calculated the ratio, and took the average value.

Data statistical analysis

SPSS 18.0 software was used for data analysis. Continuous variables were expressed as mean ± standard deviation and were analyzed by a *t*-test. The measurement data were analyzed using the chi-square test, and $P < 0.05$ indicated that the difference was statistically significant.

Results

The results of the three groups by DCE-MRI are shown in Table 1. Statistical software 18.0 was used for data analysis, and the *P*-values obtained were 0.042, 0.024, and 0.034, respectively, indicating that the comparison of the results between the three groups by DCE-MRI at 21 sec, 1 min, and 2 min showed significant differences.

The results of the three groups by MRS are shown in Table 2. Statistical software 18.0 was used to conduct statistical analysis on the data, and the *P*-values obtained were all < 0.05, indicating that the comparison between the spectral analysis results of the three groups was statistically significant, and there were significant differences.

The comparison results between the DCE-MRI and the MRS in diagnosis of prostate cancer are shown in Table 3.

Table 1 The comparison of the three groups by DCE-MRI

Groups	*n*	$\overline{\chi} \pm s$		
		21 s	1 min	2 min
Prostate cancer group	60	1.01 ± 0.09	1.51 ± 0.23	1.56 ± 0.20
Hyperplasia group	60	0.90 ± 0.09	1.23 ± 0.20	1.10 ± 0.16
Control group	60	0.80 ± 0.08	0.98 ± 0.19	0.97 ± 0.04
P value		0.042	0.024	0.034

Table 2 The comparison of the three groups by MRS

Indicators	Prostate cancer group	Hyperplasia group	Control group	*P* value
Cho/Cit	2.45 ± 1.01	0.38 ± 0.23	0.28 ± 0.13	< 0.05
(Cho + Cr)/Cit	2.83 ± 0.65	0.59 ± 0.34	0.39 ± 0.14	< 0.05

Table 3 The comparison between the DCE-MRI and the MRS in diagnosis of prostate cancer

Methods	Sensitivity (%)	Specificity (%)	Accuracy (%)
DCE-MRI	76.32	95.45	89.97
MRS	72.13	93.02	90.79
DCE-MRI + MRS	89.67	95.78	94.34

Discussion

Currently, the main detection methods for prostate cancer include PSA level examination, ultrasound-guided puncture biopsy, and MRI. Among them, the specificity of PSA level examination is low. Thus, it is difficult to distinguish benign lesions from prostate cancer and prostatic hyperplasia just from PSA levels [9–10]. The accuracy of ultrasound-guided puncture biopsy is relatively high, but the results are subjective and invasive. MRI is a non-invasive imaging method with high resolution for soft tissues. It can accurately and quickly distinguish the situation of different anatomical regions in the prostate. Coronal, transversal, and sagittal imaging can show the relationship between the gland and the surrounding structure in the pelvic cavity in a three-dimensional space, and the effect on tumor invasion of the nerves, blood vessels, capsule, bladder, seminal vesicle, and rectum is clear and obvious. Fat suppression of T2-weighted images (T2WI) clearly showed peripheral prostate cancer in patients better than other imaging studies [11]. However, MRI also has certain disadvantages, such as lack of specificity and high cost [12]. Furthermore, various functional imaging techniques such as diffusion-weighted imaging (DWI), DCE-MRI, and MRS have been gradually developed, and the advantages of MRI in the diagnosis of prostate cancer with high accuracy have been widely studied in clinical medicine [13–16].

DCE-MRI reflects the morphological and functional information of various parts of the prostate with its dynamic enhancement method. In this study, the relative signal strength values and strengthening methods are consistent with the results of other similar studies. The main manifestations of our results are as follows: the reinforcement of the normal peripheral zone was slow and uniform, and no obvious abnormal reinforcement was observed; the enhancement peak of prostate hyperplasia appeared later; prostate cancer appeared as a fast-forward and fast-out enhancement method, which strengthens the earliest peak appearance, reaching approximately 1.0 at 21 s after contrast injection. The different expression, peak value, and presenting time of these three types of enhancement methods are closely related to the blood supply of the study participants. It can be seen that the density of normal peripheral microvasculature was significantly lower than that of benign prostatic hyperplasia and prostate cancer, and the enhancement degree was significantly lower as well [17].

It has been reported that MRS analysis shows that the peak value of Cho significantly increases and the peak value of Cit significantly decreases or disappears in a prostate cancer [18]. In this study, it can be seen that the ratio of (Cho + Cr)/Cit and Cho/Cit in the prostate cancer group was compared with the data of the prostate hyperplasia and control groups, and the differences were significant, indicating that the results of this study were consistent with those of other studies. It can also be seen that the marked increase in the Cho peak and the marked decrease or disappearance of the Cit peak are one of the characteristic manifestations of prostate cancer in MRS. The Cho/Cit and (Cho + Cr)/Cit ratios are important bases for the diagnosis of prostate cancer [19]. The contents of Cho and Cit in prostate cancer show significantly abnormal changes. In this study, the changes in the above metabolites showed characteristic crest changes in the MRS spectrum analysis, which was also consistent with other research results [20–21]. Patients with prostate cancer

had Cho/Cit ≥ 1.0, (Cho + Cr)/Cit ≥ 2.0, and neither benign prostatic hyperplasia nor normal prostate tissue had abnormal changes in the above metabolites, with a specificity of 93.02%. The results indicate that it has high value in the diagnosis and of prostate cancer. However, the MRS examination required a long time and is affected by signals from surrounding tissues of the prostate. Thus, the spectrum was prone to clutter, leading to inaccurate measurements.

From the discussion above, it can be seen that DCE-MRI combined with MRS can greatly improve the value of MRI in the diagnosis of prostate cancer.

Conflicts of interest

The authors indicated no potential conflicts of interest.

References

1. Li M, Zhang SW, Ma JH, *et al*. A comparative study on incidence trends of prostate cancer in part of cities and counties in China. Chin J Urol (Chinese), 2009, 30: 368–370.
2. Siegel RL, Miller KD, Jemal A. Cancer statistics, 2016. CA Cancer J Clin, 2016, 66: 7–30.
3. Collin SM, Martin RM, Metcalfe C, *et al*. Prostate-cancer mortality in the USA and UK in 1975–2004: an ecological study. Lancet Oncol, 2008, 9: 445–452.
4. Zheng RS, Zeng HM, Zhang SW, *et al*. Estimates of cancer incidence and mortality in China, 2013. Chin J Cancer, 2017, 36: 384–389.
5. Xu JQ, Humphrey PA, Kibel AS, *et al*. Magnetic resonance diffusion characteristics of histologically defined prostate cancer in humans. Magn Reson Med, 2009, 61: 842–850.
6. Langer DL, van der Kwast TH, Evans AJ, *et al*. Intermixed normal tissue within prostate cancer: effect on MR imaging measurements of apparent diffusion coefficient and T2 – sparse versus dense cancers. Radiology, 2008, 249: 900–908.
7. Langer DL, van der Kwast TH, Evans AJ, *et al*. Prostate cancer detection with multi-parametric MRI: logistic regression analysis of quantitative T2, diffusion-weighted imaging, and dynamic contrast-enhanced MRI. J Magn Reson Imaging, 2009, 30: 327–334.
8. Knight SP, Browne JE, Meaney JFM, *et al*. Quantitative effects of acquisition duration and temporal resolution on the measurement accuracy of prostate dynamic contrast-enhanced MRI data: a phantom study. MAGMA, 2017, 30: 461–471.
9. Vos PC, Hambrock T, Hulsbergen-van de Kaa CA, *et al*. Computerized analysis of prostate lesions in the peripheral zone using dynamic contrast enhanced MRI. Med Phys, 2008, 35: 888–899.
10. Cheikh AB, Girouin N, Colombel M, *et al*. Evaluation of T2-weighted and dynamic contrast-enhanced MRI in localizing prostate cancer before repeat biopsy. Eur Radiol, 2009, 19: 770–778.
11. McMahon CJ, Bloch BN, Lenkinski RE, *et al*. Dynamic contrast-enhanced MR imaging in the evaluation of patients with prostate cancer. Magn Reson Imaging Clin N Am, 2009, 17: 363–383.
12. Bonekamp D, Macura KJ. Dynamic contrast-enhanced magnetic resonance imaging in the evaluation of the prostate. Top Magn Reson Imaging, 2008, 19: 273–284.
13. Kim CK, Park BK, Kim B. High-b-value diffusion-weighted imaging at 3 T to detect prostate cancer: comparisons between b values of 1000 and 2000 s/mm^2. AJR Am J Roentgenol, 2010, 194: W33–W37.
14. Casciani E, Polettini E, Carmenini E, *et al*. Endorectal and dynamic contrast-enhanced MRI for detection of local recurrence after radical prostatectomy. AJR Am J Roentgenol, 2008, 190: 1187–1192.
15. Wang XY, Zhou LP, Li FY, *et al*. MR spectroscopy of prostate cancer: correlation study of metabolic characters with Gleason score. Chin J Radiol (Chinese), 2006, 40: 1181–1184.
16. Zhang P. Dynamic contrast enhanced MRI and PSA for diagnosis and differentiation of prostate cancer. J Prac Med Techniq (Chinese), 2009, 16: 168–170.
17. Shi H, Wu LB, Ding HY, *et al*. Prostate cancer: diagnostic value of dynamic contrast-enhanced MRI, diffusion weighted imaging and 3D ^{1}H-MR spectroscopy. Chin J Radiol (Chinese), 2006, 40: 678–683.
18. Wu DQ, Chen ZQ. An investigation on the feasibility of using MRS for the diagnosis of prostate diseases by comparing MRS with pathological results. Funct Mol Med Imaging (Electro Edit) (Chinese), 2016, 5: 842–847.
19. Westphalen AC, Kurhanewicz J, Cunha RMG, *et al*. T2-weighted endorectal magnetic resonance imaging of prostate cancer after external beam radiation therapy. Int Braz J Urol, 2009, 35: 171–182.
20. Fuchsjäger M, Akin O, Shukla-Dave A, *et al*. The role of MRI and MRSI in diagnosis, treatment selection, and post-treatment follow-up for prostate cancer. Clin Adv Hematol Oncol, 2009, 7: 193–202.
21. Nong SJ, Guan YB, Wang ZW, *et al*. Clinical study of IL-18 and NANOG gene polymorphisms in prostate cancer patients. Oncol Transl Med, 2018, 4: 247–254.

DOI 10.1007/s10330-020-0414-4
Cite this article as: He YK, Wang M, Deng HP, *et al*. Application of dynamic contrast-enhanced magnetic resonance imaging (DCE-MRI) combined with magnetic resonance spectroscopy (MRS) in prostate cancer diagnosis. Oncol Transl Med, 2021, 7: 31–34.

Oncology and Translational Medicine
DOI 10.1007/s10330-020-0460-0
February 2021, Vol. 7, No. 1, P35–P40

CASE REPORT

Meningeal melanocytoma in the cerebellopontine angle: A rare case report and review of the literature

Minhai Dong[1, 2], Qungen Xiao[1], Jinyang Hu[1], Xiaopeng Li[1], Dongsheng Guo[1], Baofeng Wang[1] (✉)

[1] Department of Neurosurgery, Tongji Hospital, Tongji Medical College, Huazhong University of Science and Technology, Wuhan 430030, China
[2] Department of Neurosurgery, The First Affiliated Hospital of Guangxi Medical University, Nanning 530021, China

Abstract

Primary meningeal melanocytoma (MM) in the cerebellopontine angle (CPA) region is an extremely rare neoplasm that originates from the melanocytes in the leptomeninges. These lesions are usually misdiagnosed as they mimic other common CPA lesions through their nonspecific presenting symptoms, signs, and radiological characteristics. Here, we report a 47-year-old Chinese female patient who presented with a 1-month history of the right-sided tongue numbness and 1-week history of the right-sided face numbness that had been worsening for 2 days. The tumor, in the right CPA region, showed a slight isointensity on T1-weighted image and mixed signal intensity on T2-weighted image. The clinical presentation, surgical treatment, and pathologic characteristics were determined. The tumor was microsurgically resected and gross-total resection was achieved. The tumor revealed a solid, capsulated, brown-black lesion. Immunohistochemistry showed that the tumor cells were positive for human melanoma black-45 (HMB-45), melanoma antigen (MelanA), S100, SOX10, and BRAF, confirming the final diagnosis of meningeal melanocytoma. Ultimately, no signs of radiological local recurrence were observed during the two-year follow-up. Collectively, meningeal melanocytoma is difficult to distinguish from common tumors in the CPA region before operation due to the lack of specificity in imaging and symptoms. Complete surgical resection is the best therapeutic option for this tumor. Although the tumor is commonly considered as a benign lesion, recurrence and metastasis are common, and pathogenesis remains unclear.

Received: 13 October 2020
Revised: 14 November 2020
Accepted: 5 December 2020

Key words: meningeal melanocytoma; cerebellopontine angle; pathology; therapy

Primary meningeal melanocytomas (MMs), first reported by Limas and Tio in 1972 [1] are extremely rare primary brain tumors, accounting for only about 0.07% of all tumors in the central nervous system (CNS), with an annual incidence of 1 case per 10 million individuals [2–3]. MMs are benign lesions originating from the melanocytes of the leptomeninges, and they often present in the leptomeninges adjacent to the medulla oblongata and anterolateral spinal cord because of the abundance of melanocytes here [1]. MMs can occur in different areas of the brain but are commonly seen in the region of the foramen magnum [1], the posterior fossa [4], cervical spinal region [5–7], anterior cranial fossa [8], and the sellar region [9]. However, they rarely occur in the cerebellopontine angle (CPA) region [10–11]. To the best of our knowledge, only ten studies of MMs in the CPA have been published.

Here, we elucidate a case of a pathologically diagnosed MM in the CPA region, which had been treated at our department. We focus on the clinical presentation, surgical treatment, and pathologic characteristics, and review the related literature.

✉ Correspondence to: Baofeng Wang. Email: wbf620@163.com

Clinical summary

History and physical examination

A 47-year-old Chinese woman presented with right-sided tongue numbness for one month and right-sided face numbness for one week, which had been worsening for 2 days prior to admission. She had no headache, hearing loss, or other manifestations of cranial nerve dysfunction. After admission, physical examination findings showed decreased sensation on the right side of the tongue and right-sided mild facial paralysis. There were no mucocutaneous or ocular pigmented lesions. Our study was conducted in accordance with the declaration of Helsinki, and was approved by the Ethics Committee of Tongji Hospital of Wuhan. Written informed consent was obtained from the patient.

Imaging findings

Preoperative computed tomography (CT) displayed a slight hyperdense and well-circumscribed lesion in the right CPA region (Fig. 1a). MRI also revealed a solid oval mass (26 mm × 19 mm) attached to the dura of petrosal surface in the right CPA. The lesion was isointense on T1-weighted image (Fig. 1b) and of mixed signal intensity on T2-weighted image (Fig. 1c), and it showed intense and homogenous enhancement after gadolinium administration (Fig. 1d and 1e). No evidence of angiopathic abnormalities was found on magnetic resonance angiography scan (Fig. 1f).

Therapeutic intervention

The right retrosigmoid suboccipital approach was performed and the lesion was microsurgically resected under continuous intraoperative neurophysiologic monitoring. Microscopy revealed a brown-black solid lesion in the right CPA region. The tumor seemed to derive from the dura mater, and the brainstem was slightly compressed. The lesion was a slightly soft, well-circumscribed brown-black pigmented tumor, and a gross-total resection was achieved.

Pathological results

Tumor sections stained with hematoxylin and eosin (H&E) comprised of a large number of spindle-shaped cells, with a strip distribution and focal storiform pattern, and could be markedly observed in tumor tissues (Fig. 2a). Many spherical nucleus cells that contained granules of dark brown pigment were distributed among the tumor cells (Fig. 2b). However, there were rare mitotic images and areas of necrosis in the region of the tumor. The tumor cells showed strongly positive staining for some relatively special markers of meningeal melanocytoma including HMB-45, MelanA, S100, SOX10, and BRAF (Fig. 2c–2g). Furthermore, cellular proliferative activity assessed by Ki67 labeling index was low, approximately 5% (Fig. 2h). The final diagnosis of MM was established according to

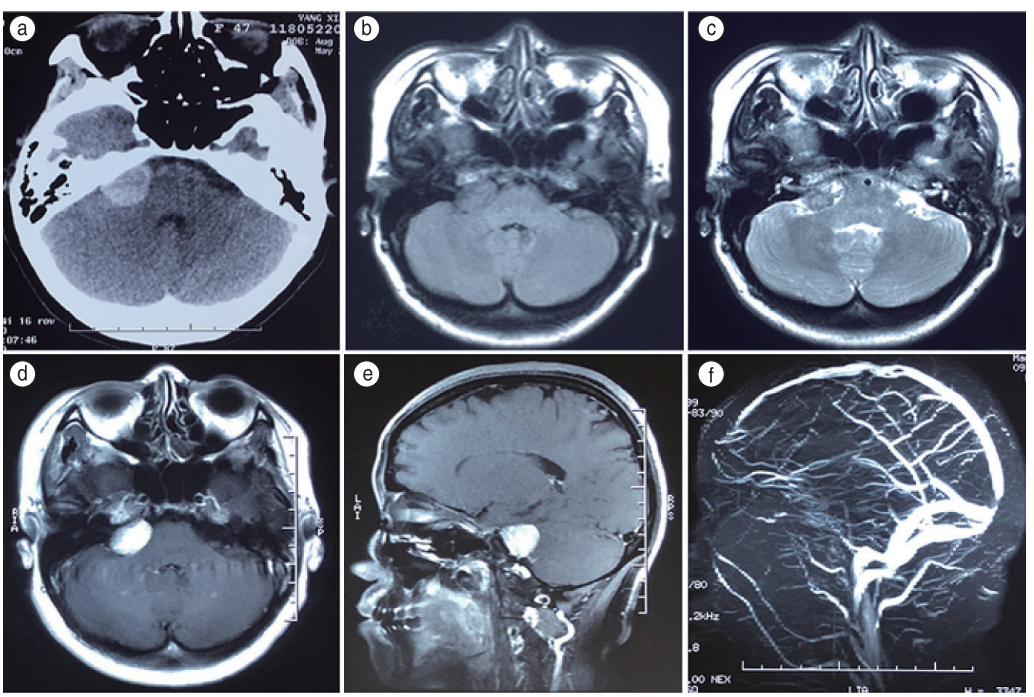

Fig. 1 Imaging findings (a) CT showed a hyperdense and well-circumscribed lesion in the right cerebellopontine angle (CPA) region; (b and c) The lesion was isointense on T1-weighted sequences (b) and of mixed signal intensity on T2-weighted sequences (c); (d and e) T1-weighted images presented intense and homogenous enhancement in the right CPA; (f) Magnetic resonance angiography (MRA) scan showed no obvious abnormity

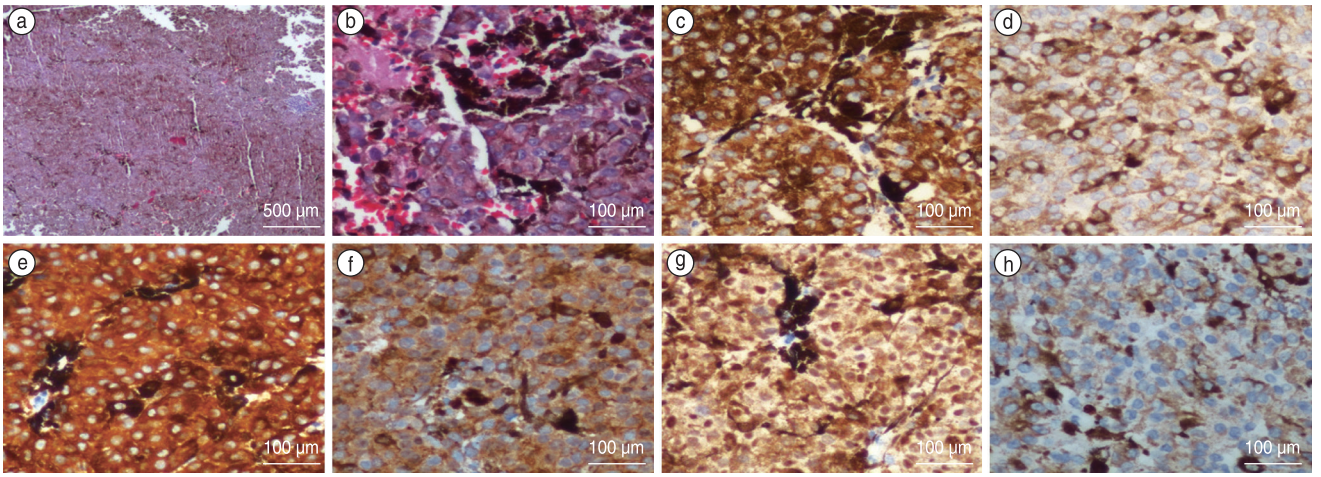

Fig. 2 Histopathological findings. (a and b) Tumor cells arranged in fascicles interspersed with melanin-containing cells in H&E staining; (c–h) The tumor cells were positive for HMB-45 (c), Melan A (d), S100 (e), SOX10 (f), BRAF (g), and Ki67 (h). (× 200)

the histopathological and immunohistochemical results.

Follow-up

Postoperatively, the symptoms eventually resolved, and there was no focal neurologic deficit or complications associated with surgery upon discharge. The patient underwent neither radiotherapy nor chemotherapy after surgery. During the two-year follow-up, no evidence of local recurrence was observed (Fig. 3a and 3b).

Discussion

Primary pigmented tumors of the leptomeninges, which include pigmented meningioma, primary central nervous system (CNS) malignant melanoma, melancholic schwannoma, melanoblastosis, and MMs, are rare lesions in the brain [12–13]. MMs are exceptionally rare benign tumors of the central nervous system [8, 12]. Additionally, the occurrence of meningeal melanocytoma in the CPA region is extremely uncommon, with only ten cases previously described in relevant literature (Table 1). Although the tumor attaching to the meninges often grossly resembles meningioma on radiology [10, 14–15], MMs are ultrastructurally similar to melanoma in their histology and pathology [14–16]. Gratifyingly, they commonly shows a favorable clinical prognosis [17]. Importantly, because the biological behavior, management, and prognosis of MMs is different from meningioma, it is necessary to distinguish those tumors in order to make a suitable therapeutic strategy and prognosis for MM.

Lacking distinctive clinical symptoms, MMs are often difficult to distinguish from some usual lesions of the CPA before operation, such as vestibular schwannomas, meningiomas, and epidermoid tumors. Preoperative

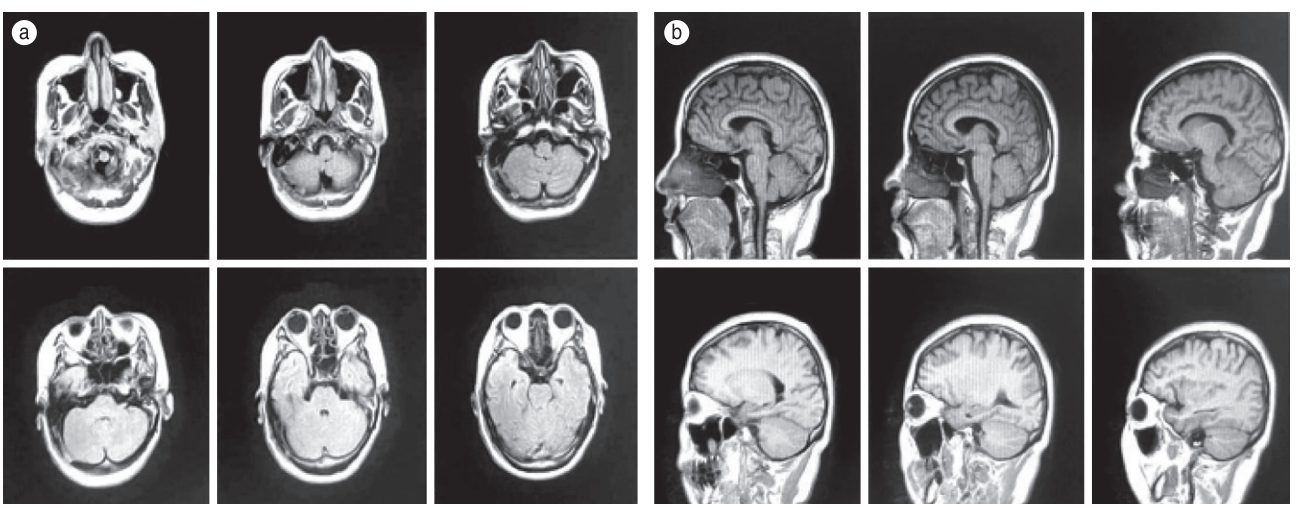

Fig. 3 Imaging results of 2 years after operation (a and b). There is no recurrence of the tumor on magnetic resonance imaging

Table 1 Cases of meningeal melanocytoma of CPA

Case and reference	Age/sex	Tumour lacation	T1: T2 weighted imaging	Treatmecnt	Immunohistoche mical finding	Ki67(%)	Recurrence Time of Dead
Prabhu,1993 [32]	67/Women	CPA	N	S	HMB45(+)S100(+)	–	NR/4month(D)
Gardiman,1996 [33]	19/Men	CPA	N	S	Vimentin(+)S100(+)HMB45(–)	–	NR
Gardiman,1996 [33]	43/Men	CPA	N	S	Vimentin(+)S100(+)HMB45(–)	–	Re/5month(D)
Clarke,1998 [21]	30/Women	CPA	Hyper-intensity; N	S&R	Vimentin(+)S100(+)	–	Re/6month(D)
Hamasaki, 2002 [18]	59/Men	CPA	Hyper-intensity; Hypo-intensity	S&R	HMB45(+)S100(+)HMB45(-)	–	NR/2 years
Horst, 2005 [26]	38/Men	CPA	Hyperintense; iso-hypointense	S	MelanA(+)	–	Re/5 years
Gupta, 2007 [13]	58/Women	CPA	Heterogeneously Hyperintense; hypointense	S	HMB45(+)vimentin(+)MelanA(+) EMA(–)	–	NR
Masaaki, 2011 [34]	43/Women	CPA	Hyperintense; hypointense	S	HMB45(+)S100(+)	4%–5%	Re/20 month
Gjergji, 2011 [10]	47/Men	CPA	Hyperintense; iso-hypointense	S	–	10%	Re/20 month
Rasha, 2018 [11]	46/Men	CPA	Hyperintense; hypointense	S	S100(+)	–	N
This case	47/Women	CPA	Iso-hypointense; Heterogeneously Hyperintense	S	HMB45(+)BRAF(+)MelanA(+) S100(+)SOX10(+)	5%	NR

CPA: cerebellopontine angle; N: no evidence; S: surgical; R: radiotherapy; Re: recurrence; B: biopsy; NR: not recurrence; D: dead

imaging studies are also nonspecific and inconclusive for MMs, leading to frequent preoperative misdiagnoses. On CT scan, MMs appear as a well-circumscribed, iso- to slightly hyperdense lesion with dural attachment [18–19]. Congruently, the tumor, in our case, was hyperdense and well-circumscribed on CT scan. The signal pattern of MMs on MRI scan varies widely, depending on melanin and presence of hemorrhage. Generally, the tumor was hyperintense or isointense on T1-weighted sequences and isointense or slightly hypointense on T2-weighted sequences with homogeneous enhancement on contrast-enhanced MRI [9, 19]. Recently, Shoko summarized the characteristic image features of 14 cases of intracranial MMs documented in English literature and found that eleven cases showed hyperintensity on T1-weighted images and were hypointense on T2-weighted images [20]. However, the MM in our case was isointense on T1-weighted sequences, with homogenous enhancement after gadolinium administration, and of mixed signal intensity on T2-weighted sequences, which is not consistent with the general characteristic MRI features of MMs. The degree and distribution of the melanin pigments and presence of hemorrhage in the tumor might have resulted in an uncommon presentation in the MRI in our case. We then summarized the MRI features of MMs in the CPA region in the English literature, which are generally in line with the characteristic MRI features, with high signal intensity on T1-weighted images and low signal intensity on T2-weighted images (Table 1). Collectively, it is difficult to provide preoperative value through MRI studies in the diagnosis of meningeal melanocytoma.

The definitive diagnosis of MM and the differential diagnosis are best achieved postoperatively through histopathological and immunohistochemical studies. The histopathological characteristics of MMs have been documented [10]. Briefly, the general morphology of MMs usually presents as an encapsulated black or dark brown solid lesion that is tightly attached to the underlying meninges [13], as seen in the present case. Microscopically, there are several melanin granules in the tumor cells. It can obviously be observed that tumor cells with prominently spherical nuclei are arranged in bundles and enriched with melanin pigments. Characteristic immunohistochemical reaction of this lesion includes a positive response to HMB-45, Melan-A, Vimentin, and S-100 [8, 12, 21]. HMB-45 and Melan-A are two specific markers detectable in most melanocytic lesions, and S-100 and vimentin are indicators of cells with mesenchymal origin. However, the antigen of EMA and Leu-7 are usually negative, differentiating MMs from melanotic meningioma and melanotic schwannoma [4, 22]. The differential diagnosis between MM and malignant melanoma can sometime be difficult as they share some common histological features. However, melanocytomas are characterized by nuclear pleomorphism, necrosis, and a lack of or decreased mitosis. Importantly, Ki-67 labeling index, which is an important marker to evaluate malignancy and predict the recurrence of tumors, is often expressed less than 5% in MMs and more than 10% in malignant melanomas [9, 23]. In this case, we found that the lesion was enriched with melanin, and the cells were arranged in sheaf with obvious nuclei. Immunohistochemical findings showed the antigens of HMB45, BRAF, MelanA, S100, and SOX10 to be positive, and the Ki-67 labeling index was approximately 5%, which corresponded with the pre-descriptive characteristics of MM on pathology and immunohistochemistry.

Although MMs are histologically benign tumors, malignant transformation and recurrence have been reported, despite complete surgical removal. In 2003, Uozumi *et al* reported the first case of malignant transformation of an intracranial MM. The patient

underwent gross total removal of the MM. However, four years later, the patient underwent radiotherapy and an additional operation because of a local recurrence. Histopathological examination revealed a malignant melanoma originating from a melanocytoma, and the patient died from cerebrospinal fluid dissemination. [24] Wang *et al* also presented a case of malignant transformation of an intracranial supratentorial MM which recurred as malignant melanoma 3 years after total resection [25]. Roser *et al* described a case of malignant transition of an intracranial melanocytoma into a melanoma 12 years after subtotal tumor resection of the initial tumor. The patient died 4 months after the second operation from a rapid diffuse meningeal spread of the tumor, despite a combination of whole brain radiotherapy and chemotherapy [23]. As for the recurrence of MMs, Koch *et al* also reported a patient with MM of the CPA who suffered a first local recurrence 5 years after surgical resection and a second local recurrence 6 years after diagnosis, with tumor cells seeding to the intracerebral and spinal meninges (Table 1) [26]. Naturally, the frequent phenomenon of malignant transformation or recurrence has prompted researchers to explore its pathogenesis. There are a few possible causes for the transformation or recurrence of MMs: first, most scholars believe that MMs exhibit relatively benign characteristics [27]; second, the region of the CPA is complicated, which precludes complete removal of the tumor [3]. However, with respect to the present case, no sign of local recurrence was observed at the postoperative two-year follow-up.

To the best of our knowledge, there is no specific guideline for the management of the MMs as they are rare tumors. The best therapeutic option for MMs is complete removal of the tumor whenever possible [28]. Rades reviewed 89 patients with MMs and found that the five-year survival rate and the five-year local control were 100% and 80%, respectively, in patients with complete resection, but only 46% and 18%, respectively, in those with incomplete resection [29], indicating the vital role of complete resection in the outcome of MMs. Complete tumor removal was also achieved in the present case, and no recurrence was observed at the postoperative two-year follow-up. However, failure of complete resection of the lesion can be attributed to several factors, such as poor tumor location, involvement of vital structures or skull base dura [8], excessive tumor bleeding [9, 21], and excessive tumor volume [30]. Noteworthy, Rades also found that the five-year survival rate was 100% in patients with combined incomplete resection and postoperative radiotherapy versus 46% in patients with incomplete resection only [29], suggesting that postoperative radiotherapy should be advised in cases of incomplete resection. Other cases of MMs, wherein tumors were partially removed by surgery and postoperative radiotherapy was beneficial, have been reported. Kurita *et al* described a case of MM from the Meckel's cave, wherein gamma knife radiotherapy was performed after the tumor was partially removed. The tumor showed marked shrinkage without complication after three years of irradiation [31]. Hamasaki *et al.* also presented a patient, with residual MM tumor in the CPA region, who underwent radiosurgery and showed no evidence of regrowth or metastasis 24 months later (Table 1) [18]. Clarke reported another case of MM in the CPA, wherein radiotherapy was performed after the tumor was partially removed. Although regrowth of the residual tumor was observed, the tumor was much less vascular after radiotherapy and a complete resection was achieved upon second operation (Table 1) [21]. Kuo *et al* reported that the survival time of MM between surgery alone and surgery plus radiotherapy was not significantly different. However, adjuvant radiotherapy showed a trend towards improved survival [28]. In our retrospective study for MM of the CPA, all 8 patients with CPA MM underwent surgical treatment, of which 2 patients underwent surgery plus adjuvant radiotherapy and 6 patients underwent surgery solely. The observed survival time was 4 months to 5 years. Table 1 shows the clinical characteristics and prognosis of the 11 cases of CPA MM. Therefore, to the best of our knowledge and based on the published data, complete removal of the tumor is the best therapeutic option for MM, and postoperative radiotherapy appears to improve both local control and survival. However, further clinical evidence-based research is needed to draw a definite conclusions regarding the benefits of radiotherapy in MM treatment. Although MM is rare in the central nervous system, it is often misdiagnosed as common tumors in the CPA region before surgical resection due to the lack of specificity in imaging and in the patient's symptoms. Although the tumor is usually considered to be benign, recurrence and metastasis have also been reported. Total resection is the best therapeutic option. Some adjuvant treatments, such as chemotherapy and radiotherapy, can be selectively considered. However, their curative effect needs further verification.

Conflicts of interest

The authors indicated no potential conflicts of interest.

References

1. Limas C, Tio FO. Meningeal melanocytoma ("melanotic meningioma"). Its melanocytic origin as revealed by electron microscopy. Cancer, 1972, 30: 1286–1294.
2. Balakrishnan R, Porag R, Asif DS, *et al*. Primary intracranial melanoma with early leptomeningeal spread: a case report and treatment options available. Case Rep Oncol Med, 2015, 2015: 293802.
3. Adib SD, Ebner FH, Bornemann A, *et al*. Surgical management of primary cerebellopontine angle melanocytoma: outcome, recurrence and additional therapeutic options. World Neurosurg, 2019, 128:

e835–e840.
4. O'Brien TF, Moran M, Miller JH, *et al*. Meningeal melanocytoma. An uncommon diagnostic pitfall in surgical neuropathology. Arch Pathol Lab Med, 1995; 119: 542–546.
5. Bydon A, Gutierrez JA, Mahmood A. Meningeal melanocytoma: an aggressive course for a benign tumor. J Neurooncol, 2003, 64: 259–263.
6. Kim OH, Kim SJ, Choo HJ, *et al*. Spinal meningeal melanocytoma with benign histology showing leptomeningeal spread: case report. Korean J Radiol, 2013, 14: 470–476.
7. Yin M, Ma J, Ye J, *et al*. 8-year follow-up for woman with spinal meningeal melanocytoma in S1 nerve root: case report and literature review. World Neurosurg, 2019, 129: 143–147.
8. Lin B, Yang H, Qu L, *et al*. Primary meningeal melanocytoma of the anterior cranial fossa: a case report and review of the literature. World J Surg Oncol, 2012, 103: 135.
9. Wang F, Ling S. Primary meningeal melanocytoma in sellar region, simulating a nonfunctioning pituitary adenoma: case report and literature review. World Neurosurg, 2018, 112: 209–213.
10. Vreto G, Rroji A, Xhumari A, *et al*. Meningeal melanocytoma of the cerebellopontine angle as the unusual cause of superficial siderosis. Neuroradiology, 2011, 53: 927–930.
11. Elbadry R, Elazim AA, Mohamed K, *et al*. Primary meningeal melanocytoma of the cerebellopontine angle associated with ipsilateral nevus of Ota: A case report. Surg Neurol Int, 2018, 9: 245.
12. Litofsky NS, Zee CS, Breeze RE, *et al*. Meningeal melanocytoma: diagnostic criteria for a rare lesion. Neurosurgery, 1992, 31: 945–948.
13. Gupta A, Ahmad FU, Sharma MC, *et al*. Cerebellopontine angle meningeal melanocytoma: a rare tumor in an uncommon location. Case report. J Neurosurg, 2007, 106: 1094–1097.
14. Jellinger K, Böck F, Brenner H. Meningeal melanocytoma. Report of a case and review of the literature. Acta Neurochir (Wien), 1988, 94: 78–87.
15. Maiuri F, Iaconetta G, Benvenuti D, *et al*. Intracranial meningeal melanocytoma: case report. Surg Neurol, 1995, 44: 556–561.
16. Ahluwalia S, Ashkan K, Casey AT. Meningeal melanocytoma: clinical features and review of the literature. Br J Neurosurg, 2003, 17: 347–351.
17. Perrini P, Caniglia M, Pieroni M, *et al*. Malignant transformation of intramedullary melanocytoma: case report. Neurosurgery, 2010, 67: E867–869; discussion E69.
18. Hamasaki O, Nakahara T, Sakamoto S, *et al*. Intracranial meningeal melanocytoma. Neurol Med Chir, 2002, 42: 504–509.
19. Samadian M, Nejad AM, Bakhtevari MH, *et al*. Primary meningeal melanocytoma in the left temporal lobe associated with nevus ota: a case report and review of the literature. World Neurosurg, 2015, 84: 567–573.
20. Gamoh S, Tsuno T, Akiyama H, *et al*. Intracranial meningeal melanocytoma diagnosed using an interdisciplinary approach: a case report and review of the literature. J Med Case Rep, 2018, 12: 177.
21. Clarke DB, Leblanc R, Bertrand G, *et al*. Meningeal melanocytoma. Report of a case and a historical comparison. J Neurosurg, 1998, 88: 116–121.
22. Wang H, Zhang S, Wu C, *et al*. Melanocytomas of the central nervous system: a clinicopathological and molecular study. Eur J Clin Invest, 2013, 43: 809–815.
23. Roser F, Nakamura M, Brandis A, *et al*. Transition from meningeal melanocytoma to primary cerebral melanoma. Case report. J Neurosurg, 2004, 101: 528–531.
24. Uozumi Y, Kawano T, Kawaguchi T, *et al*. Malignant transformation of meningeal melanocytoma: a case report. Brain Tumor Pathol, 2003, 20: 21–25.
25. Wang F, Qiao G, Lou X, *et al*. Malignant transformation of intracranial meningeal melanocytoma. Case report and review of the literature. Neuropathology, 2011, 31: 414–420.
26. Koch HJ, Roeber S, Zimmermann UW, *et al*. Spinal and cerebral leptomeningeal seeding from a melanocytoma of the cerebello-pontine angle. Wie Med Wochenschr, 2005, 155: 360–364.
27. Radner H, Blümcke I, Reifenberger G, *et al*. The new WHO classification of tumors of the nervous system 2000. Pathology and genetics. Pathologe, 2002, 23: 260–283.
28. Kuo KL, Lin CL, Wu CH, *et al*. Meningeal melanocytoma associated with nevus of ota: analysis of twelve reported cases. World Neurosurg, 2019, 127: e311–e320.
29. Rades D, Schild SE, Tatagiba M, *et al*. Therapy of meningeal melanocytomas. Cancer, 2004, 100: 2442–2447.
30. Sun J, Wang C, Shu Q, *et al*. A case report on intermediate-grade malignant meningeal melanocytoma with elevated cell proliferation index. Int J Clin Expe Pathol, 2015, 8: 11698–11703.
31. Kurita H, Segawa H, Shin M, *et al*. Radiosurgery of meningeal melanocytoma. J Neurooncol, 2000, 46: 57–61.
32. Prabhu SS, Lynch PG, Keogh AJ, *et al*. Intracranial meningeal melanocytoma: a report of two cases and a review of the literature. Surg Neurol, 1993, 40: 516–521.
33. Gardiman M, Altavilla G, Marchioro L, *et al*. Meningeal melanocytoma: a rare lesion of the central nervous system. Tumori, 1996, 82: 494–496.
34. Mikamoto M, Seo Y, Ito T, *et al*. A case of meningeal melanocytoma in the cerebellopontine angle. No Shinkei Geka, 2011, 39: 859–864.

DOI 10.1007/s10330-020-0460-0
Cite this article as: Dong MH, Xiao QG, Hu JY, *et al*. Meningeal melanocytoma in the cerebellopontine angle: A rare case report and review of the literature. Oncol Transl Med, 2021, 7: 35–40.

Oncology and Translational Medicine
DOI 10.1007/s10330-020-0463-3

Februry 2021, Vol. 7, No. 1, P41–P44

CASE REPORT

Ewing sarcoma/primitive neuroectodermal tumor of the ureter: A case report and literature review

Qian Zhou[1, 2], Guobo Du[2], Jie Tang[1], Yujia Wang[1], Yu Xiao[1], Bangxian Tan[2] (✉)

[1] North Sichuan Medical College, Nanchong 637000, China
[2] Department of Oncology, Affiliated Hospital of North Sichuan Medical College, Nanchong 637000, China

Abstract

Ewing sarcoma/primary neuroectodermal tumors are rare, invasive, and small round blue cell tumors. There are few reports of its occurrence in the urinary system. Here, we present the first middle-aged female patient whose Ewing sarcoma primary site was in the ureter. The main clinical manifestation was intermittent hematuria. She was in good health after complete surgical resection and adjuvant radiotherapy. To date, there has been no recurrence or metastasis. Accurate early diagnosis and appropriate treatment can help prolong survival. 18F-fluorodeoxyglucose positron emission tomography/computed tomography is expected to be an effective means of evaluating treatment effects and detecting metastasis and recurrence. In this article, besides introducing a case of Ewing sarcoma/primitive neuroectodermal tumor of the ureter, we review the literature to discuss the current status of diagnosis and treatment.

Received: 19 October 2020
Revised: 27 December 2020
Accepted: 15 January 2021

Key words: Ewing sarcoma (ES); primitive neuroectodermal tumor (PNET); ureter; positron emission tomography/computed tomography (PET/CT)

In 1918, Stout described, for the first time, a solid tumor originating from the ulnar nerve, which was later named primitive neuroectodermal tumor (PNET). Subsequently, Ewing discovered a sarcoma he named after himself—Ewing sarcoma (ES)—composed of long bones' undifferentiated cells. In 1973, Hart and Earle proposed that PNET is a malignant small round cell tumor originating from the neural crest [1]. According to the location, PNET can be divided into central PNET and peripheral PNET (pPNET). Because pPNET and ES share the same chromosomal translocation, approximately 85% of ES and pPNET present a specific t(11;22)(q24;q12) balanced translocation, which in 2002, the World Health Organization classified as the ES family of tumors that also includes Askin tumors (ES of the chest wall).

ES/PNET is a highly malignant and extremely rare small round cell tumor, showing varying degrees of neuroectodermal differentiation, which usually occurs in children and adolescents. ES/PNET mainly affects the bones or soft tissues but is not common in the urinary tract. It is mostly reported in case forms, such as in the kidney and bladder, but rare in the ureter. It is challenging to make a preoperative diagnosis and identify other diseases based on clinical symptoms and imaging findings. The diagnosis mainly depends on histological biopsy, immunohistochemistry (IHC), and gene detection. Complete surgical resection combined with adjuvant radiotherapy and chemotherapy is the primary treatment method, whereas a new type of targeted immunotherapy is now being investigated in clinical trials [2].

Case presentation

On July 29, 2019, a 45-year-old woman presented with painless gross hematuria for 3 months. There was no obvious abnormality in patient history, family history, or physical examination. Ultrasound, magnetic resonance imaging, and 18F-FDG PET/CT examination showed that the lower part of the right ureter and bladder triangle was 1.8 cm × 1.5 cm × 0.8 cm, and the presence of a tumor

✉ Correspondence to: Bangxian Tan. Email: tbx_nsmc@126.com

was considered (Fig. 1a–1e). The urine smear showed squamous epithelium and lymphocytes; laboratory examination revealed mild anemia (hemoglobin, 101 g/L). After that, the right kidney was removed, and ureterectomy was performed. A lower ureteral neoplasm was observed during the surgery, and lumen stenosis with rough mucosa was found. An intraoperative frozen section evaluation of the ureter suggested invasive urothelial carcinoma (Fig. 2a). The patient recovered well after surgery.

Histological examination of the excised specimen indicated that the right ureteral carcinoma had infiltrated the muscular layer of the wall, but the rest of the tissues were not involved. The tumor was composed of small round blue cells, suggesting the presence of ES/PNET (Fig. 2b). IHC showed that the cells were CD99 diffusely positive, CD117(+), Fli-1(–), cytokeratin (CK, –), desmin(–), chromogranin (CgA, –), synaptophysin (SYN, –), WT-1(–), CD56(–), and S-100(–). These results supported the diagnosis (Fig. 2c). Fluorescence in situ hybridization (FISH) detection revealed a EWSR1 gene (22q12) breakage, consistent with that in ES/PNET. The patient received volumetric modulated arc radiotherapy 1 month after the surgery, with a total dose of 50.4 Gy in 28 fractions at the tumor bed and pelvic drainage area. During the same period, she was simultaneously administered chemotherapy with lobaplatin (40 mg) once a week. After the second administration of chemotherapy, the patient had severe leukopenia and third-degree myelosuppression, which improved after symptomatic support. No severe complications or abnormal lesions were found during the follow-up period. It has been 16 months since the initial diagnosis. At present, the patient receives oral capecitabine maintenance therapy with a

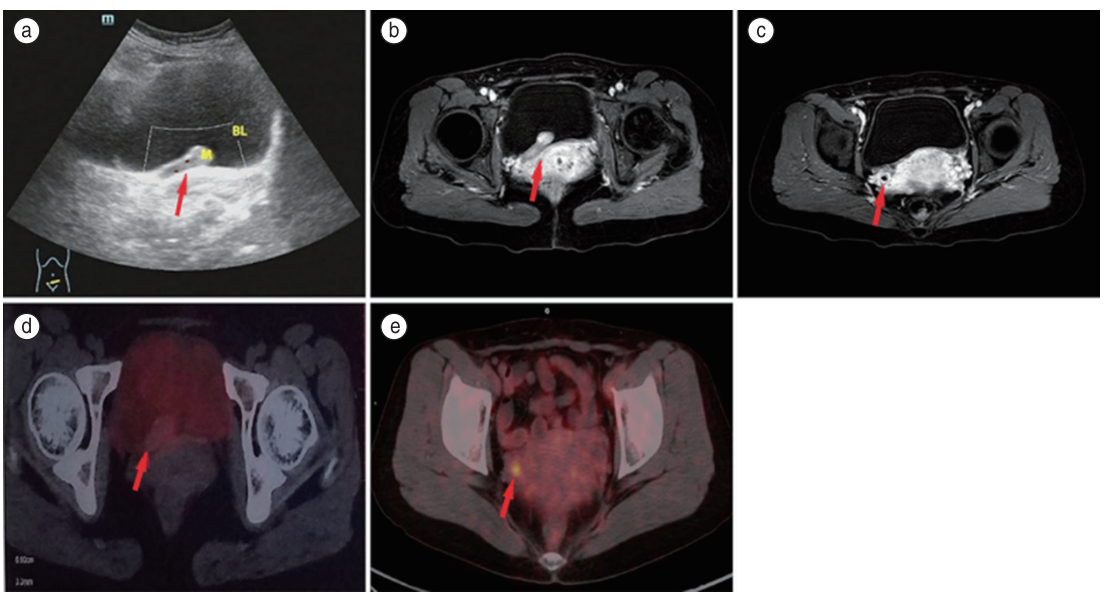

Fig. 1 US, MRI and PET/CT images of tumor. (a) US image shows hypoechoic nodule can be seen in the triangle of the bladder, with regular shapes and clear boundaries; (b, c) Enhanced axial MRI images show abnormal signal shadow in the bladder triangle, thickening of the ureteral wall with dilation; (d, e) 18F-FDG PET/CT images show solid nodules in the right ureter and bladder triangle with increased radioactivity uptake. US, ultrasound; MRI, magnetic Resonance Imaging; 18F-FDG PET/CT, 18F-fluorodeoxyglucose positron emission tomography/computed tomography

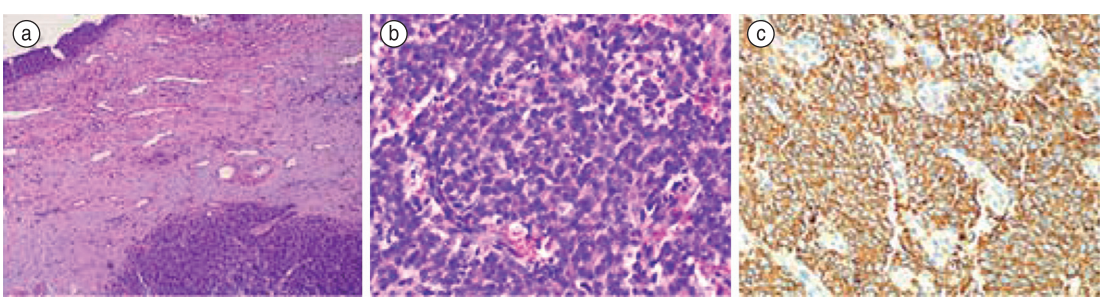

Fig. 2 Histologic and immunohistochemical images of tumor. (a) Cancer cells in the interstitium showed invasive growth (× 100); (b) Microscopically, histologic analysis of hematoxylin and eosin staining (× 200) revealed that the tumor was composed of small blue round cells; (c) Immunohistochemical staining showed positive expression for CD99 (× 400)

good mental state, appetite, and sleep state and is being closely followed up.

Discussion

Principal findings

The clinical and imaging findings of urinary ES/PNET are not specific, and most of the symptoms are related to the involved site; thus, a direct diagnosis is difficult, and ES/PNET is easily misdiagnosed as other common space-occupying diseases. Extraosseous ES is highly malignant, aggressive, and easily metastasizes or recurs in the early stage. Although patients show obvious local clinical signs, occult metastases may also exist in most localized diseases, resulting in a short survival period; the 5-year disease-free survival rate is approximately 45% to 55%, and the 3-year survival rate is 60%. Histopathologically, ES/PNET is mainly characterized by small round blue cells of equal size, evident nucleoli, fine nuclear chromatin, and sparse or vacuolar cytoplasm. IHC and molecular genetics play an essential role in diagnosis and differentiation. CD99 (MIC-2 gene product) and FLi-1 are sensitive indices for diagnosis, but their specificity is not high; they can also be expressed in small round cell tumors such as lymphoma and rhabdomyosarcoma and can be distinguished by combining with other biomarkers such as neuron-specific enolase (NSE), vimentin, desmin, CK, CgA, SYN, and S-100. EWS dual-color, breakable-apart rearrangement probe FISH detection is a highly sensitive and specific diagnostic technique, which combined with CD99 is the preferred diagnostic method, and the combination of CD99 and FLi-1 can improve specificity.

There is no standard treatment guided by evidence-based medicine. Usually, a comprehensive treatment mode of surgery is adopted, supplemented by radiotherapy and chemotherapy, and the most commonly used chemotherapy regimens are VCD + IE (VCD: vincristine+cyclophosphamide+doxorubicin; IE: ifosfamide+etoposide). Some studies have proposed that sandwich therapy (neoadjuvant chemotherapy+surgery+adjuvant chemotherapy) can be used for ES/PNET, and radiotherapy can be used as a postoperative adjuvant or an alternative in locally advanced disease that is not amenable for surgery [3]. Thorough surgical resection is important for the control of local diseases. The 2-year overall survival rate of patients undergoing surgery is approximately 80%, whereas the survival rate of patients who do not undergo surgery is 30%. Despite the aggressive treatment strategy, the prognosis of ES/PNET is still frustrating, with a median overall survival of approximately 26.5 months. Kuroda *et al* [4] have pointed out that the average age at the time of diagnosis is 27.7 years, and whether metastasis is present at the time of diagnosis is a critical factor influencing prognosis. The 5-year survival rates of metastatic and localized diseases are 22% and 55%, respectively. Young age may be a protective factor. Some studies have shown that the prognosis of adults is worse than that of children, and this difference may derive from the dose of chemotherapy drugs and the duration of local treatment [5]. In addition, the tumor size and location of the central axis are also adverse prognostic factors. At present, there are no definite protocols for the follow-up period. The authors believe that if conditions permit, the follow-up period should be extended to monitor the changes in the disease or even carry out a lifetime follow-up.

A case of a middle-aged woman with ureteral ES/PNET is presented for the first time in this article. Thus far, only five cases of ureteral ES/PNET have been reported in the English literature [6–10] (Table 1). These patients were treated for abdominal pain or hematuria. Among them, three minor patients underwent surgery and chemotherapy, and two of them could be traced to follow-up; the longest disease-free survival time was 8 years. An adult male relapsed twice after surgery and radiochemotherapy and died of disseminated disease. Another elderly female patient only underwent surgery, and there was no obvious abnormality in the examination at 6 months follow-up. Our patient was in good condition

Table 1 Characteristics of 5 patients with ureteral ES/PNET

Case No.	Gender	Age (years)	Location	Symptoms	Treatment	Prognosis
1	Female	17	Right ureter	Right flank pain and hematuria	Surgery+ chemotherapy	None
2	Male	45	Left ureter	Painless hematuria	Surgery+ chemotherapy+ palliative radiotherapy	Relapsed 3 years after the first operation, relapsed 7 years after the second operation, and died of metastasis 2 years later
3	Male	12	Right ureter	Abdominal pain	Surgery+ chemotherapy	Disease-free survival 8 months after surgery
4	Male	12	Right ureter	Abdominal pain	Surgery+ chemotherapy	Disease-free survival for 8 years without recurrence
5	Female	69	Left ureter	abdominal pain and hematuria	Surgery	Followed up for 6 months without recurrence and metastasis

ES/PNET, Ewing's sarcoma/primary neuroectodermal tumor

after complete surgical resection and radiotherapy, and there was no recurrence or metastasis 11 months after the completion of treatment. Unfortunately, our patients did not receive standard systemic chemotherapy because of long-term leukopenia. Currently, only maintenance monotherapy is administered, which requires close observation and follow-up. This patient underwent a systemic PET/CT scan before surgery to rule out other possible lesions. Some studies [11] have pointed out that this examination can also be carried out during follow-up to evaluate treatment response, distant metastasis, and recurrence.

Conclusion

Urinary tract ES/PNET is a rare disease. The most fundamental challenge is an accurate preliminary diagnosis, combined with active systematic treatment and close follow-up to improve the prognosis and survival time. With the increasing application of IHC markers, the regulation of tumor transformation, growth, and metastasis is becoming increasingly sophisticated, and potential therapeutic targets and diagnosed cases will increase. The establishment of a global database for these rare malignant tumors will also contribute to improving treatment strategies.

Conflicts of interest

The authors indicated no potential conflicts of interest.

References

1. Hart MN, Earle KM. Primitive neuroectodermal tumors of the brain in children. Cancer. 1973, 32: 890–897.
2. PDQ Pediatric Treatment Editorial Board. Ewing Sarcoma Treatment (PDQ®): Health Professional Version. In: PDQ Cancer Information Summaries. Bethesda (MD): National Cancer Institute (US). 2002–2021.
3. Gupta V, Raju KVVN, Sridhar D, *et al*. Primary Ewing's sarcoma/primitive neuroectodermal tumour of the cervix: a rare tumour. Indian J Surg Oncol, 2020,11: 162–165.
4. Kuroda M, Urano M, Abe M, *et al*. Primary primitive neuroectodermal tumor of the kidney. Pathol Int, 2000, 50: 967–972.
5. Gupta AA, Pappo A, Saunders N, *et al*. Clinical outcome of children and adults with localized Ewing sarcoma: impact of chemotherapy dose and timing of local therapy. Cancer, 2010, 116: 3189–3194.
6. He Y, Sun N, Zhang W, *et al*. Ewing sarcoma/primitive neuroectodermal tumor of the urogenital system in children: a retrospective observational case series. J Pediatr Urol, 2019, 15: 556.e1–556.e7.
7. Charny CK, Glick RD, Genega EM, *et al*. Ewing's sarcoma/primitive neuroectodermal tumor of the ureter: a case report and review of the literature. J Pediatr Surg, 2000, 35: 1356–1358.
8. Huang KH, Shun CT, Huang SY, *et al*. Primary primitive neuroectodermal tumor of the urinary tract. J Formos Med Assoc. 2006,105: 1008–1012.
9. Song HC, Sun N, Zhang WP, *et al*. Primary Ewing's sarcoma/primitive neuroectodermal tumor of the urogenital tract in children. Chin Med J (Engl), 2012, 125: 932–936.
10. Li XX, Bi JB. Ureteral Ewing's sarcoma in an elderly woman: A case report. World J Clin Cases, 2019, 7: 3372–3376.
11. Doroudinia A, Ahmadi S, Mehrian P, *et al*. Primary Ewing sarcoma of the kidney. BMJ Case Rep, 2019, 12: bcr-2018-227198.

DOI 10.1007/s10330-020-0463-3
Cite this article as: Zhou Q, Du GB, Tang J, *et al*. Ewing sarcoma/primitive neuroectodermal tumor of the ureter: A case report and literature review. Oncol Transl Med, 2021, 7: 41–44.

Oncology and Translational Medicine
DOI 10.1007/s10330-020-0450-0

February 2021, Vol. 7, No. 1, P45–P47

CASE REPORT

Megakaryocyte aplastic thrombocytopenia after CAR T-cell therapy in a patient with multiple myeloma: A case report

Shangqin Liu (✉), Chengsi Gui

Department of Hematology, Zhongnan Hospital of Wuhan University, Wuhan 430071, China

Abstract

Chimeric antigen receptor (CAR) T-cell therapy is an effective new treatment strategy for hematologic malignancies. The success of CAR T-cell therapy in treating leukemia and lymphoma has promoted its development for multiple myeloma (MM), and the initial results of CAR T cell therapy have been encouraging. CAR T-cell therapy target antigens that have been clinically evaluated in MM; these antigens include CD19, B cell maturation antigen (BCMA), CD38, and CD138. A barrier to the widespread use of CAR T-cell therapy is its toxicity, primarily cytokine release syndrome (CRS), and neurologic toxicity. This study reports a patient with refractory MM who also developed megakaryocyte aplastic thrombocytopenia after receiving CAR T-cell therapy; such a case or the unusual side effects involving medications are yet unreported. There are risks in using cyclosporine and other immunosuppressants that may lead to MM recurrence as the use of such substances is contradictory to previous treatments; therefore, we temporarily administered platelet infusion as supportive care. Thus far, the condition of the patient has been steady and the patient regularly takes blood test in the hospital.

Received: 16 October 2020
Revised: 5 November 2020
Accepted: 25 November 2020

Key words: megakaryocyte aplastic thrombocytopenia; chimeric antigen receptor (CAR) T cell therapy; multiple myeloma; case report

A 51-year-old female sought treatment at Tongji Hospital in Wuhan in August 2018 after reportedly experiencing pain in her left lower back. Complete bone marrow aspiration was performed, and multiple myeloma (34.5% bone marrow plasma cells, 25.5% naïve plasma cells) was diagnosed; 13q14 deletion, IGH separation, and 1q21 amplification were identified using fluorescence in situ hybridization (FISH). Furthermore, immunoglobulin testing was performed, and an M protein level of 31.6 g/L (accounting for 34.2%) was recorded. Serum immunofixation electrophoresis indicated the presence of immunoglobulin A lambda lanes, and the level of serum-free light chain was 850 mg/L for lambda lanes. Later, the patient received three cycles of bortezomib, doxorubicin, and dexamethasone (PAD) chemotherapy and three cycles of bortezomib, lenalidomide, and dexamethasone (VRD) chemotherapy from August 2018 to January 2019. After chemotherapy, bone marrow aspiration was performed and indicated 4% bone marrow plasma cells, and MRD testing indicated that 0.62% of the nucleated cells were phenotypically abnormal monoclonal plasma cells.

In March 2019, the patient received one dose of 47 mg fludarabine for three days and one dose of 400 mg cyclophosphamide for three days prior to anti-BCMA and anti-CD38 CAR T cell infusion. Two weeks later, bone marrow aspiration indicated that the bone marrow hyperplasia was no longer active, and megakaryocytes were observed. MRD results indicated the absence of nucleated cells. Moreover, the immunoglobulin test indicated an M protein level of 0.8 g/L (accounting for 1.2%). CAR T-cell immunodetection indicated an increase in human IL-10 (7.13 pg/mL). Then, the patient was discharged. Furthermore, the blood of the patient was tested every three months. In March 2020, her blood test indicated thrombocytopenia. Subsequently, she was

✉ Correspondence to: Shangqin Liu. Email: ubeliu@aliyun.com

treated with Sheng platelet capsules, caffeic acid tablets, and platelet transfusion; however, no marked effects were noted. On May 13, 2020, she was admitted to our hospital.

Her physical examination results were normal, and her blood count was as follows: 3.79 × 10^9/L WBC, 3.04 × 10^{12}/L RBC ↓, 103 g/L HB ↓, 4 × 10^9/L PLT ↓, 101.60 fL ↑ MCV; her direct Coombs test results, COVID-19 antibody and platelet specificity, and tissue-associated fusion antibody test results were all normal. The immunoglobulin test indicated the disappearance of M protein. Bone marrow aspiration indicated morphological remission after MM treatment. Moreover, bone marrow hyperplasia was decreased, and granulocyte, mononuclear cell, and lymphocyte levels were normal; however, her megakaryocyte count was extremely low; only one was counted, and her platelet levels were also low.

Currently, our diagnosis of the disease is megakaryocyte aplastic thrombocytopenia, which might have resulted from CAR-T treatment. As for the treatments, we transitorily provided treatment for hemostasis by infusing platelets; thus far, the patient's condition has remained stable.

Discussion

CAR T-cell therapy is an effective new treatment for hematologic malignancies. CARs are proteins that incorporate an antigen recognition domain and T cell signaling region. After gene modification, CARs expressed by T cells can specifically recognize and eliminate malignant cells that express the target antigens. The target antigens must be expressed on MM cells; importantly, they must be absent or restricted to healthy tissues. CAR T-cell therapy targets antigens that have been clinically evaluated in MM; these antigens include CD19, B cell maturation antigen (BCMA), CD38, and CD138. BCMA is a tumor necrosis factor (TNF) receptor superfamily 17 (TNFRSF17) that plays a central role in regulating B cell maturation and differentiation into plasma cells (PC).

Therefore, BCMA is an excellent target owing to its preferential expression in plasma cells [1]. Trial reports have indicated that BCMA CAR T therapy has strong effects in relapsed or refractory MM and can induce complete tumor remission [1–2]. CD38 is a multifunctional cell surface protein that has receptor and enzymatic functions. It is consistently expressed on malignant plasma cells, making it a suitable target for CAR T cell therapy. Moreover, it is generally expressed at low levels in various hematological and solid tissues. Altogether, this triggered the development of various therapeutic CD38 antibodies, and early clinical data show a marked activity in MM; however, the potential of CAR T cells does not guarantee safety when targeting widely expressed proteins [3–5].

Multiple hematologic toxicities may occur following CAR T cell infusions [2, 6]. In previous trials, most cytopenia cases occurred early after CAR T cell infusion and were attributable to cyclophosphamide and fludarabine conditioning chemotherapy [7]; however, the periods of some cytopenia cases can last for prolonged periods. In this case, the patient continued to experience cytopenia and platelet crisis one year after receiving CAR T-cell therapy. Based on bone marrow aspiration result, we considered that bone marrow was depressed by cyclophosphamide and fludarabine conditioning chemotherapy, and megakaryocyte aplastic may be due to CAR T cell therapy targeting megakaryocyte precursor cells; however, the underlying mechanisms remain unclear.

As there are risks in using cyclosporine and other immunosuppressants that may lead to MM recurrence, we temporarily administered platelet infusions for support care as we waited for the CAR T cells to be expended, and observed whether blood cells would gradually return to normal.

CAR T-cell therapy is an effective new treatment strategy for hematologic malignancies. It is still being tested in clinical trials, and the initial results have been encouraging. CAR T-cell therapy remains relatively new and the management of CAR T-cell toxicities is in early stage. Further animal experiments are needed to assess different immunosuppressive thresholds and to determine whether immunosuppressants can be used, whether they have an impact on clinical long-term remission, and when they are appropriate for use.

Conflicts of interest

The authors indicated no potential conflicts of interest.

References

1. Sellner L, Fan F, Giesen N, *et al*. B-cell maturation antigen-specific chimeric antigen receptor T cells for multiple myeloma: clinical experience and future perspectives. Int J Cancer, 2020, 147: 2029–2041.
2. Ali SA, Shi V, Maric I, *et al*. T cells expressing an anti–B-cell maturation antigen chimeric antigen receptor cause remissions of multiple myeloma. Blood, 2016, 128: 1688–1700.
3. Ghosh A, Mailankody S, Giralt SA, *et al*. CAR T cell therapy for multiple myeloma: where are we now and where are we headed? Leuk Lymphoma, 2018, 59: 2056–2067.
4. Grywalska E, Sosnowska-Pasiarska B, Smok-Kalwat J, *et al*. Paving the way toward successful multiple myeloma treatment: chimeric antigen receptor T-cell therapy. Cells, 2020, 9: 983.
5. van de Donk NW, Janmaat ML, Mutis T, Lammerts VBJ, *et al*. Monoclonal antibodies targeting CD38 in hematological malignancies and beyond. Immunol Rev, 2016, 270: 95–112.
6. Brudno JN, Kochenderfer JN. Recent advances in CAR T-cell toxicity: Mechanisms, manifestations and management. Blood Rev, 2019, 34: 45–55.

7. Brudno JN, Maric I, Hartman SD, *et al*. T cells genetically modified to express an anti-B-cell maturation antigen chimeric antigen receptor cause remissions of poor-prognosis relapsed multiple myeloma. J Clin Oncol, 2018, 36: 2267–2280.

DOI 10.1007/s10330-020-0450-0
Cite this article as: Liu SQ, Gui SC. Megakaryocyte aplastic thrombocytopenia after CAR T-cell therapy in a patient with multiple myeloma: A case report. Oncol Transl Med, 2021, 7: 45–47.

Contribution Invitation of Oncology and Translational Medicine

Oncology and Translational Medicine is an international professional academic periodical on oncology and translational medicine. The Journal, with the authors from around world, especially from China, is dominated in introducing the clinical experience of diagnosis and treatment as well as leading scientific research achievement in the tumor and translational medicine domain, in addition to report basic theory researches which help instruct the clinical practice of oncology and closely connect with the discipline. All the manuscripts are published in English, bimonthly issued both internal and external, 48–64 pages, 16 opens domains, art paper in offset printing, with layout by international customs, unified issuing number: ISSN 2095-9621 / CN 42-1865/R.

Oncology and Translational Medicine uses an online submission system. After reading the Information for Contributors, you must go to ***http://otm.tjh.com.cn*** to submit.

Manuscripts' arrangements are expected to meet the *Uniform Requirement for Manuscripts Submitted to Biomedical Journals* (*the 5th edition*) basically, which was laid down by Internal Medical Journals Edition Committee. Specific requirements for manuscripts are as follows:

Submission process

Manuscripts must be submitted by one of the authors of the manuscript, and should not be submitted by anyone on their behalf. The submitting author takes responsibility for the article during submission and peer review. Manuscripts should be scientific, advanced, pragmatic, concise, clear, well-arranged, well-informed and data-accurate. Provided the manuscript is to be printed, full text will be published in English. To facilitate rapid publication and to minimize administrative costs, *Oncology and Translational Medicine* accepts online submission.

During submission you will be asked to provide a cover letter. Please use this to explain why your manuscript should be published in the journal and to elaborate on any issues relating to our editorial policies detailed in the instructions for authors.

Files can be submitted as a batch, or one by one. The submission process can be interrupted at any time – when users return to the site, they can carry on where they left off. Each manuscript should include title page, abstract, key words, text, acknowledgement, authors' disclosures of potential conflicts of interest, reference, tables, charts and captions, starting each of these sections on a new page, numbered consecutively, beginning with the title page.

T*itle page*: It contains the title of the article, which should be concise but informative. The names of all authors are to be placed under the title in sequence, and personal signatures in the same sequence are a must. Pay attention to accuracy of the title, the names of all authors with their affiliations and the contacting methods in English (address, postcode, telephone and fax number, Email address, etc.).

A*bstract and key words:* A structural abstract of no more than 250 words is to be put on the second page. It should embody four parts, objectives, methods, results and conclusion. It's desirable to employ the third person to write, not "this article" or "the author" in stead of. Supply three to eight key words or short phrases, and terms from the medical subject heading (MeSH) list Index Medicus should be adopted, each word being separated by semicolon.

F*igures and Tables:* Each figure and table is demanded to be numbered consecutively with the order given in the text, typed in separate sheets, and headed by a concise title. Attach all tables after the text. Place explanatory materials in footnotes below the table, and illustrate in footnotes all non-standard abbreviations used in table. The Journal takes the "Three Lines" form of table, requiring the data of the table in accordance with the significant digits of the same index (in the text). Only professional quality glossy photographs and black and white drawings are acceptable. Table numbers, subjects, names of the authors and an arrow indicating "top" should be affixed to the back of each table with soft pencil. If any images of people are involved, it must be granted by the persons in written. Magnification and staining should be indicated when pertinent (esp. pathological pictures concerned).

R*eferences:* References should be listed in the order as mentioned in the text using Vancouver style. References are supposed to be sequentially listed according to GB7714-87 The Rules of References after the Manuscript, being marked by numbers in square brackets in the order as mentioned in the text. The authors must have read the references themselves. List the authors of the reference up to three and， "et al" if more than three. Names of journals should be abbreviated on the basis of the Index Medicus. Every reference should be symbolized by beginning and ending pages. Authors ought to check all references for accuracy and, at the same time, to correct text citation, listing all the citation orderly in Arabian number at the bottom of the text before submitting the articles. The following are two examples of reference style:

1 Bold RJ, Ota DM, Ajani JA, *et al*. Peritoneal and serum tumor markers predict recurrence and survival of patients with respectable gastric cancer. Gastric Cancer, 1999, 2: 1–7.

2 Weinstein L, Swartz MN. Pathologic properties of invading microorganisms. In: Sodeman WA Jr, Sodeman WA, eds. Pathologic physiology: mechanisms of disease. 8th ed. Philadelphia: Saunders, 1974. 457–472.

Assistance with the process of manuscript preparation and submission is available from the customer support team (dmedizin@sina.com).

Publication and peer review processes

Submitted manuscripts will be sent to peer reviewers, unless they are either out of scope or below threshold for the journal, or the presentation or written English is of an unacceptably low standard. They will generally be reviewed by two experts with the aim of reaching a first decision as soon as possible. Statistical reviewers are also used where required (for a full list of our statistical advisers, please click here). Reviewers are asked to declare any competing interests and have to agree to open peer review, which works on two levels: the authors receive the signed report and, if the manuscript is published, the same report is available to the readers. Reviewers are asked whether the manuscript is scientifically sound and whether it is of sufficient significance for publication. In cases where there is strong disagreement either among peer reviewers or between the authors and peer reviewers, advice is sought from a member of the journal's Editorial Board. The journal allows a maximum of two revisions of any manuscript. All appeals should be directed to the Medical Editor. The ultimate responsibility for editorial decisions lies with the Editor-in-Chief.

Other specification

Numbers are required in Arabian. Units of measurement are to be presented in metric units, such as m, cm, mm, mmHg, μm, nm, L, dL, mL, μL, kg, g, mg, μg, kcal, ℃, etc. Abbreviations and terms in simplified forms should be displayed in whole words or phrases at the first time, directly followed by its abbreviation, for example, nasopharyngeal cancer (NPC), When the terms are to be mentioned the second time, the shortened forms in question are acceptable. The abbreviations ought to be standard ones. Any abbreviations in title and abstract are not allowed.

If some Funds subjects of the studies are involved in the manuscripts, be it winning national, ministerial, provincial funds or concerning the special and strategic program, all should be given clear indication in the title page (the Funds number is to be needed), and the copy of the Funds certificate a plus.

It's advisable of you to send us a English-polish certificate from foreign experts (English or American for the best), with inclusion of their personal signatures. Without such certificate, we will invite foreign specialist accordingly to examine and revise your manuscript at the cost on your part. Please indicate your approval when contribute.

Manuscripts must be accompanied by a introduction letter from the author's institution. The letter should contain (1) institution's review and remarks over the manuscript, (2) a statement of no duplicate publication or submission elsewhere of any part of the text, (3) a statement that no secretes or classified information are involved, (4) a statement of no signature or other relationships problems that might lead to a conflict of interest.

To reduce errors in typesetting and to speed up publication, authors are encouraged to submit manuscripts on disk. Disks should not be sent until the manuscript has been accepted and all revisions have been made. The revised manuscript should be saved in paper pattern as well as in pure text pattern, and the saving pattern must clearly indicated on the disk. The editors will not accept a disk without accompanying printouts of all the files on the disk nor without the original manuscript.

Under conditions prescribed by Copyright Law and under considerations of some context of the Journal, manuscripts which are acknowledged receipts but no further notice in the following 3 months may be in the course of examine. If contribution elsewhere is a want, please contact with the editor first because double contribution to different journals with the same manuscripts are not permitted. Keep all the manuscripts for no original manuscript will be returned.

Authors are responsible for the manuscripts they submitted. The Journal, on the basis of Copyright Law, is entitled to revise and abridge the manuscripts. Any amendments concerning the original meaning will be referred to the author for consideration.

Once the manuscript was adopted into the inclusion of the press, the Journal has the rights to publish the manuscript by means of electronic medium or in disc edition. Any part of the manuscript should on no condition be reprinted without our approval.

Every manuscript will be charged 50 yuan (RMB) for being taken care of. When post the manuscript, please remit the money via post office simultaneously (Do not enclose the money with the manuscript). After inclusion of the manuscript, a relevant fees for space of page is to be added. The publisher will provide three copies of the journal free of charge, if the manuscript is accepted.

Address of Editorial Office: Editorial Office of *Oncology and Translational Medicine*, Tongji Hospital, 1095 Jiefang Dadao, Wuhan 430030, China; Tel.: +86-27-69378388; Email: dmedizin@sina.com; Website: http://otm.tjh.com.cn.

Call For Papers
Oncology and Translational Medicine

(CN 42-1865/R, ISSN 2095-9621)

Dear Authors,

Oncology and Translational Medicine (OTM), a peer-reviewed open-access journal, is very interested in your study. If you have unpublished papers in hand and have the idea of making our journal a vehicle for your research interests, please feel free to submit your manuscripts to us via the Paper Submission System.

Aims & Scope

- Lung Cancer
- Liver Cancer
- Pancreatic Cancer
- Gastrointestinal Tumors
- Breast Cancer
- Thyroid Cancer
- Bone Tumors
- Genitourinary Tumors
- Brain Tumor
- Blood Diseases
- Gynecologic Oncology
- ENT Tumors
- Skin Cancer
- Cancer Translational Medicine
- Cancer Imageology
- Cancer Chemotherapy
- Radiotherapy
- Tumors Psychology
- Other Tumor-related Contents

Contact Us
Editorial office of Oncology and Translational Medicine
Tongji Hospital
Tongji Medical College
Huazhong University of Science and Technology
Jie Fang Da Dao 1095
430030 Wuhan, China
Tel.: 86-27-69378388
Email: dmedizin@tjh.tjmu.edu.cn;
dmedizin@sina.com

Oncology and Translational Medicine (OTM) is sponsored by Tongji Hospital, Tongji Medical College, Huazhong University of Science and Technology, China (English, bimonthly).

OTM mainly publishes original and review articles on oncology and translational medicine. We are working with the commitment to bring the highest quality research to the widest possible audience and share the research work in a timely fashion.

Manuscripts considered for publication include regular scientific papers, original research, brief reports and case reports. Review articles, commentaries and letters are welcome.

About Us

- Peer-reviewed
- Rapid publication
- Online first
- Open access
- Both print and online versions

For more information about us, please visit:
http://otm.tjh.com.cn

中国科技核心期刊

（中国科技论文统计源期刊）

收录证书

CERTIFICATE OF SOURCE JOURNAL

FOR CHINESE SCIENTIFIC AND TECHNICAL PAPERS AND CITATIONS

ONCOLOGY AND TRANSLATIONAL MEDICINE

经过多项学术指标综合评定及同行专家评议推荐，贵刊被收录为“中国科技核心期刊”（中国科技论文统计源期刊）。

特颁发此证书。

中国科学技术信息研究所

Institute of Scientific and Technical Information of China

北京复兴路 15 号 100038　　www.istic.ac.cn

2020年12月

证书编号：2019-G616-0093

有效期至：2021年12月